RL-TR-96-66
Final Technical Report
May 1996

OPTICALLY CONTROLLED SHF SATCOM ARRAY (OCSSA)

Harris Corporation

G.R. Diemond, R.M. Montgomery, and J.T. Gallo
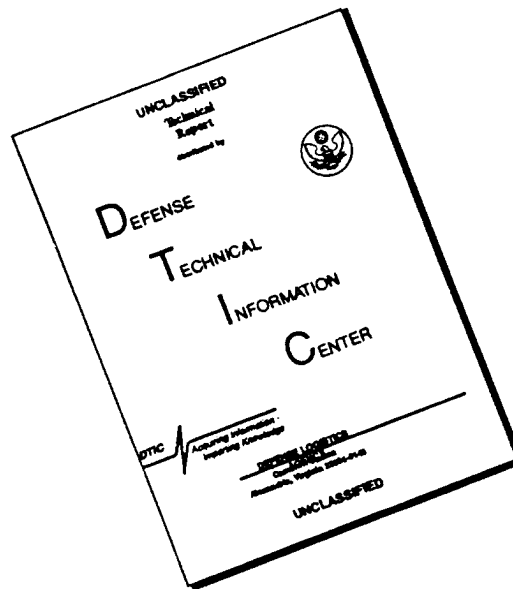
APPROVED FOR PUBLIC RELEASE; DISTRIBUTION UNLIMITED.

19960730 093

Rome Laboratory
Air Force Materiel Command
Rome, New York
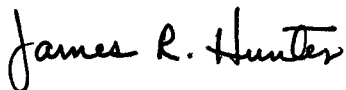
DTIC QUALITY INSPECTED 1

DISCLAIMER NOTICE

THIS DOCUMENT IS BEST
QUALITY AVAILABLE. THE COPY
FURNISHED TO DTIC CONTAINED
A SIGNIFICANT NUMBER OF
PAGES WHICH DO NOT
REPRODUCE LEGIBLY.

This report has been reviewed by the Rome Laboratory Public Affairs Office (PA) and is releasable to the National Technical Information Service (NTIS). At NTIS, it will be releasable to the general public, including foreign nations.
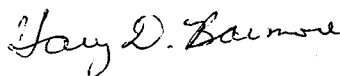
RL-TR- 96-66   has been reviewed and is approved for publication.

APPROVED:

James R. Hunter

JAMES R. HUNTER
Project Engineer

FOR THE COMMANDER:

Gary D. Barmore

GARY D. BARMORE, Major, USAF
Deputy Director of Surveillance & Photonics

If your address has changed or if you wish to be removed from the Rome Laboratory mailing list, or if the addressee is no longer employed by your organization, please notify Rome Laboratory/ (OCPC), Rome NY 13441. This will assist us in maintaining a current mailing list.

Do not return copies of this report unless contractual obligations or notices on a specific document require that it be returned.

REPORT DOCUMENTATION PAGE

Public reporting burden for this collection of information is estimated to average 1 hour per response, including the time for reviewing instructions, searching existing data sources, gathering and maintaining the data needed, and completing and reviewing the collection of information. Send comments regarding this burden estimate or any other aspect of this collection of information, including suggestions for reducing this burden, to Washington Headquarters Services, Directorate for Information Operations and Reports, 1215 Jefferson Davis Highway, Suite 1204, Arlington, VA 22202-4302, and to the Office of Management and Budget, Paperwork Reduction Project (0704-0188), Washington, DC 20503.

1. AGENCY USE ONLY (Leave Blank)	2. REPORT DATE	3. REPORT TYPE AND DATES COVERED
	May 1996	Final Oct 94 – Nov 95

4. TITLE AND SUBTITLE

OPTICALLY CONTROLLED SHF SATCOM ARRAY (OCSSA)

5. FUNDING NUMBERS
C – F30602-94-C-0294
PE – 63726F
PR – 2863
TA – 92
WU – 71

6. AUTHOR(S)

G.R. Diemond, R.M. Montgomery, and J.T. Gallo

7. PERFORMING ORGANIZATION NAME(S) AND ADDRESS(ES)
Harris Corporation
Government Aerospace Systems Division
P.O. Box 94000
Melbourne FL 32902

8. PERFORMING ORGANIZATION REPORT NUMBER

N/A

9. SPONSORING/MONITORING AGENCY NAME(S) AND ADDRESS(ES)

Rome Laboratory/OCPC
25 Electronic Pky
Rome NY 13441-4515

10. SPONSORING/MONITORING AGENCY REPORT NUMBER

RL-TR-96-66

11. SUPPLEMENTARY NOTES

Rome Laboratory Project Engineer: James R. Hunter/OCPC/(315) 330-7045

12a. DISTRIBUTION/AVAILABILITY STATEMENT

Approved for public release; distribution unlimited.

12b. DISTRIBUTION CODE

13. ABSTRACT (Maximum 200 words)

Users of Defense Satellite Communications Systems (DSCS) will place increasing demands on the throughput of the systems. Increased reliance on DSCS to send and receive large amounts of data to high performance ground terminals means more high performance will be expected in future DSCS satellites. As the system capability increases, use of DSCS by more mobile platforms will become more popular. Photonics technology promises to enable DSCS growth with wider bandwidth systems and smaller packages. A top-down system engineering study that identifies where and how photonic approaches may enhance system performance is described. This study produced two unique array designs for DSCS airborne and satellite applications. Both are described in terms of performance characteristics at the array and DSCS link levels. The airborne array uses a unique switched delay beamformer that achieves 100% usage of all the delays all of the time. No additional lasers for frequency multiplexing are required. This hardware compression means there are no overhead hardware penalties due to time delays not switched into a signal path. The satellite array design uses a LO multiplexing scheme to produce simultaneous independent multiple beams. The hardware to produce four beams measures approximately 4" by 4" by 30".

14. SUBJECT TERMS

Phased array, Photonic control, Optical control

15. NUMBER OF PAGES
126

16. PRICE CODE

17. SECURITY CLASSIFICATION OF REPORT	18. SECURITY CLASSIFICATION OF THIS PAGE	19. SECURITY CLASSIFICATION OF ABSTRACT	20. LIMITATION OF ABSTRACT
UNCLASSIFIED	UNCLASSIFIED	UNCLASSIFIED	UL

Table of Contents

List of Figures

List of Tables

1.0   Introduction

Current and future users of the DSCS will place increasing demands on the throughput of the system. Increased reliance on DSCS to send and receive large amounts of data to high performance ground terminals means more high performance will be expected in future DSCS satellites. In addition, as the system capability increases, use of DSCS by more mobile platforms will become more popular.

Photonic technology promises to create the necessary hardware for the DSCS growth with wider bandwidth systems and smaller packages with equal or better performance than existing RF designs.

The current DSCS III satellite, although it has a multiple beam antenna, can produce <u>only one beam at a time</u>. Thus only users within a single custom satellite footprint can access the system through the high performance array. Significant enhancement to the current system can be obtained if the array could produce <u>multiple simultaneous customized beams</u> allowing traffic to be directed among a wide range of users simultaneously. Photonic technology can provide the technology to allow growth to simultaneous multiple beams without the multiplication effect seen in RF designs. It is anticipated that going from one to four beams, for example, will require significantly less than twice the hardware compared to the quadrupling of RF hardware.

Another, thus far largely untapped, group of users are aircraft that can provide or receive reconnaissance and mission critical data through DSCS. Most Satellite Communication (SATCOM) links are designed to pass large amounts of data to and from large, fixed ground terminals. To achieve sufficient performance with an airborne terminal requires large aperture antennas to close the link and to avoid interference with other satellites and users. On aircraft, the problem is to find enough real estate to provide sufficient aperture size while maintaining wide angular coverage. Large apertures with wide scan angles and wide bandwidth establishes the need to incorporate true-time delays in the array architecture.

Photonic technology can provide the medium for the airborne time delay hardware, allow the systematic use of large distributed arrays, and perhaps reduce the size of the terminal hardware by incorporating portions of the signal processing along with the antenna control and distribution.

1.1   Program Objectives

To explore the possibilities for airborne and satellite photonic phased arrays, the government has begun initiatives to explore applying photonic technologies to the DSCS system. Initial concept developments have been defined and the definition of the next phase of technology demonstrations using EDM's is underway.

Advanced development of the OCSSA airborne and satellite phased arrays must be preceded by demonstrations that show the technology risk has been bounded. Following the array definitions documented in this report, the next steps in this effort, is to build and test breadboard hardware defined specifically to demonstrate key technology components of the proposed FSD OCSSA system.

The objectives of this first effort are to achieve maximum progress toward the EDM definition and to present a relevant and significant demonstration of some portion of the concepts conceived in this first phase.

1.2 Study Philosophical Direction

The primary challenge in this first phase is to merge array and photonic technologies. A successful merger would solve one technologies weaknesses with the other's strengths and vice versa. Additionally, the merger should extend the system's capabilities. Table 1.2-1 summarizes the primary strengths and weaknesses of the two technologies.

Table 1.2-1   Technology Strengths and Weaknesses

phased arrays	strengths	weaknesses
	beam agility	complexity
	multiple beams	cost
	conformal	size
		weight

photonics	strengths	weaknesses
	wideband	noise figure
	instantaneous processing	conversion efficiency
	low loss fiber	switching speeds
	light weight fiber	

Adding some complexity to the task is the expected differences between the airborne and satellite phased arrays. The two sets of requirements for the arrays forecast significant differences between the two arrays. Table 1.2-2 lists both sets of array characteristics. Significant differences in the array approaches can be expected.

Table 1.2-2   Two Different Array Requirements

Airborne Array	Satellite Array
single beam	multiple beam
non-adaptive	adaptive
wide scan	narrow scan
conformal	planar
tracking	non-tracking

For successful insertion into either array, the photonic approach must show clear performance, cost, or physical advantage. Each architectural trade for photonic application is a three-way trade of photonic integration level versus risk, performance, cost, or physical payoff, and versus time frame. A design capable of applications in the short term must use techniques with lower risks in order to be competitive. A lower risk approach means less integration and lower payoff.

A design that promises higher payoff will require larger levels of integration and therefore higher risk. This approach may require technology breakthroughs before it can be fully realized.

With that prelude, there are two major assertions made at the beginning of the study. First, the airborne array is assumed to have a near term application. If a

competitive design is available today, an application could be found. The airborne array configuration is therefore a low risk approach with photonic integration at the component level.

The satellite array is assumed to be a longer term application. The design cycle for a new DSCS satellite may be years away. The satellite array approach is therefore a very highly integrated approach that promises huge improvements in size and weight over its RF equivalent.

An additional comment is necessary to insure the reader understands the approach taken in this study. The results presented in this report are derived from a top-down system engineering study that identifies where and how photonic approaches may enhance system performance. Rather than start with a set of photonic components and design upward to see what system performance is possible, this study defines the system link, the required array performance, and then transfers the requirements down to photonic building blocks. The photonic hardware necessary to provide a useful DSCS link is defined. The study task flow is illustrated in Figure 1.2.
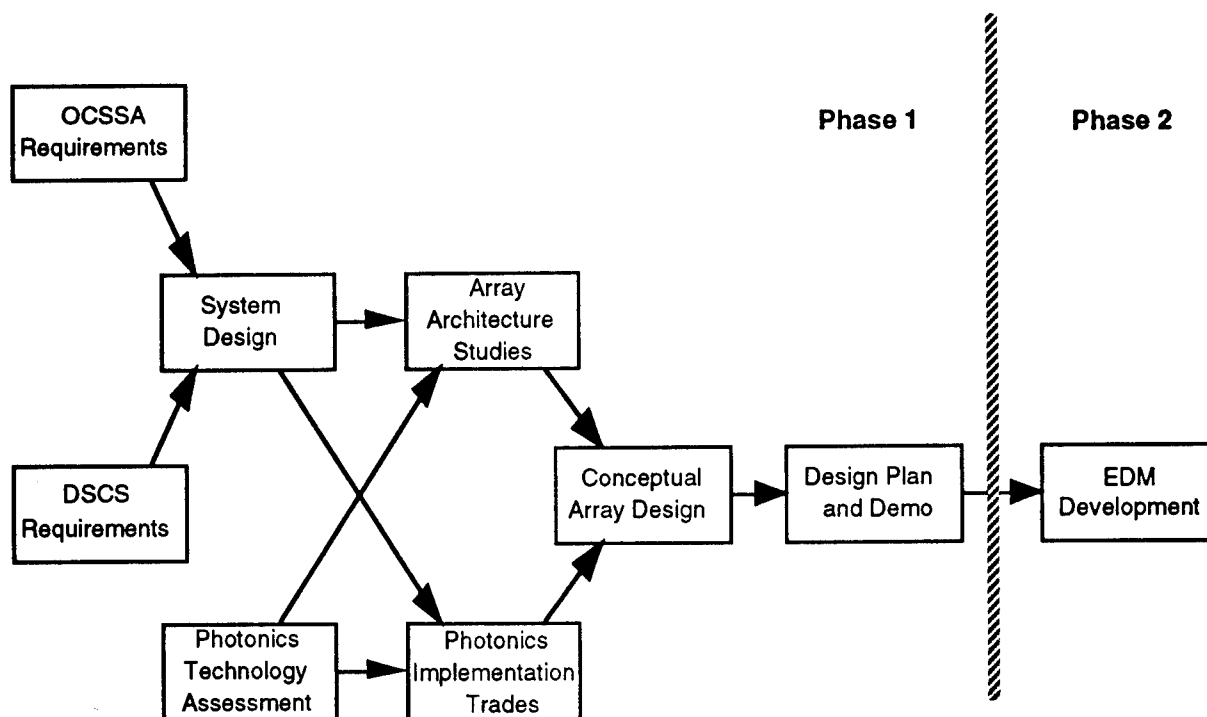
Figure 1.2   OCSSA Top-Down Task Flow

1.3   Summary of Results

This first OCSSA study has produced two unique array designs for the DSCS airborne and satellite applications. Both arrays have been described in terms of performance characteristics at the array and DSCS link levels. Physical descriptions of both arrays have been developed

The airborne array uses a unique switched delay beamformer approach that achieves 100% usage of all the delays all of the time. No additional lasers for frequency multiplexing is required. This form of hardware compression means there is no

overhead hardware penalties due to time delays not switched into a signal path. The airborne array performance on the airframe has been characterized showing the coverage difficulties due to the rotodome. Physically, the array hardware approaches the size and weight envelopes of a conventional RF feed array using photonic technology available today.

Two issues remain for the airborne array. With more detailed study of the hardware configuration, can the switched delay beamformer ever compete with the integrated MMIC RF technology that can produce a three-bit phase shifter at S-band on a 40 by 70 mil GaAs chip? Secondly, the study specification of 256 elements on the transmit array produces wide beamwidths that cannot meet the terminal certification requirements for the DSCS system. System access may be limited or additional assets may have to be rented to prevent interference.

The satellite array design derived on this study uses a unique LO multiplexing scheme to produce simultaneous independent multiple beams. The resulting hardware to produce four beams measures only about 4" by 4" by 30". Growth to more beams is accomplished by adding an additional dual frequency laser and a modified SLM. Size growth from one to two beams is less than 10% and less than 25% for four beams. RF hardware growth in the existing DSCS satellite array for a second beam is 100% and 300% for growth to four beams.

The major issue for the satellite array is when a suitable 1.3 micron SLM might be developed. A second issue, like the airborne array, is based on the study requirement of 256 elements spaced 2 wavelengths apart. The resulting beamwidth is roughly the same size as the existing DSCS III satellite array. A larger aperture with more elements would improve coverage selectivity.

This study has shown that photonic-controlled arrays are rapidly becoming viable for missions like the DSCS. Realistic expectations on the advantages and improvements of a photonic beamformer will hasten their acceptance.

2.0   System Design

During the System Design task of the OCSSA Study, the array strawmen designs given in the SOW were characterized. Included in this activity were loss budgets, G/T and EIRP predictions, and pattern performance predictions

2.1   Airborne Arrays

The airborne receive and transmit arrays are specified to have separate receive and transmit apertures. This decision eliminates the packaging problem inherent in full duplex arrays. Diplexing the two bands behind each array element presents a difficult problem at higher frequencies.

2.1.1 Airborne Receive Array Characteristics

- **Strawman**
  The airborne strawman array requirements given in the SOW are:

  - 7.25-7.75 GHz
  - ±75° scan
  - 256 elements
  - one beam
  - circular polarization
  - true time delay
  - receiver noise figure = 6 dB

- **Lattice**
  The lattice for the receive array is a square grid. Although this choice tends to make the 256 element smaller than a hexagonal grid, the square grid pays some dividends in the selections of the feed network. The justification for the square grid is discussed in section 4.4.

  - element spacing in square grid = 0.775 inches

  - aperture area = 154 square inches

  - aperture size = 12.4 inches square

  - 3 dB beamwidth = 8.1 degrees (assuming some amplitude taper)

- **Gain**

  The receive array loss budget is shown in Table 2.1.1

Table 2.1.1   Airborne Receive Array Loss Budget

scan loss @ 75° scan	8.2 dB	non-ohmic
mispointing loss	0.5	non-ohmic
quantization loss	0.2	non-ohmic
rms phase error	0.5	non-ohmic
rms amplitude error	0.2	non-ohmic

amplitude taper	0.7	non-ohmic
polarization loss	0.5	non-ohmic
active mismatch	0.5	non-ohmic
radome	0.3	ohmic
element loss	0.3	ohmic

total loss = 11.9 dB

- directivity = 29.3 dB
- array gain at 75° scan = 17.4 dB

- **G/T**

The G/T calculation for the receive array is based on the model shown in Figure 2.1.1.
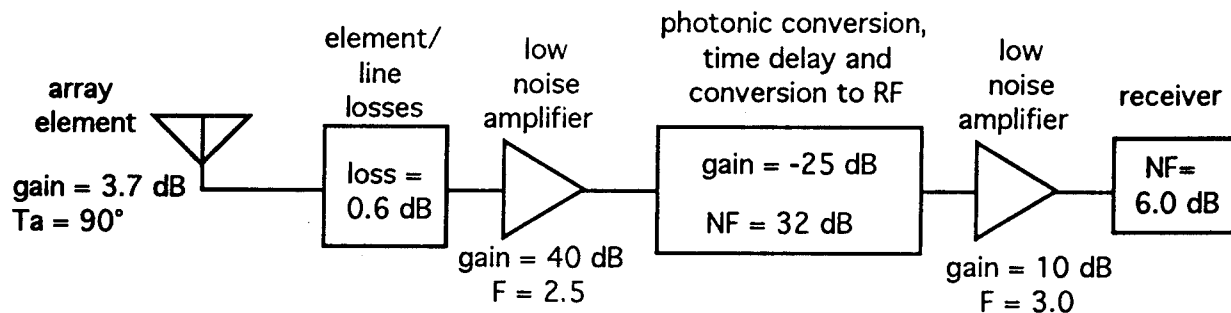
Figure 2.1.1 Airborne Receive Array G/T Model

With the values shown in the figure, the receive array G/T is -9.27 dB/°K at the maximum 75° scan position.

2.1.2 Airborne Transmit Array Characteristics

- **Strawman**

The airborne strawman transmit array requirements given in the SOW are:

- 7.9-8.4 GHz
- ±75° scan
- 256 elements
- one beam
- circular polarization
- true time delay
- 47 dBW EIRP

- **Lattice**

The lattice for the transmit array is a frequency scaled version of the receive array.

- element spacing in square grid = 0.715 inches
- aperture area = 130.8 square inches
- aperture size = 11.4 inches square
- 3 dB beamwidth = 8.0 degrees (assuming some amplitude taper)

- **EIRP**

The transmit array EIRP calculation are made assuming the same aperture budget as the receive array.

- directivity = 29.3 dB
- array gain at 75° scan = 17.4 dB
- array transmitted power = 29.7 dBW
- element transmitter power = 3.6 Watts

- **Airborne Transmit Array Thermal Considerations**

An additional item requiring consideration is the thermal density of the transmit array. With elements packed closely together, due to wide scan and square lattice, and each transmitting 3.6 Watts, the thermal load created by the transmit aperture will require special heat removing techniques. The total heat dissipated by each element could reach 10 Watts. In addition, because the array is top-mounted, it is subject to solar loading effects.

For the purposes of the discussion in this study, it is assumed that the transmit array will require liquid cooling in order to protect it from thermal damage. This is a worst case position. Limiting operation to in-flight would help some. Increasing the aperture size so that each element has less RF power would also reduce the thermal management challenge.

2.1.3 Airborne Array Beam Count

A consideration in choosing a beamformer approach for the airborne array beamformers is the number of 3 dB beamwidths required to cover the full 75° scan volume. Assuming a 8 degree beamwidth, square lattice, and symmetrical azimuth and elevation scan, each plane requires a minimum of 14 beams to cover ±75°.

2.1.4 Airborne Array Tracking

Flying on a maneuvering airframe, the DSCS arrays must track the satellite in order to maintain the link. Generally, there are two options for tracking on an aircraft: monopulse and command pointing. A monopulse approach requires multichannel receiving systems to detect two orthogonal pointing errors. This technique is very accurate and can be designed to handle fairly rapid motion.

Command pointing, on the other hand, is much more simple since it does not need receivers to sense the position. The aircraft, from its on-board sensors can tell the

array the airframe location and orientation. The array can calculate the direction to the desired geosynchronous DSCS satellite and select the beam position.

Since the beamwidths are relatively fat and the dynamics of the aircraft are slow compared to a tactical fighter, command pointing would appear to be adequate. With an eight degree beamwidth and 30 degree per second roll rate, it takes 266 milliseconds to roll from one beam peak to another.

Should the array design grow to achieve smaller beamwidths, some type of automatic tracking would be required. Fortunately, the DSCS satellite has a beacon signal that can be used to maintain track continuously through the receive channel. The transmit array pointing will be slaved to the receive beam position.

2.1.5 Airborne Array Coverage

An airborne platform can communicate with a satellite only when in a line-of-sight of the satellite and when the airframe does not interfere with the array patterns. Both conditions have been simulated and their results presented in this section.

● **Airborne Array Satellite Visibility**

Predicting satellite visibility is basically a vector problem. A level flying aircraft at a specified altitude is positioned at a point above the earth and a geometric calculation indicates if the desired satellite or satellites can be seen by the airframe within the scan volume of the phased array.

For the calculations on the study, level flight at an operational altitude of 35000 feet was assumed. It is also assumed that there is only one array on the airframe and that its boresight is in the direction of the airframe zenith.

Two cases are shown in Figures 2.1.5-1 and 2.1.5-2: 75° and 60° maximum scan. The advantage of the 75° scan is obvious from the data. The 60° case was added because, with only one array on top of the airframe, scan performance in the pitch plane is limited by the electromagnetic effects of the conductors. If it is assumeed that the pitch plane has less visibility, the the 75° scan coverage holds for the airframe flying East-West while the 60° scan case represents an aircraft flying North-South.
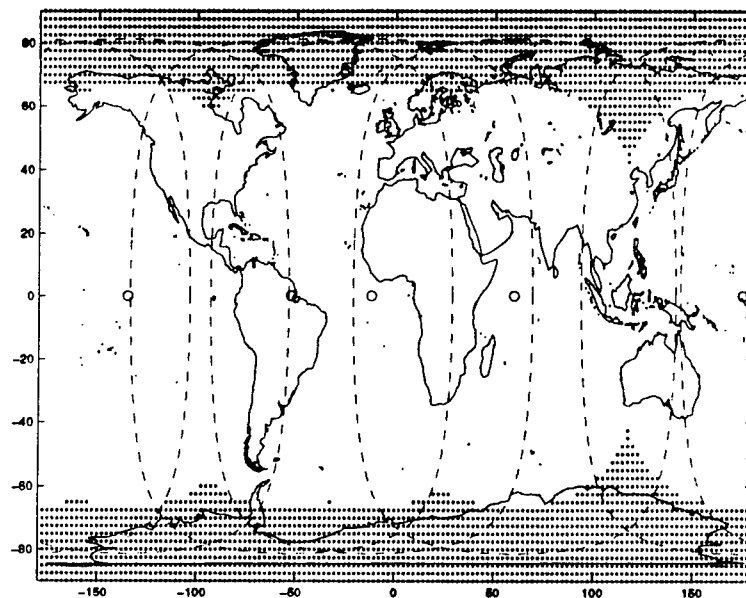
Figure 2.1.5-1   DSCS Visibility for an Airborne Array at 75° Scan
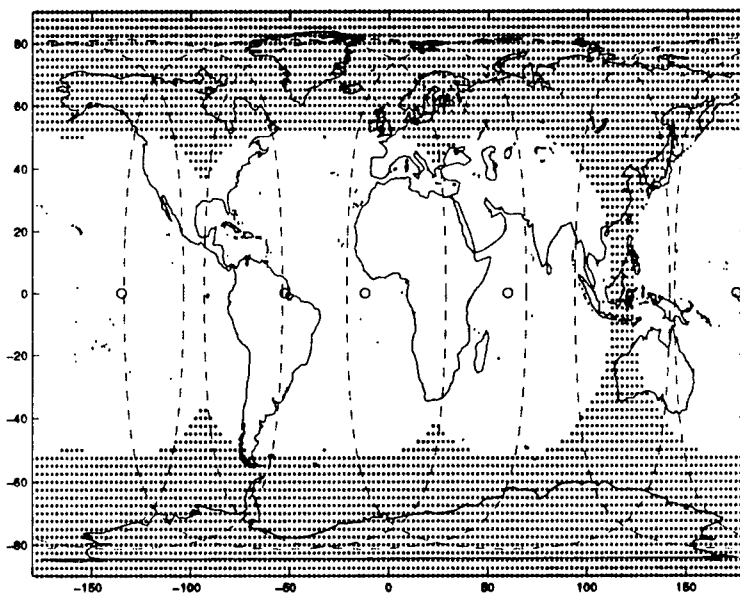
Figure 2.1.5-2   DSCS Visibility for an Airborne Array at 60° Scan

- ### Airborne Array Free Space Patterns

    Figure 2.1.5-3 shows simulated patterns of the airborne array in free space, i.e. containing no effects from the aircraft fuselage. Scan positions shown are boresight, 30°, 60°, and 75° scan. The scan loss at 75° scan is consistent with the 8.2 dB number used in the array aperture budgets.
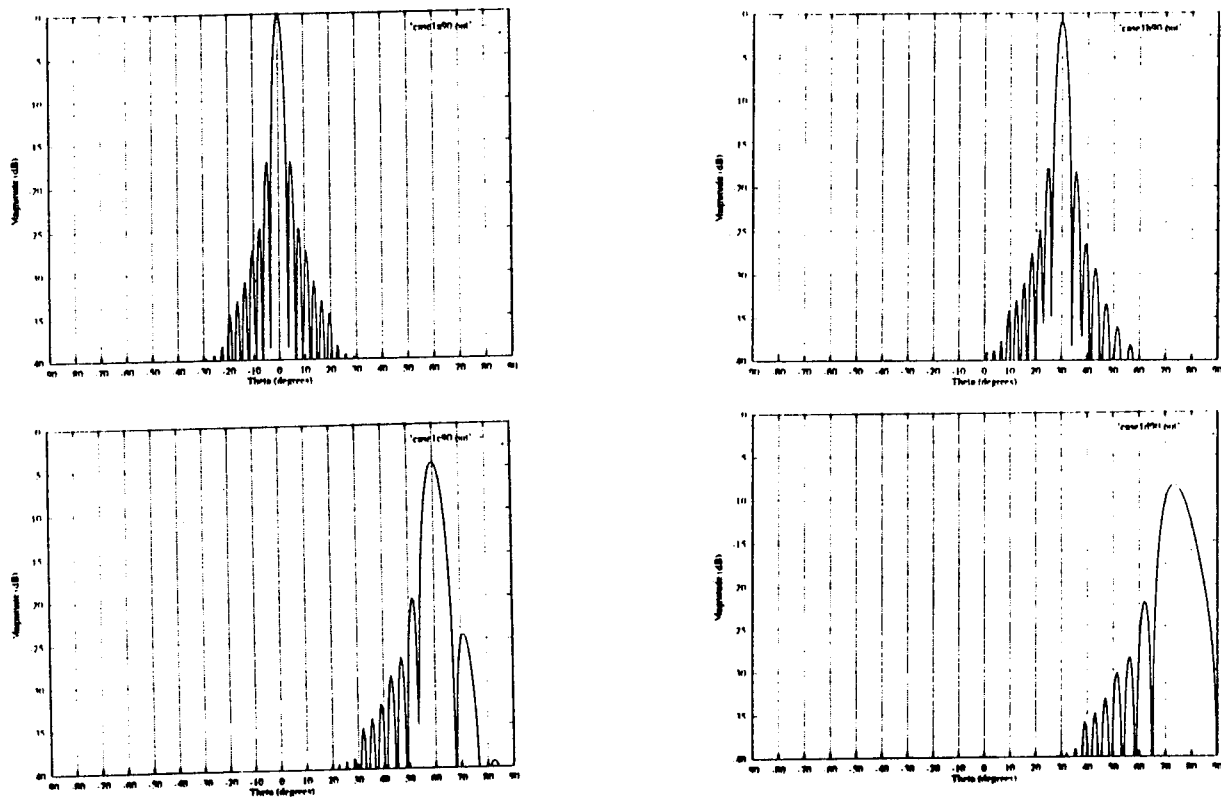
Figure 2.1.5-3   Airborne Array Free Space Patterns

• Airborne Array Airframe Blockage

Complex airframes can significantly distort antenna patterns reducing coverage . For the present study, an airframe like that shown in Figure 2.1.5-4 can be expected to present significant problems in the pitch plane. Useful locations for the DSCS array are limited to the area just aft of the cockpit and forward of the rotodome. Intuitively, the array should be as far forward as possible. This not only reduces the rotodome blockage but minimizes multipath effects of the wings.
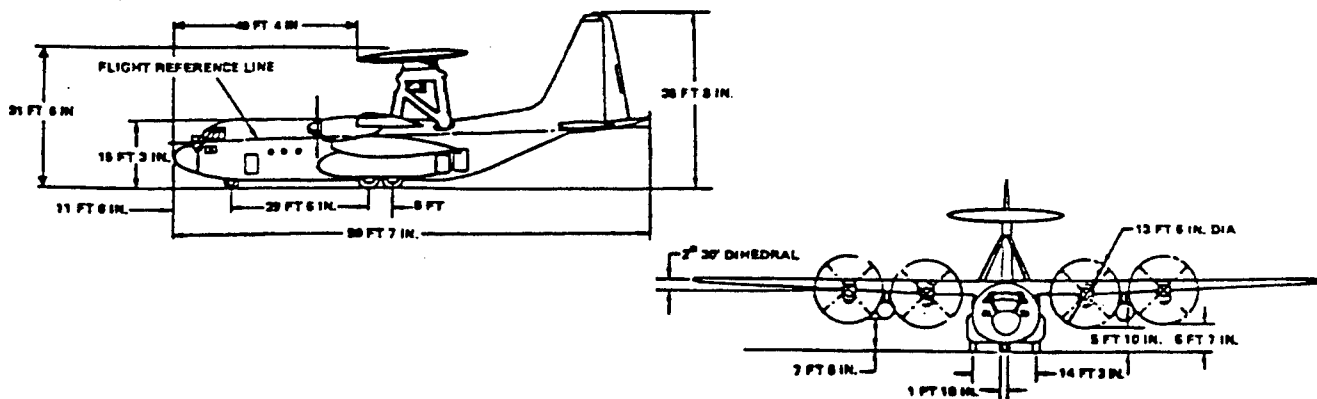
Figure 2.1.5-4   OCSSA Airborne Platform

Modeling a two-dimension scanning array on a complex groundplane is a difficult and time consuming effort. On the OCSSA study, emphasis was placed on the pitch plane effects only. Thus only a linear array positioned on the centerline had to be analyzed. A similar airframe model was modified to the required dimensions. A plot of the computer model is shown in Figure 2.1.5-5.
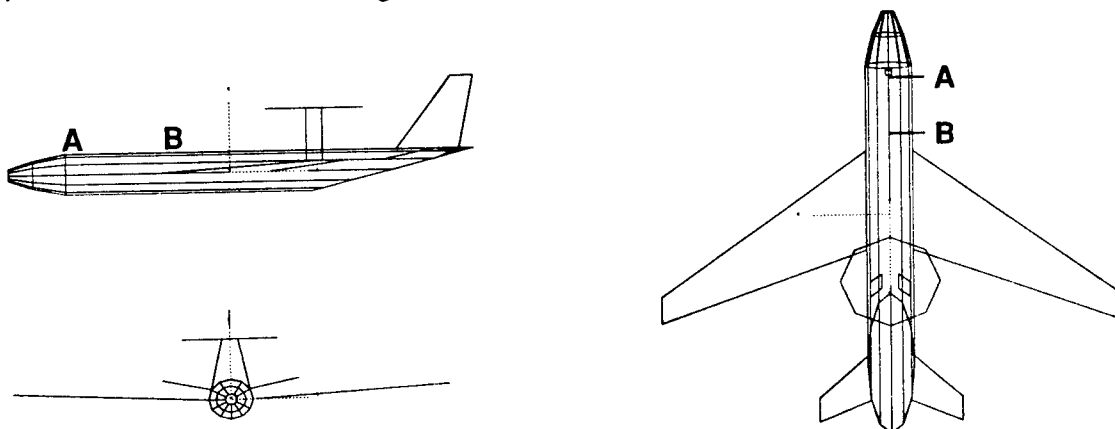
Figure 2.1.5-5   Computer Model of the OCSSA Airborne Platform

Next two monopole patterns were placed at the A & B locations shown in Figure 2.1.5-5 for simulation of the pitch plane performance. This exercise served to bound the level of blockage and the sensitivity to airframe location. Figure 2.1.5-6 shows the two monopole patterns. As expected, the forward-most location is required. At that position, the pattern is starting to just starting to break-up at 75° from zenith.

Monopole Pitch Plane Pattern at Position A

Monopole Pitch Plane Pattern at Position B
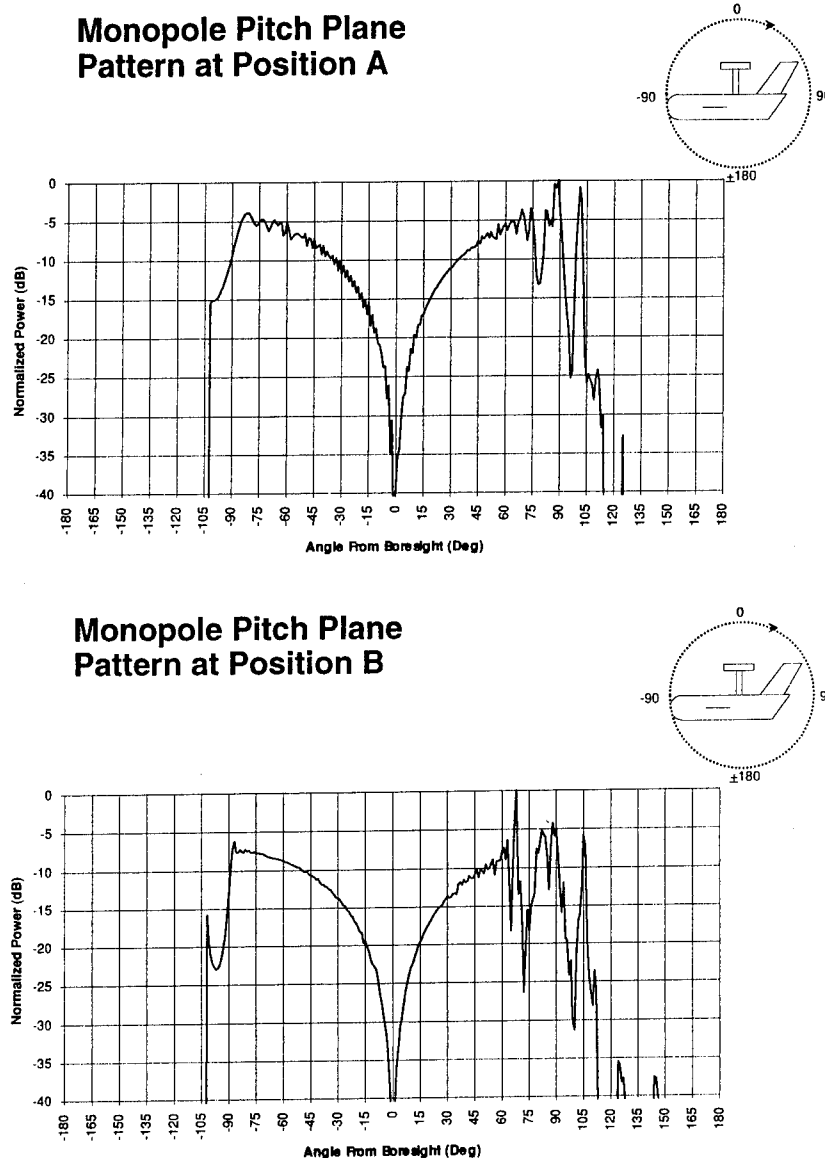
Figure 2.1.5-6   Pitch Plane Monopole Patterns

The final step in the simulation was to position a 16 element array along the top airframe centerline at position A and examine pitch plane scan performance. This linear array is a suitable model for the square array in the pitch plane only. The complete set of patterns run are shown in Appendix A. Of particular interest is the patterns scanned toward the rotodome at 60° and 75°. these two patterns are shown in Figure 2.1.5-7.

As expected, the scanned pattern at 75° is virtually useless. Fifteen degrees closer to boresight, at 60° scan, the pattern is quite well-behaved.

16-Element Linear Array
Pitch Plane, +60° Scan

16-Element Linear Array
Pitch Plane, 75° Scan
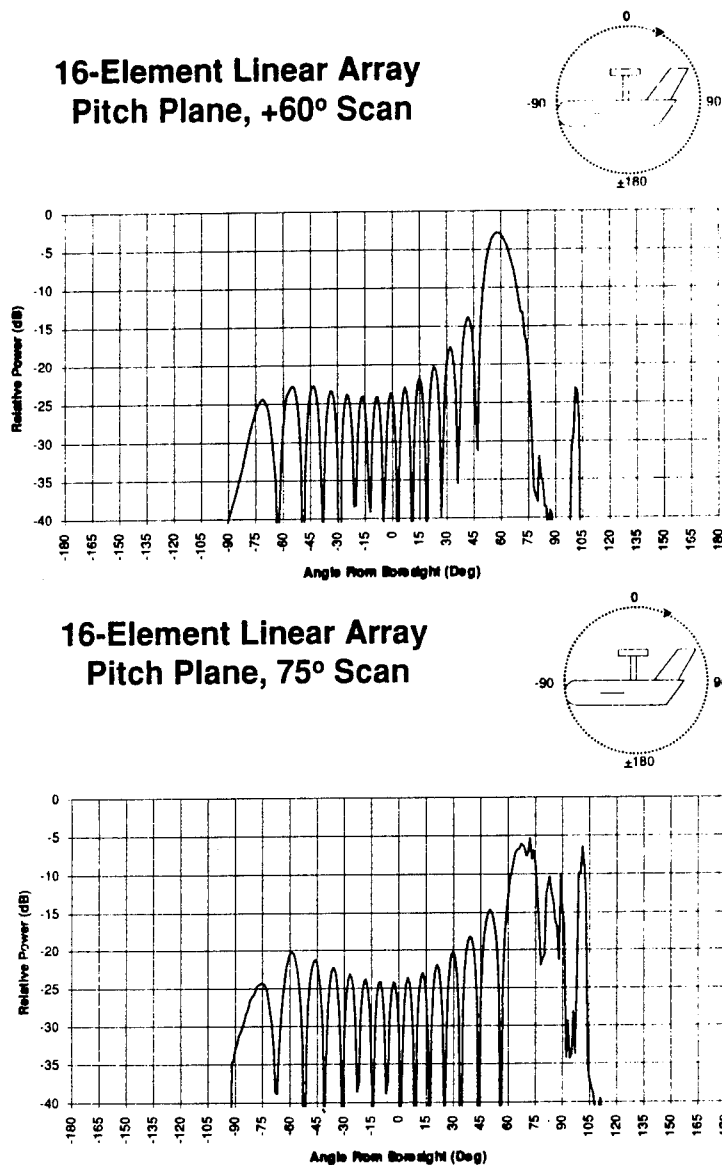
Figure 2.1.5-7   Pitch Plane Array Patterns

• **Airborne Array Coverage Conclusions**

Putting together all of the visibility and airframe blockage effects seen in the simulations, the following conclusions can be made:

1) 75° scan coverage gives excellent satellite visibility

2) On the airframe, coverage to 75° scan is expected to be satisfactory in the roll plane and in the forward upper quadrant of the pitch plane.

2-9

3) Coverage in the aft upper portion of the pitch plane is usable at least to 60°

4) On the basis of the above statements, the 75° visibility curve shown in Figure 2.1.5-2 is applicable to all East-West flights and to southbound flights in the Northern hemisphere and northbound flights in the southern hemisphere.

5) The 60° visibility curve in Figure 2.1.5-1 applies to northbound flights in the northern hemisphere and southbound flights in the southern hemisphere.

2.1.6 Airborne Array DSCS Certification Requirements

In order to operate in the DSCS network, ground terminal antennas must meet a set of requirements in order to prevent interference with other DSCS users and efficient use of the satellite transponder resources. These requirements are found in the DSCS Certification Requirements Document [1] (see references at the end of this report).

The requirements applicable to the OCSSA include control carrier stability, extraneous emissions, antenna beamwidth, antenna sidelobes, antenna pointing accuracy, and transmit carrier level control.

The sidelobe level specified in power level is shown in Figure 2.1.6. These values must hold for any antenna less than 100 wavelengths across. The OCSSA array meets that criteria but it is so small that it has no problem keeping sidelobe gain below these numbers.
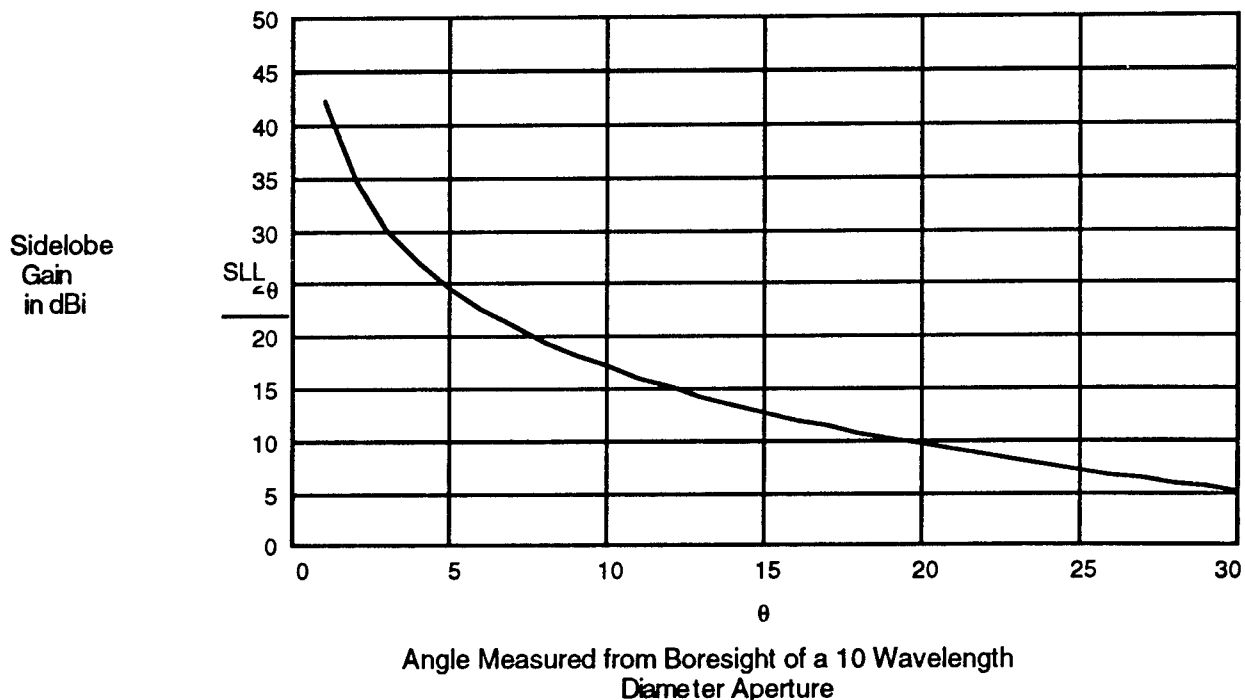
Figure 2.1.6 DSCS Certification Sidelobe Levels

The certification requirements for tracking states that over a 24 hour period, the pointing loss of any antenna shall not exceed 0.4 dB for systems using tracking and 1

dB for systems not using tracking. Again, the OCSSA design should not have any difficulty meeting this requirement because of its wide beams and motion compensation.

The last pertinent specification, antenna beamwidth, presents a problem for the OCSSA airborne array strawman. The certification requirement requires that antennas have a 3 dB beamwidth of four degrees or less to prevent interference to/from DSCS on-orbit spares. The current OCSSA arrays have eight degree beamwidths.

Achieving all certification requirements is not an easy task, even for large ground antennas. Questions were sent to DSA, who coordinates access to DSCS, about any relaxation for airborne terminals. At this time the certification specifications do apply to airborne terminals.

The effect of reducing the beamwidth is to increase both array sizes to over 1000 elements. This represents a significant increase in size which will make an airborne array location difficult to find. It also may require more sophisticated tracking hardware to stay locked up as the airframe moves.

For the purpose of this study, the arrays remain at the current size of 256 elements. Operation within the DSCS system will still be possible with the terminal but it may have to wait for clearance when other users are not using the system. Alternatively, the OCSSA user might have to rent multiple transponders to prevent interference to other on-orbit DSCS assets.

In terms of the array design, the 256 element array could be used as a building block for larger arrays in the future. Use of subarray techniques is a natural application for time-delay array feeds.

2.1.7 Airborne Array Physical Goals

In order to define a measuring stick to compare the hardware sizes, a couple of previous designs were examined. By scaling their hardware to the same element count and frequency as OCSSA, physical goals can be identified. Because of the low risk approach to the airborne OCSSA arrays, the physical size and weight of the array must at least compare favorably with an airborne RF array.

Based on a previous 1156 element airborne array, the OCSSA airborne array goals are 249 cubic inches and 31 pounds for the receive array and 350 cubic inches and 45 pounds for the transmit array. The transmit array includes passages for circulation of coolant.

2.2   Satellite Arrays

2.1.1   Satellite Receive Array

•   **Strawman**
The satellite strawman array requirements given in the SOW are:

- 7.9-8.4 GHz
- 256 elements
- 2 wavelength spacing
- circular polarization
- four simultaneous beams
- receiver noise figure = 6 dB

- **Lattice**

The lattice for the receive array is a hexagonal grid. Maximum scan is assumed to be ±10°.

- element spacing = 2.81 inches in x and 1.623 inches in y
- aperture area = 2347 square inches
- aperture diameter = 54.7 inches
- 3 dB beamwidth = 2.0 degrees (assuming some amplitude taper)

- **Gain**

The receive array loss budget is shown in Table 2.2.1

Table 2.2.1 Satellite Receive Array Loss Budget

scan loss @ 10° scan	0.05 dB	non-ohmic
mispointing loss	0.8	non-ohmic
quantization loss	0.2	non-ohmic
rms phase error	0.5	non-ohmic
rms amplitude error	0.2	non-ohmic
amplitude taper	0.7	non-ohmic
polarization loss	0.5	non-ohmic
active mismatch	0.5	non-ohmic
radome	0.3	ohmic
element loss	0.3	ohmic

total loss = 4.25 dB

- directivity = 41.7 dB
- array gain at 10° scan = 37.5 dB

- **G/T**

The G/T calculation for the receive array is based on the model shown in Figure 2.2.1.
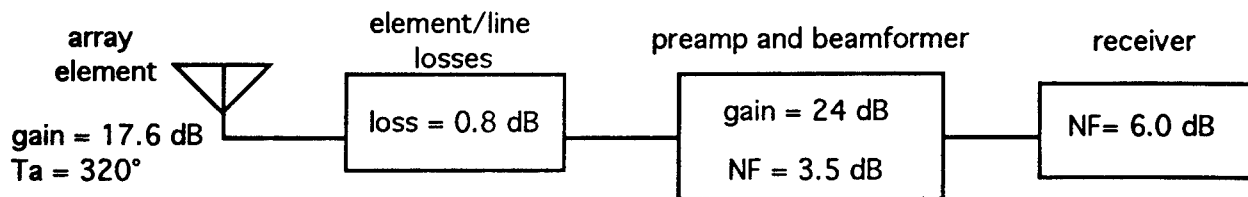
Figure 2.2.1 Satellite Receive Array G/T Model

With the values shown in the figure, the receive array G/T is 9.3 dB/°K at the maximum 9° scan position.

2.2.2 Satellite Transmit Array

- **Strawman**

  The satellite strawman transmit array requirements given in the SOW are:

  - 7.25-7.75 GHz
  - 256 elements
  - 2 wavelength element spacing
  - circular polarization
  - 4 simultaneous beams
  - 50 dBW EIRP

- **Lattice**

  The lattice for the transmit array is a frequency scaled version of the receive array.

  - element spacing = 3.05 inches in x and 1.76 inches in y
  - aperture area = 2757 square inches
  - aperture diameter = 59.2 inches
  - 3 dB beamwidth = 2.0 degrees (assuming some amplitude taper)

- **EIRP**

  The transmit array EIRP calculation are made assuming the same aperture budget as the receive array.

  - directivity = 41.7 dB
  - array gain at 9° scan = 37.5 dB
  - array transmitted power = 12.5 dBW
  - element transmitter power = .017 Watts

2.2.3 Satellite Array Beam Count

A consideration in choosing a beamformer approach for the satellite array beamformers is the number of beam positions required to cover the earth surface. Assuming a 2 degree beamwidth, approximately 61 beams are required to cover the volume assuming 3 dB crossovers. Figure 2.2.3 shows the beam position superimposed over the earth diameter. Each beam footprint has a diameter of about 1051 miles.
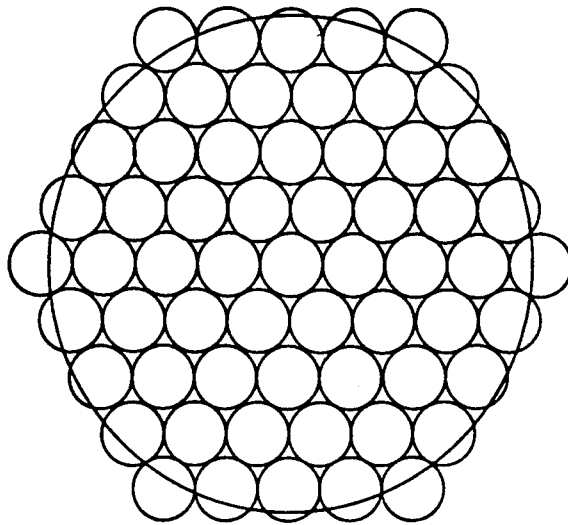
Figure 2.2.3 Satellite Array Beam Count

2.2.4 Satellite Array Patterns

Figure 2.2.4 shows the patterns of a satellite array in free space. With the wide element spacing, grating lobes are not unexpected. Several techniques for minimizing these effects could be applied to the design. The grating lobes would cause few problems with the link since they are not directed toward the earth. However, the reduced efficiency would required some adjustments.
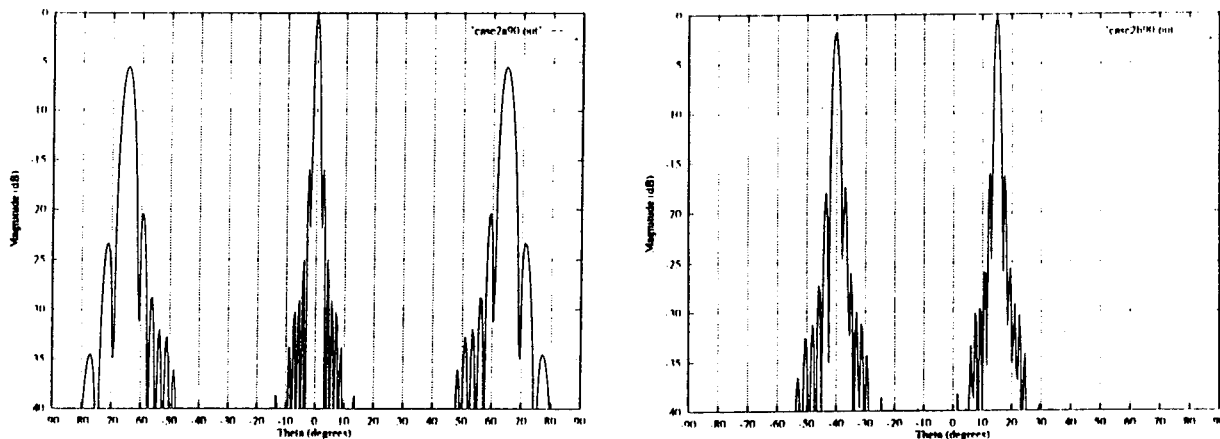
Figure 2.2.4 Satellite Array Patterns

2.2.5 Current DSCS III Array Description

The OCSSA photonic arrays are intended to increase the DSCS satellite capability. As a benchmark, the DSCS III arrays are characterized below:

Receive Array
- 61 horns feeding a passive lens
- hexagonal grid
- one beam
- multiple horn combinations for footprint customizing
- 2° beamwidth
- -5 to -6 dB crossover among three beams

Transmit Array
- 19 horns feeding a passive lens
- hexagonal grid
- 3.6° beamwidth
- multiple horn combinations for footprint customization
- -5 to -6 dB crossover among three beams

2.2.6 Satellite Array Physical Goals

The benchmark for the satellite arrays is the existing DSCS III arrays. If a photonic array that can handle four simultaneous beams can meet the current one-beam receive array cylindrical envelope, a success can be claimed.

Current DSCS III

receive array
- 100 pounds
- 60" diameter
- 45" long

transmit array
- xx pounds

OCSSA satellite

receive array goals
- 100 pounds
- 60" diameter
- 45" long

transmit array goals
- xx pounds

2.3 DSCS Link Calculations

The performance of the OCSSA antenna designs in the DSCS system is calculated in an end-to-end link model. Characteristics of the user's airborne terminal, the appropriate DSCS transponder, and a selected ground terminal are all used in the model.

For the purposes of OSCCA calculations, a pair of ground terminals was selected to help bound the performance. In addition, two satellite performance numbers were used in the calculations: existing DSCS III and a transponder of the same performance with the OSCCA satellite arrays.

- **Ground Terminals**

AN/TSC-86

EIRP = 77.7 dBW

G/T = 27 dB/°K

AN/WSC-6

EIRP = 61.0 dBW

G/T = 12.5 dB/°K

- **Satellite Configurations**

<u>DSCS III</u>
EIRP = 34 dBW
G/T = 31.5 dB/°K
Transmit gain = 24.7 dB
Receive gain = 30.4 dB

<u>OCSSA</u>
EIRP = 50.0 dBW
G/T = 28.2 dB/°K
Transmit gain = 37.5 dB
Receive gain = 37.5 dB

- **Link Calculation Results**

The plotted results of the DSCS end-to-end link calculations for all eight permutations of satellite, ground terminal and uplink and down link versus signal bandwidth are shown in Appendix B. To effect a comparison table, the bandwidth of each link permutation that has 0 dB margin was selected and entered into Table 2.3.

Table 2.3 DSCS Bandwidths at Zero dB Margin

satellite	ground terminal	aircraft transmit bandwidth	aircraft receive bandwidth
DSCS III	AN/TSC-86	1600 kHz	13 kHz
DSCS III	AN/TSC-6	900 kHz	13 kHz
OCSSA	AN/TSC-86	14 MHz	500 kHz
OCSSA	AN/TSC-6	14 MHz	500 kHz

Two comments can be made about the results. First, the aircraft transmit bandwidth to the DSCS III is limited by the satellite and ground terminal. Second, the aircraft transmit bandwidth to the OCSSA satellite and the aircraft receive bandwidths to both satellites are limited by the airborne array.

3.0 Photonic Technology Assessment

This section describes the technology tradeoffs which are available when choosing the photonic components for a phased array system design. The general form of a photonic link is shown in Fig 3.0.

```
┌─────────────┐              RF from
│   Signal    │              Antenna
│   Laser     │              Element
└─────────────┘                 │
       │                        │
       ▼                        ▼
┌─────────────┐         ┌─────────────────┐
│  Modulator  │◄────────│       RF        │
│             │         │  Preamplifier   │
└─────────────┘         └─────────────────┘
       │
       ▼
┌─────────────┐
│  Photonic   │
│ Processing  │
│(Beamforming)│
└─────────────┘
       │
       ▼
┌─────────────┐              RF
│Photodetector│─────────►    to
│             │              Terminal
└─────────────┘
```
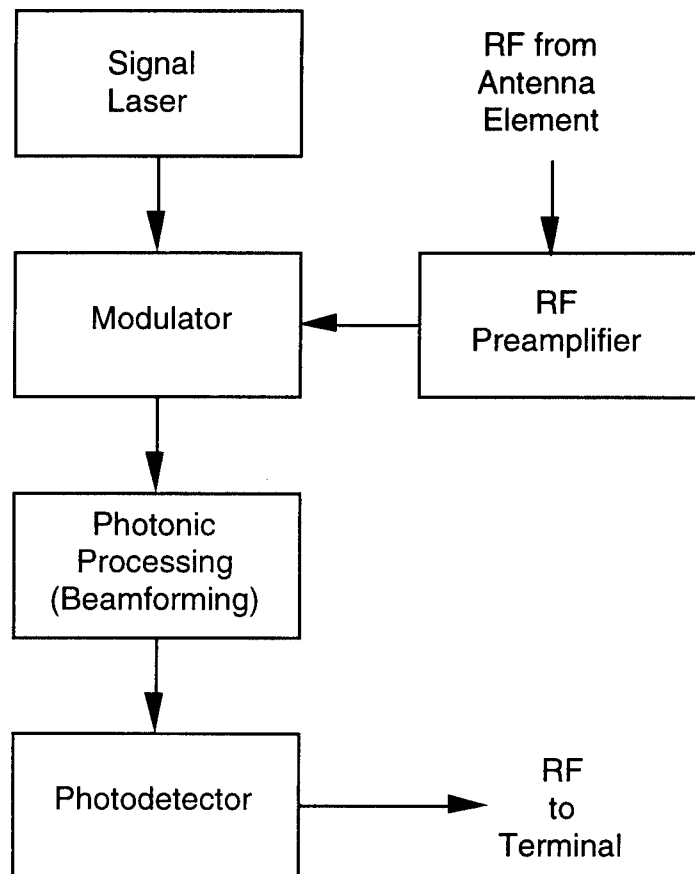
Figure 3.0   Photonic Link Model

The link consists of six components or subsystems:

1. Microwave preamplifier-to make up for link loss and preserve
    noise figure

2. Laser - to provide the optical carrier

3. Modulator- for imposing the microwave signal on the light

4. Photonic Processor (Switch network or phase shift network)

5. Distribution elements- (fibers)

6. Photodetector- for converting the modulated light back to
   microwave signals.

In the system analysis the preamplifier laser, modulator, detector combination is treated as a communication link which is characterized by noise figure, one dB compression point and microwave loss. The switching and delay components can be analyzed separately to determine their optical loss and their impact on the amplitude and phase response of the optical link.

The actual tradeoffs must be performed in an iterative manner when the detailed design stage is reached because of the strong interaction between various component selections. These tradeoffs are made in consideration of the overall system impact as related to system performance, power, size, weight, and reliability.

An additional critical component , especially for the satellite array is the spatial light modulator (SLM). The technology discussion on the SLM is deferred to Section 5.3.3. The SLM, more than any other photonic component, requires technology advances viable in the proposed design in Section 5.0 The remaining components discussed in this section are selected based on nearer term performance expectations.

3.1 Preamplifier

The range of parameters available for the system design dictate an insertion loss for broadband photonic networks of approximately 20-40 dB. In order to achieve an overall noise figure of 4 dB a preamplifier with gain exceeding this loss must be provided. MMIC preamplifier technology is an essential element of the overall photonic link technology.

3.2 Laser

There are a wide variety of laser choices available to provide carrier power for photonic systems. The driving requirements affecting laser selection are: laser noise (RIN or "Relative Intensity Noise"), available wavelength, power efficiency, size, weight, and environmental sensitivity. Two broad categories dominate the laser trade off; semiconductor diode lasers, and diode pumped solid state lasers.

Diode lasers, as a class, are better than diode pumped solid state lasers in the areas of efficiency, size, weight, and environmental robustness. However, presently available diode lasers frequently fall short of system requirements in noise level (RIN) and broadband linear modulation capability.

Laser sources with 30 to 50 milliWatts of fiber coupled power with a relative intensity noise level of less than 150-160 dB/Hz are generally available.

The diode pumped YAG is available in three configurations: Nonplanar ring, rod, and microchip. The non planar ring is a mature, commercially available technology which lies in the commercially important 1.3 micron wavelength range. Another attractive and viable source a strained quantum well diode laser operating at 0.98 micron. This is a simple, efficient device.

However, It does pose risks associated with photorefractive damage, marginal RIN performance, and non "standard" wavelength.

The microchip YAG laser is also a viable choice. It features small size and simplicity of this design. The microchip is commercially available at a power level of 25 milliWatts at the present time.

3.3   Modulator

The most widely used modulation method for phased array applications is intensity modulation. That is, the laser power is modulated in direct proportion to the microwave signal strength. Power or intensity modulation has the advantage that the receiver is unaffected by the phase or frequency of the received light. This insensitivity to phase is important because of the long delay paths involved in typical antenna systems. Coherent modulation schemes, those requiring optical phase integrity, are seldom used unless optical phase manipulation is an integral and essential part of the antenna processor. This is because of the complexity involved with optical phase recovery/compensation and the minimal link performance improvement offered.

3.3.1   Direct vs External Modulation

A simple method of producing intensity modulation is modulation of a diode laser by modulating the drive current. Since, to first order, the light power output is linearly related to the current above threshold, a linear power modulation results. However, the design parameters for the laser are restricted by requirement to produce a broadband, low noise, linear source. Because of these restrictions directly modulated laser sources with acceptable linearity and RIN levels are not available at power levels above 10 milliWatts. The sources available above 10 milliWatts have poor RIN performance. They also present severe impedance matching difficulty when one must design for low insertion loss and to meet tight amplitude/phase budgets. Typical values for the real component of driving point impedance for laser diodes is approximately 5 Ohms. These devices are widely used in TV transmission systems operating in the low GigaHertz frequency range.

In the final analysis, the high RIN noise for devices operating in the 10 GHz frequency range, coupled with unstable and nonuniform (from device to device) impedance characteristics forces the choice to indirect modulation techniques.

A much broader range of laser types is available for use in an externally modulated system since there is no requirement to design good modulation characteristics into the laser itself.

3.3.2 External Modulator Design Trades

There are several technologies for producing a broadband external modulator but The choices narrow quickly to semiconductor and lithium noibate material systems when a restriction of commercially available technology is applied. A lithium niobate waveguide Mach-Zehnder structure is the clear choice for the external modulator because of its technical maturity, proven

performance, availability, and design flexibility.

A diagram of a waveguide Mach-Zehnder modulator is shown in Fig. 3.3.2-1.
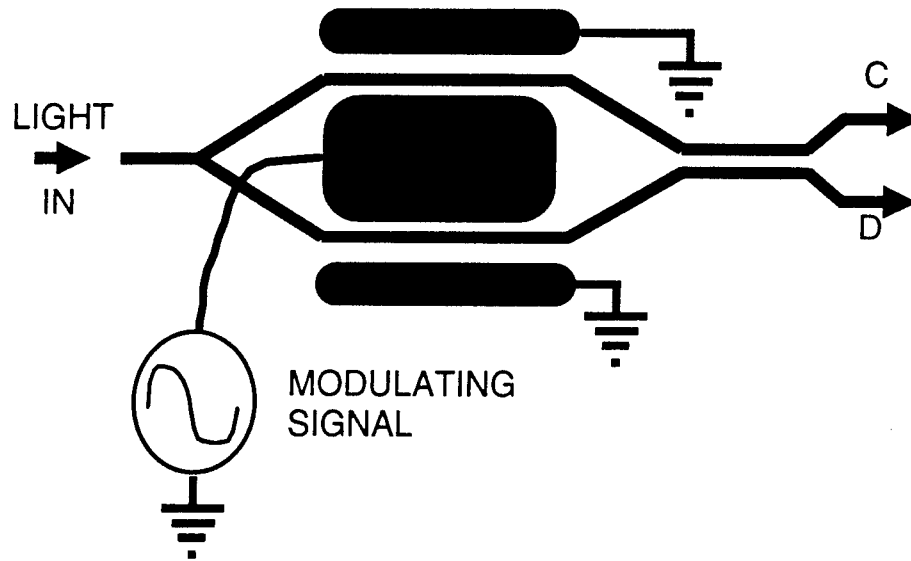
Figure 3.3.2-1 Waveguide Mach-Zehnder Modulator

This device is conventionally implemented as a pair of waveguide electro-optic phase modulators in a balanced bridge or interferometer configuration. The interferometer structure is symmetric while the phase modulators are driven with an antisymmetric field distribution. The modulating electric field is parallel to the crystal z axis on one side and antiparallel to the z axis on the other side.

There are two basic forms in widespread use: the first is implemented on z-cut lithium niobate (crystal z axis normal to the surface) and the second is implemented on x-cut lithium niobate (z axis parallel to the surface). In both cases the z axis is normal to the optical waveguide. The cross section of the z-cut and x-cut modulator designs are shown in Figure 3.3.2-2.
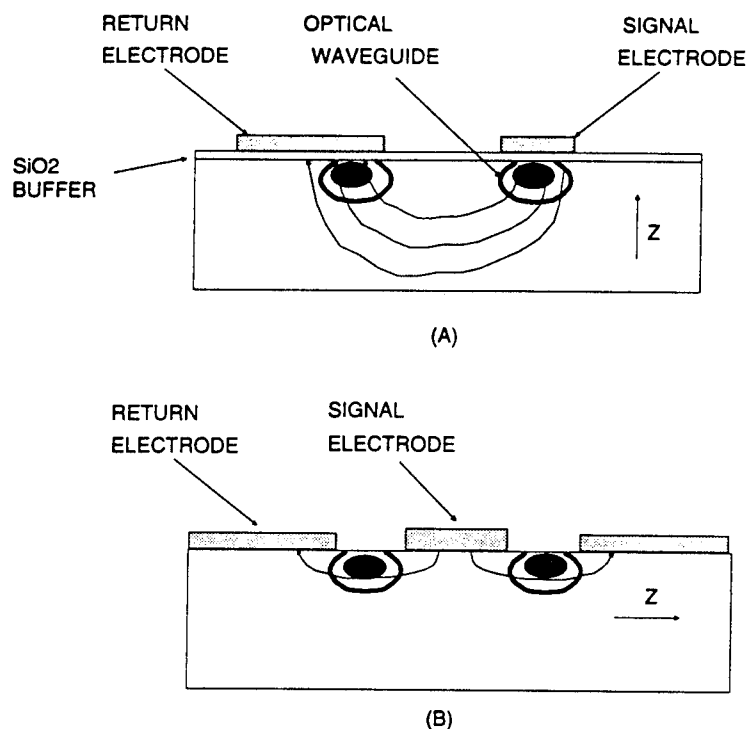
Figure 3.3.2-2   Z and X Cut Modulator Designs

The field generating electrodes are in the form of a coplanar strip transmission line. The x-cut design uses a center conductor placed between two closely spaced optical waveguides with return electrodes on the opposite sides of the waveguides. The z-cut configuration uses a signal electrode on top of one waveguide and a return electrode on top of the second waveguide.

For low frequency applications where the electrode length is short compared to the electrical wavelength on the transmission line, the electrodes may be driven as simple capacitive elements. When the electrode length is comparable to the wavelength the system must be treated as a transmission line and, for good electrical performance, the line must be terminated in its characteristic impedance. Furthermore, for good modulation bandwidth the velocity of the wave on the transmission line must be matched to the velocity of the light propagating in the underlying waveguide. The degree of phase modulation produced is proportional to the electric field strength in the optical waveguide region times the length of the interaction region.

A number of phase velocity matched modulator designs have appeared in the literature and some are available as commercial products. Notable among the published designs are one published in January '93 Photonics Technology Letters by Noguchi of NTT Corporation[2]. The NTT modulator had a 40 GHz bandwidth and a Vpi value of 4.2 Volts at 1.55 microns. (equivalent to 3.5 volts at 1.3 microns)

Also Bulmer and her co-workers at the U.S. Naval Research Laboratory[3] have produced modulators with Vpi equal to 7 Volts at 10 GHz and 15 Volts at

40 GHz. The design and fabrication technology for these modulators is clearly established. Our strategy for the demonstration system is to perform a custom design which is optimized for the bandwidth, center frequency, and link characteristics peculiar to this specific problem. We will use fundamental design rules developed on IR&D to achieve a considered balance of characteristic impedance, velocity match, clean RF response and low drive power. We are developing technology on IR&D for an advanced concept modulator which will outperform any presently available design.

The challenge of an optimum modulator design is to achieve the maximum phase shift (E times length) with the minimum microwave power while maintaining an acceptable impedance level for matching to a 50 Ohm microwave system.

A good modulator design must be a balance of the following considerations:

1. Electric field overlap; The electric fields outside the waveguide region must be held to a minimum since these fields carry power to the load but produce no electro-optic modulation.

2. Velocity match;

3. Electrical attenuation; Since lithium niobate has a dielectric constant of approximately 30 the currents in the electrodes are relatively large and attenuation in the electrodes is not negligible. When a good velocity match is achieved the electrode length is limited by the microwave attenuation for typical broadband modulators.

4. Input impedance; The transmission line in the z-cut modulator design typically has a characteristic impedance in the vicinity of 30 to 40 Ohms while the x-cut design tends to be in the range of 20 to 30 Ohms. Either design usually has a lower than ideal impedance.

3.4   Switch Network

The switch network consists of a set of switch arrays with interconnecting fiber delays. Two interacting aspects of the switch network tradeoffs are the switch technology itself and the architecture or topology of the network.

3.4.1 Optical Switch Technology

The technologies available for light wave switching include bulk electromechanical devices, membrane devices, acousto-optic deflectors, semiconductor switches and electro-optic waveguide switches.

Bulk electromechanical devices such as moveable mirrors, and moveable fibers have response times in the tens of milliseconds. Therefore they are too slow for many phased array applications.

Membrane devices have switching times in the 10 microsecond range. This switch technology is not yet mature enough to be used in present day system applications.

Acousto-optic deflectors have not been developed in the specific configuration needed for the switch. A preliminary analysis shows that approximately 100 milliWatts of RF drive power would be required for each stage of switching. Also there is considerable technical risk in the mechanical alignment, and mechanical stability in these non integrated devices.

Semiconductor switches could either be switchable gain devices or "passive" electro-optic switches. The active gain type devices are too immature for consideration at this point. Electro-optic semiconductor switches are more lossy than their lithium niobate counterpart. Also the fiber connection losses are considerably higher and the state of technical development is not mature.

Electro-optic waveguide switches in lithium niobate are the chosen technology for the most photonic switching applications. This is a relatively mature technology in that large switch arrays (up to 16X16) have been produced. Arrays of this type have been demonstrated which meet the crosstalk, switching speed, and throughput requirements for the antenna true time delay systems. Switching speeds are limited by the drive electronics and values in the 10 nanosecond range are readily achieved. Demonstrated crosstalk ratios for packaged devices are in the 20 to 30 dB range. Switching voltage is in an acceptable range of 10 to 30 Volts. Optical throughput loss is in the 3-5 dB optical range for a single 4X4 switch array or 14 dB for a (six bit) cascade of four 4X4 switches with three banks of fiber delay lines.

3.4.2 Switch Crosstalk Requirements

The reflections at fiber-switch interfaces will be held to less than 50 dB optical so that their contribution to amplitude and phase ripple will be negligible. The switch crosstalk or leakage from the desired signal path into spurious paths cannot be held to so low a level. The switch leakage into a nominally "off" path is anticipated to be in the range 20 to 30 dB optical without bias adjustment. A computation (given in the following section) of the requirement shows that the leakage must be below 23 dB. This value is just on the margin so that bias compensation may not be needed. This need will be determined by the actual switching devices procured on the demonstration program. Our design must allow for some bias adjustment at the present stage of development. We also plan to explore some laser line spreading techniques which could reduce the effect of switch leakage to a negligible level.

The model for analyzing the effect of switch isolation is shown in Figure 3.4.2. The desired signal component with delay, D, has added to it a spurious with no delay. The optical power level of the spurious component is I2 as compared to the desired signal component, where I is the optical isolation of a single switch element. The spurious component is reduced by I2 because it must traverse two switches in going through the spurious path. To determine the effect of this spurious signal on the amplitude and phase of the power envelope at the output one must take the coherent interaction of the two light signals. The two powers cannot be simply added together except under very special circumstances.

E FIELD INPUT $E_{in} = (1+(m/2)\cos(\omega_m T)\cos(\omega_c T))$

α is power leakage coefficient

E field output $E_{out} = (1+(m/2)\cos(\omega_m(T-D))\cos(\omega_c(T-D)))+$
$\alpha(1+(m/2)\cos(\omega_m T)\cos(\omega_c T))$

$P_{out} = E^2$

In Band Terms in Pout are:

$P_{ib} = m\cos(\omega_m(T-D))\cos^2(\omega_c T)+m\alpha\cos(\omega_m T)\cos(\omega_c(T-D))\cos(\omega_c T)$

$P_{ib} = (m/2)[\cos(\omega_m(T-D))+\alpha\cos(\omega_m T)\cos(\omega_c D)]$

Maximum Phase Error = α
Maximum Amplitude Error = $1+\alpha$
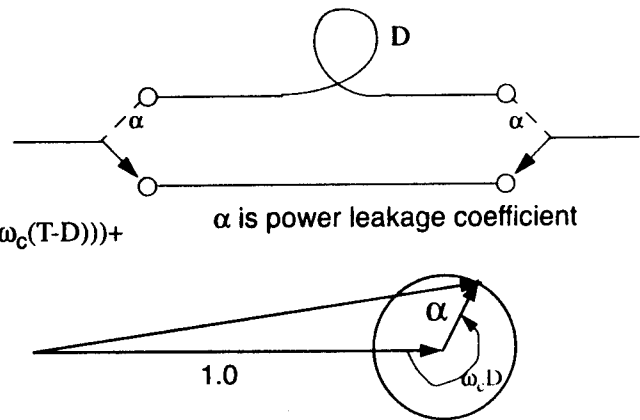
Figure 3.4.2 Switch Isolation Model

The light power in the desired signal is

$$S(t-D) = (1+a\cos(wm(t-D)))\cos(wl(t-D))$$

Where a is the depth of modulation, wm is the microwave radian frequency and wl is the light radian frequency. The electromagnetic field strength associated with this power is (in a small a approximation)

$$Ed = (1+a/2\cos(wm(t-D)))\cos(wl(t-D)).$$

The corresponding field strength of the spurious light is

$$Es = l(1+a/2\cos(wmt))\cos(wlt)$$

The resultant light power is the square of the sum of these two field values.
We now collect in band terms and drop out of band terms to determine the in band output power, Pib.

$$Pib = a/2\cos(wm(t-D))+l\cos(wlD)(a/2\cos(wmt)+a/2\cos(wm(t-D))).$$

This basic equation is essential to the quantitative understanding of the switch induced phase and amplitude ripple in the system frequency response. The right hand term in the Pib equation is the perturbing term caused by the switch leakage. It applies to each delay branch in the system. When there are multiple paths the leakage terms from each path will add together directly to first order.
A similar discussion applies to the computation of amplitude ripple. To analyze this we must focus in both parts of the spurious signal term. The first part,

3-8

$$Icos(wID)(a/2cos(wmt))$$

is undelayed. Therefore it will cycle in and out of phase with the delayed signal to create a sinusoidal amplitude ripple. The rms value of this ripple is 0.87I as it was in the phase ripple calculation.

3.5 Photodetector

The photodector is a very important element of the design. The chosen technology is an indium gallium arsenide PIN photodiode. For the 1.3 micron wavelength this has a quantum efficiency in excess of 70%. Avalanche photodiodes were dismissed because of problems of circuit complexity, stability, and minimal potential for performance improvement over the chosen PIN diode.

The interface circuit is one of the more critical design issues when stringent amplitude and phase characteristics required.

4.0   Airborne Array Design

The OCSSA airborne arrays are defined to have low risk and a minimum amount of hardware. The airborne arrays are a near-term application and are designed to achieve as much performance as possible and still be physically competitive with current RF array designs

To derive the architectural definition of the airborne arrays, several assumptions have been made:

- The receive and transmit array architectures are assumed to be identical. Thus the block diagrams and physical descriptions are essentially the same.

- The arrays are assumed to be symmetrically mounted along the top centerline of the airframe.

- The spacing between the arrays is TBD.

- The array face is flat and integrated into the skin with a radome. The small size of the aperture and the large diameter of the airframe limits the deviation form conformal. The flat face reduces array costs because it requires only a different mounting frame and radome to fit on other aircraft.

- For the current example, only one ring of dummy elements is shown around the active aperture. This is a minimum correction for array edge effects and presents the smallest possible aperture. No ring would be used if the 256 element array became a subarray of a larger array. An additional ring around the outside would reduce edge effects further.

Figure 4.0 is a top level block diagram of the OCSSA airborne array system identifying the external interfaces.
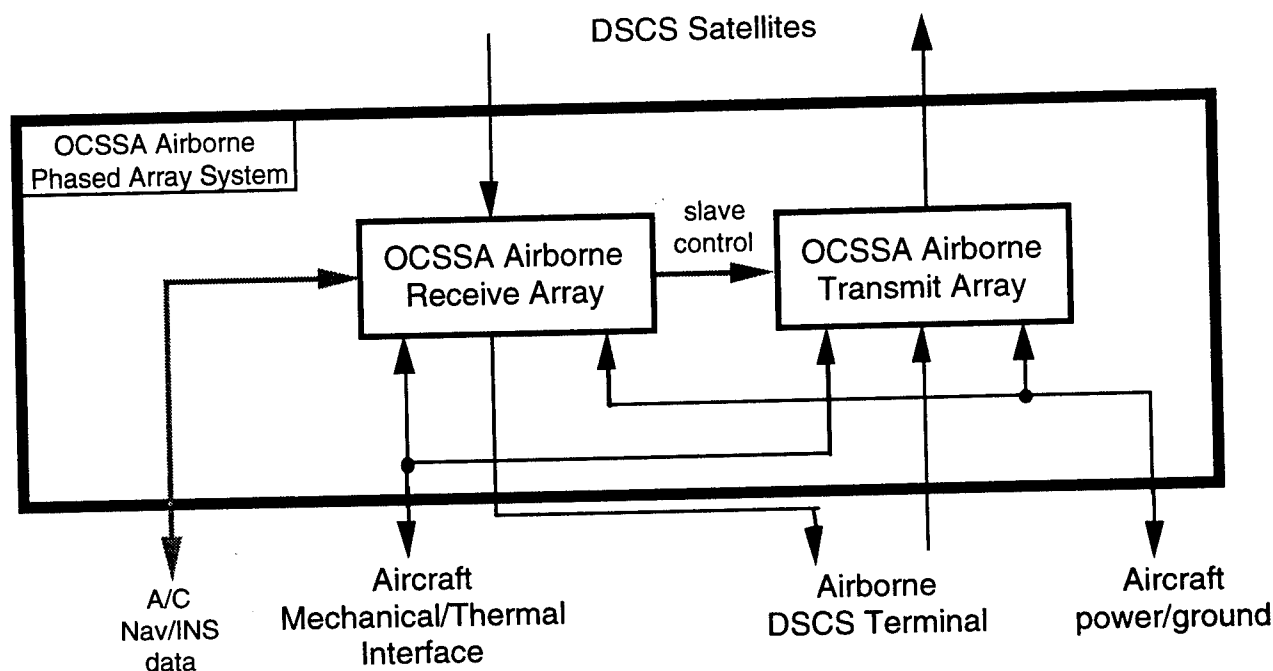

Figure 4.0   OCSSA Airborne Array System

4.1   Architecture Trades

Of the many possible design trades that are required to formulate an array baseline, three trade areas are especially pertinent to the OCSSA airborne arrays:

- wide angle scan techniques
- time delay correction
- feed technique

In the following subsections, a few notes are given on the decision processes in these trade areas.

4.1.1 Wide Angle Scan Trades

For an array to achieve wide scan capability (>60° from boresight), it must incorporate dense element packing, a non-periodic array element lattice, use non-planar apertures or multiple apertures.

- **Packing Density**

The traditional array design sets element spacing based on maximum scan requirements. As the scan volume increases, the elements must be packed more closely. High density poses two problem to this design. First, because the element count is fixed, the aperture becomes smaller as the spacing is decreased. This results in fatter beamwidths and lower gain. The second impact of closely spaced elements is the packaging and thermal problems created when elements and their RF hardware are packed closely together.

- **Aperiodic or Random Element Lattices**

When elements are placed too far apart for a given scan angle, grating lobes are created meaning multiple mainbeams. The impact on the links include less energy toward the desired direction and possible interference or jamming in the grating lobe directions. One way to avoid grating lobes is to break up the symmetries in the element lattice so the array cannot phase up in more than one direction. The element lattice can be modified either through random element location or by a more systematic, aperiodic technique.

Spreading the 256 elements using this technique results in some gain loss, higher sidelobes, and narrower beamwidths. The primary penalty paid is a more complex steering algorithm and high mechanical costs because of the reduced symmetries.

- **Nonplanar Aperture**

Modifying the apertures from planar to a spherical shape can improve the wide scanning considerably. However, changing to this shape would move the array completely into the air stream causing drag. The OCSSA arrays are defined to be conformal but that effect is only useful in the roll plane. The conformal array is planar in

the pitch plane. Additionally, the small array on a large airframes contributes only slightly to increasing the roll plane coverage.

- **Multiple Apertures**

Achieving wider coverage on an airframe often leads to multiple apertures. Using apertures on each side of the centerline can increase the roll plane coverage dramatically but the pitch plane is unaffected. Trying to increase pitch plane coverage results in fore and aft arrays that are sometimes very difficult to mount suitably.

However, even in the roll plane, two arrays mounted symmetrically from the centerline is a more expensive array because there are more total elements and, when the look direction uses one aperture, the other is "dead weight". There are adaptive techniques that could help share the apertures but the cost would still be much higher.

For the purposes of the OCSSA study, a single set of wide-scan receive and transmit arrays is selected as the baseline. The criteria is cost and complexity.

4.1.2 Time Delay Correction

One of the key advantages of photonic array feeds is the wideband capability that eliminates beam skewing and signal loss of wideband information.

Two techniques were used to quantify the delay effects on the airborne arrays. One way to quantify the effect is to calculate the S/N degradation due to energy spread and adjacent symbol interference. The loss in S/N is dependent on the bandwidth, scan angle, and aperture size. For a 12.4 inch aperture at X-band, a 6.67% signal bandwidth, and 75° maximum scan, the signal to noise loss is 0.57 dB.

An alternate technique is to quantify the pattern loss that occurs when the beam scans over the signal bandwidth. For this frequency, bandwidth, and scan angle, an array beamwidth of 6° will scan less than a quarter of its beamwidth. This translates into a gain reduction of 0.22 dB. Since the OCSSA array beamwidth is 8 degrees, the loss will be less.

The maximum delay across a 12.4 inch diameter aperture scanned to 75° is 1.02 nanoseconds. With the two above calculations, it is seen that the 256-element array does not <u>require</u> true time delay to operate over the DSCS bands. However, as future system bandwidths, both signal and system, increase in future DSCS systems, the use of true time delay will become more necessary.

4.1.3 Feed Techniques

Several single beamforming options are available to the array designer:

- constrained feeds (direct fiber or transmission line interconnects)

- unconstrained feeds (illumination of elements through free space)

- semi-constrained feeds (hybrids such as radial and constrained lenses)

A key ingredient in the selection among these options is the location of the RF/photonic interface. Figure 4.1.3 shows the set of possibilities.
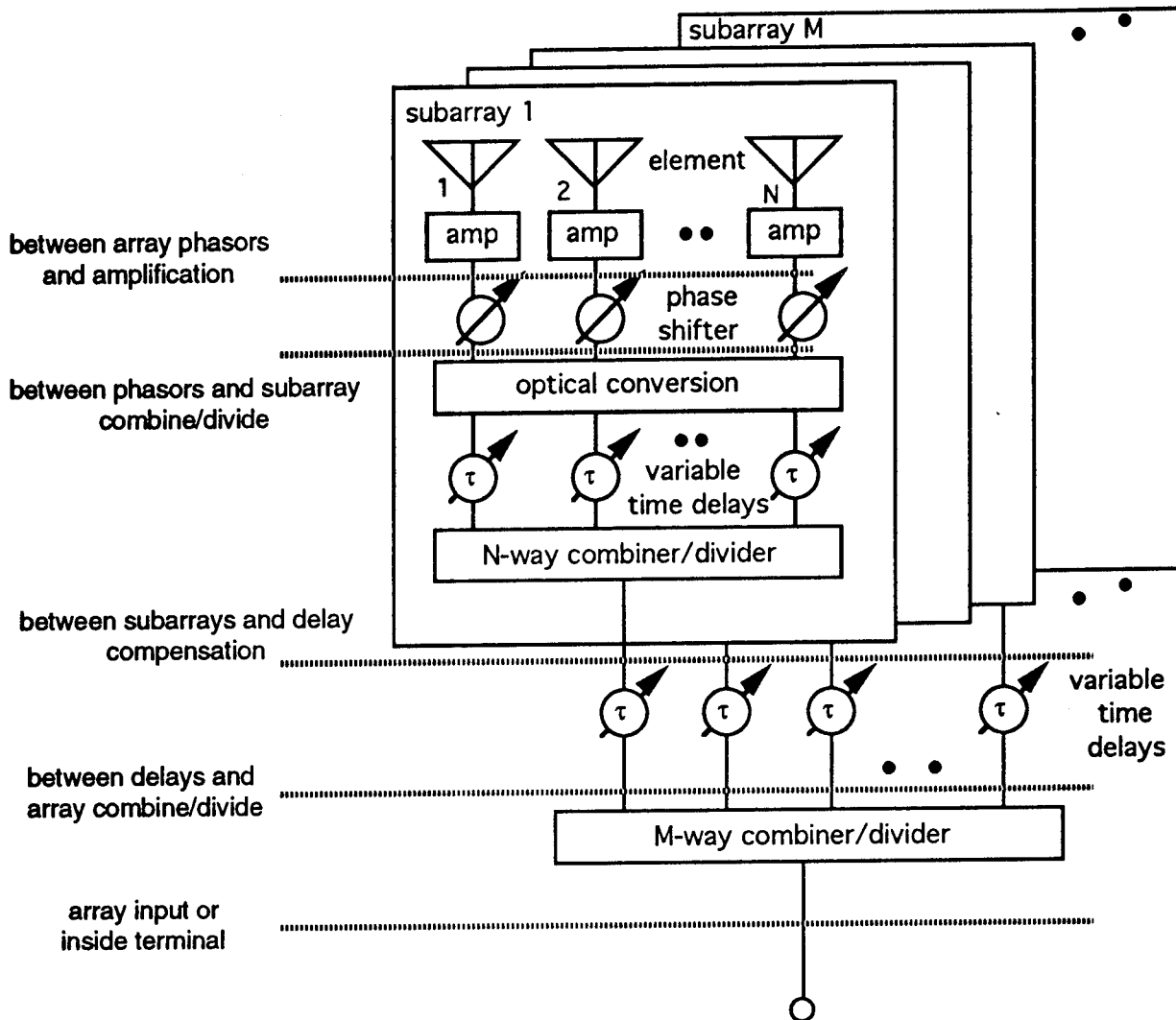
Figure 4.1.3 Photonic/RF Transition Options

For the OCSSA airborne designs, the message to maintain low complexity, low risk, and minimum hardware focused the design approach to a completely optical feed with conversion inside the element assemblies and an optical interface to the DSCS terminal. This maximizes photonic content in the array making all power division, power combining, and phasors in the optical domain.

4.2 Photonic Beamformers

Because the OCSSA study requirements specified true-time delay control of the airborne arrays, the option for the beamformer did not include photonic phase shifters. Two techniques remain, switched time delays and Fourier optic processing. As discussed at the beginning of this document, the thrust for the airborne arrays was to achieve low risk while attempting to at least compete physically with conventional RF designs.

In the literature there have been numerous discussions on ways to achieve more "hardware compression". In most of these discussions, "hardware compression" seems to mean minimizing the number of delay lines in the array. In some cases the number of delays are reduced but more sophisticated multi-frequency lasers and multiplexers are added to the hardware. The improvement in hardware compression is blurred by the addition of new hardware.

The approach taken in this study was to derive a hardware design with the absolute minimum number of passive delays and no additional hardware. The resultant beamformer has only 4 delays per element in one scan plane and 4 delays per row of elements in elevation. The array can steer to any one of 16 beam azimuth and 16 elevation positions and every delay line is switched into the beamformer all of the time. There are no pieces of hardware that are not in use 100% of the time. There is only a single optical frequency required in the beamformer.

The key step forward in the design was the use of delay matrix first discussed by Wilkinson[4] and reference in Hansen[5]. A block diagram of the matrix is shown in Figure 4.2-1. For this example, an eight element linear array is shown that can be pointed in eight directions. This beamformer uses a total of 6 delays per element to achieve the eight positions. Hardware count is 48 time delays and 48 spdt switches. Control of the matrix is extraordinarily easy because for every beam position, each row in the beamformer is set to the same position. Only three parallel control lines are necessary to switch the array to any beam position.
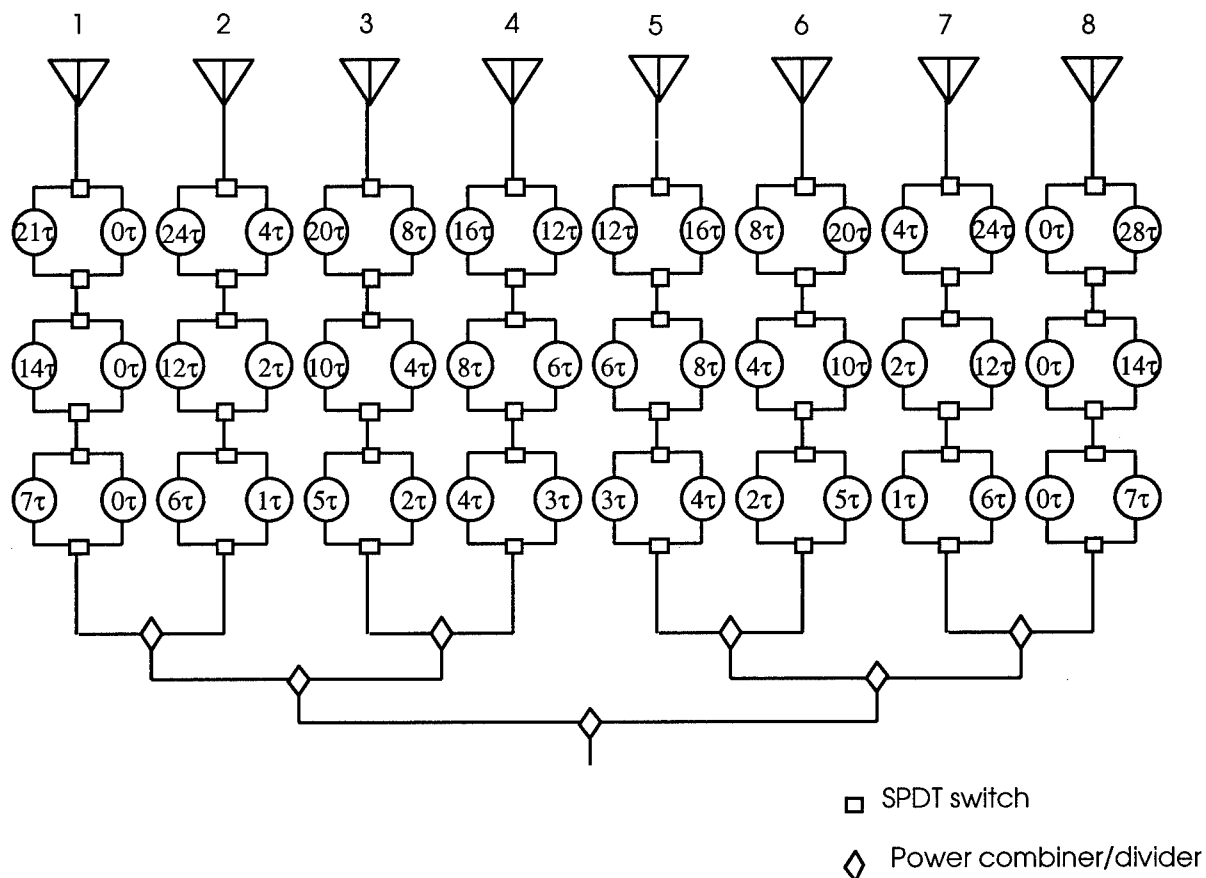

Figure 4.2-1   Wilkinson Binary Digital Delay

4-5

Despite its simplicity, an examination of the matrix shows that only 50% of the delays are used at any instant. Half of the hardware is not connected into the RF circuitry. In a conventional RF design, this is an acceptable arrangement because the phase shifter either switches in a line length or it does not. In the time delay case, the network switches in either one delay or the other. There is a much heavier penalty for unused components.

An additional simplification in the hardware can be seen if the delay networks for the outer two elements is examined. The two circuits are identical. Further study shows that at any given beam position, the delays that are not used at one end of the array are precisely the delays required by the element at the other end.

If the single pole single-throw switches are replaced by cross-bar switches, the network will create the necessary delays for two elements. If this process is continued for the rest of the elements in an even-numbered array, the network in Figure 4.2-2 is created. Now there are only 24 delays in the network and all delays are being used by the beamformer all the time.

The astute observer might notice that with an even number of elements, there can be no beam at boresight. If a boresight beam is absolutely necessary, the array requires an odd number of elements. The line feeding the center is passive containing only three passive delays.
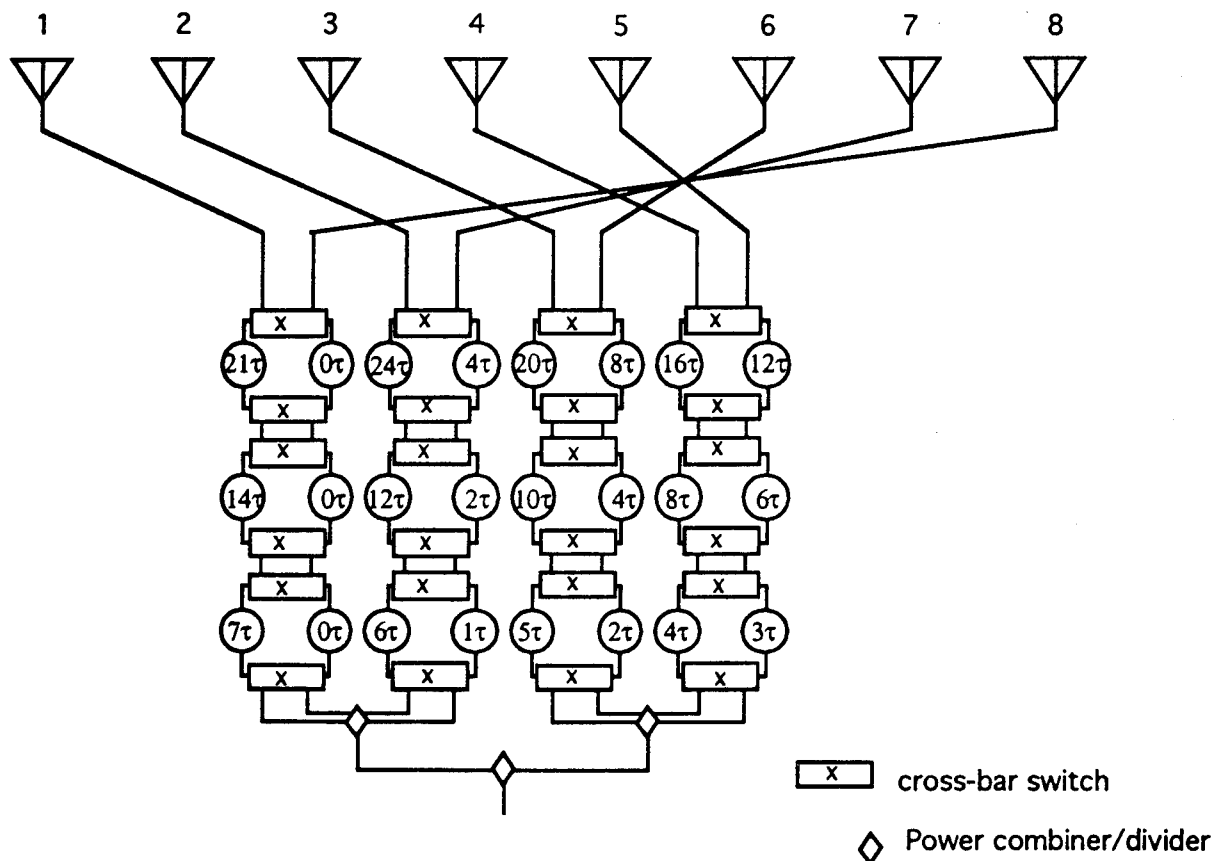

Figure 4.2-2 Full-Use Binary Digital Delay Beamformer

Throughout the photonic literature there are many techniques displayed to achieve switched time delay feed networks with minimum amount of components (hardware compression). The optical beamformer suggested for the airborne array is an extension of those concepts. By properly defining the array symmetry, it is possible to configure a set of delay networks that require only a single frequency laser and use 100% of the delays all the time. Unlike most other approaches, including most RF approaches, only 50% or less of the networks are in use at any instant. This new hardware compression minimizes the hardware overhead and gives a photonic true-time delay beamformer a chance to compete with conventional RF MMIC designs in size and weight.

The array consists of eight azimuth beamformers and one elevation beamformer. All seventeen beamformers are identical. The grouping of elements in each azimuth beamformer combines one row of sixteen elements into one beamformer. The sixteen elements are grouped in pairs to be fed by one of eight different switched delay networks in the beamformer. The elevation beamformer combines the sixteen azimuth beamformers in a like manner.

Inside each beamformer there are eight bits of delay settings meaning 16 beams in each scan plane of the array. The sum of all the delays in each different switched delay network is the same meaning physically they can theoretically be made within the same sized envelope. Each switched delay network could be implemented in an integrated circuit consisting of optical waveguide and switches.

The control scheme for the airborne array beamformer is elegant in its simplicity. At each beam position in elevation, the beamformer is fed with a four-bit word. At each azimuth position, all azimuth beamformers are in the same state meaning they also need only one four-bit word.

4.3   Baseline Definition

Based on the design studies and trades, the architecture for the airborne arrays has been selected.

A single aperture is used to minimize hardware. Better coverage might be achievable with multiple apertures, but with receive and transmit arrays already separate and the possibility of larger apertures to meet certification, obtaining sufficient surface area for multiple arrays on the airframe is unlikely.

The aperture lattice is a square grid with 16 elements in each plane. This allows the same beamformers to be used in both planes of scan.

The lattice used in the airborne arrays seems to be inconsistent with standard practice. Instead of a triangular lattice to minimize the number of elements, and therefore cost, of the array, the OCSSA airborne arrays have square grids. Using a square grid does mean about 16% more elements in a given area. This also makes the difficulty of removing heat slightly more critical because of the increased density of power in the transmit array. However, because the photonic approach moves the phasor out of the TR module, the TR module size is reduced and the phasor control interfaces to the module are no longer required.

The primary advantage of the square grid is a more modular approach to the beamformers. All of the beamformers are identical and are very hardware compressive without the need for additional lasers and offset frequencies.

A constrained, corporate feed is selected to achieve a more compact design with conventional hardware interconnects.

Photonic conversion occurs right before/after the amplifiers in the element assemblies. This achieves maximum photonic integration. Improving RF technologies have made very low-noise amplifiers and moderate output power amplifiers easily achievable for the element level conversion from optics to RF. The beamforming is done entirely photonically.

Figure 4.3 shows the array block diagram including assembly definitions and counts as well as interfaces and probable power and control distribution.
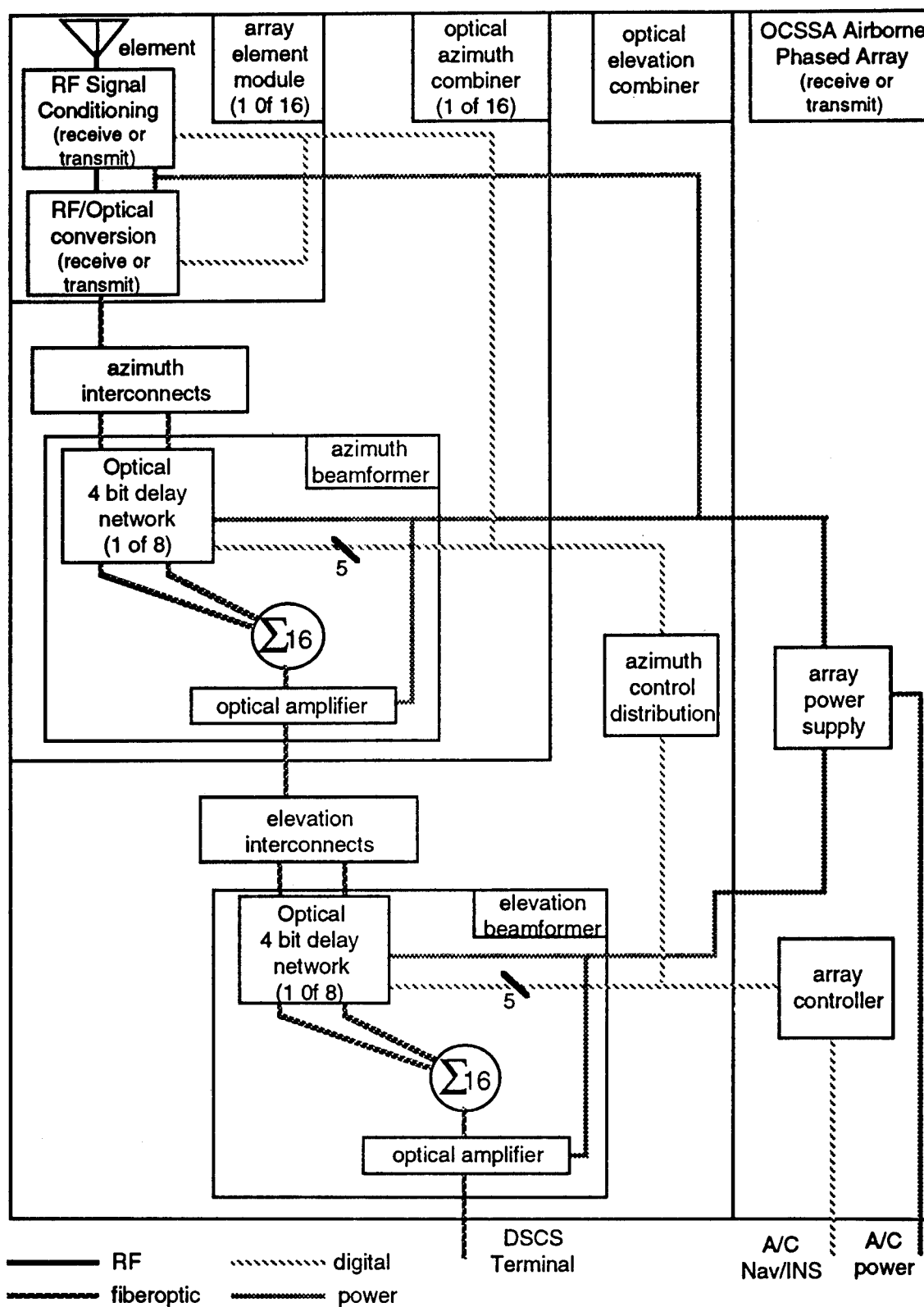
Figure 4.3   Airborne Array Baseline Block Diagram

4.3.1 Array Element Assemblies

The array element assemblies are the building blocks for the airborne arrays. These assemblies are the array cost drivers because of their cost multiplication by the number of elements. Critical importance must be placed on the low-cost and small size of all the parts in these assemblies.

The RF module at each receive array element also provides RF conditioning and optical conversion. Figure 4.3.1-1 is the definition of the receive array element. assemblies. The array element, discussed in the next subsection, requires a 90° hybrid to achieve circular polarization.

Free space

```
                    array element
                         |
                      90° hybrid
                         |
                       filter
                         |
                      limiter
                         |
                        LNA ········
                         |         :
                      Driver       :
                       Amp ······· : ············· power
                         |         :
              filter ── laser diode ········ Azimuth
                                              Interconnects
```
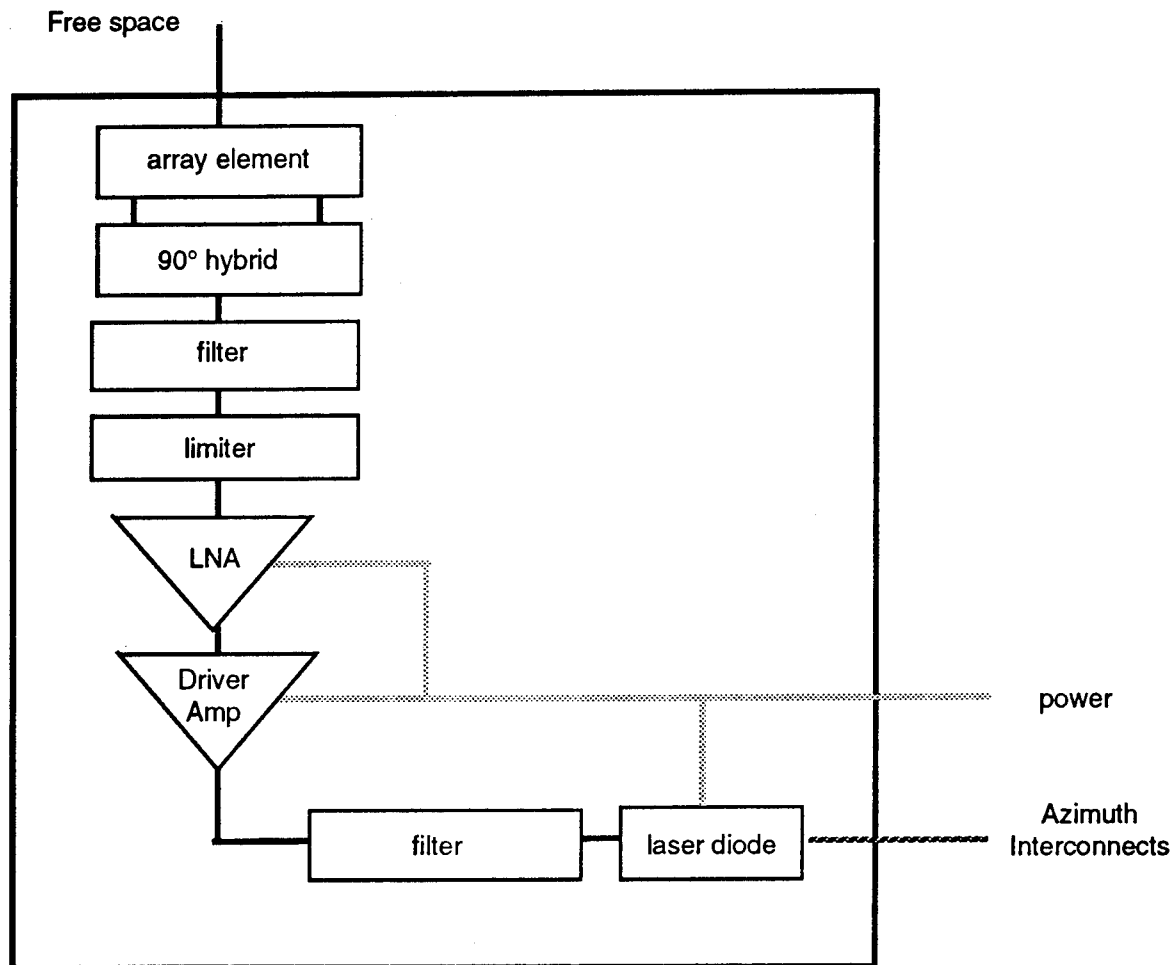
Figure 4.3.1-1   Airborne Receive Array Element Assembly

The receive path amplification consists of two stages in a typical low noise-wide dynamic range configuration. The first amplifier is an LNA with moderate gain and low noise figure. Advances in GaAs MMIC fabrication have made 1.0 dB and below noise figures achievable with yields appropriate for use in a 256 element array. The second amplifier serves two purposes: add additional gain and extend the dynamic range of the receive system through a high third order intercept point.

Filtering in the receive RF modules is also at a TBD level until more refined definitions of orientation and separation of the arrays is established. The filtering is designed to help control transmit-band power from appearing at the LNA input. Typically, this filter can require 9 poles or more. Use of limiters and physical separation of the transmit and receive arrays to achieve isolation is much more important to the receive signal path..

The receive array RF-to-optical conversion is performed by an externally modulated laser diode. At the 1.3 micron wavelength, there is ample bandwidth available on commercially available hardware to meet these requirements.

At each transmit array element, there is a RF transmit module containing RF conditioning and optical/RF conversion circuitry. Figure 4.3.1-2 is the definition of the transmit array element. assemblies. The diagram is the same as the receive array except for the photonic conversion and the amplifiers.
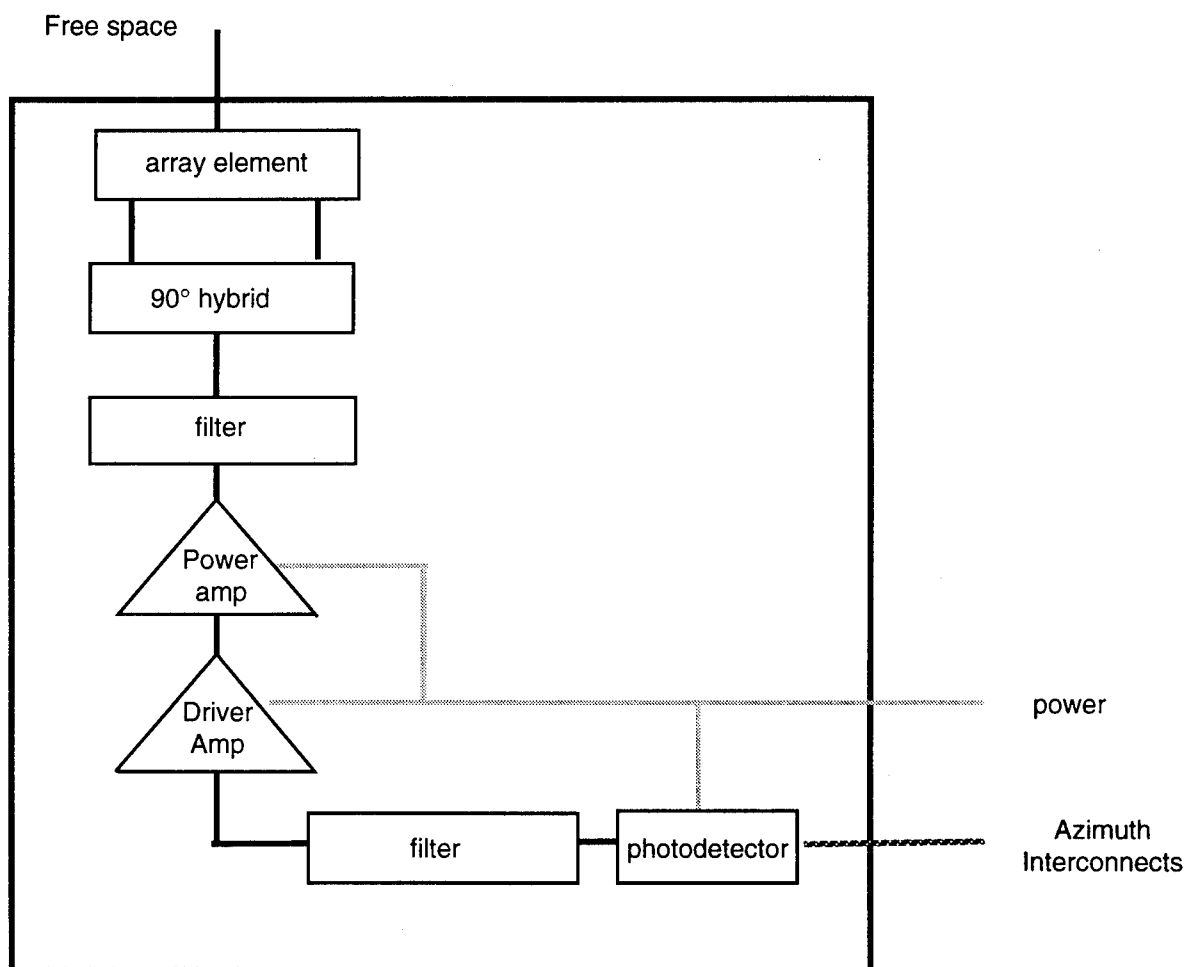

Figure 4.3.1-2   Airborne transmit Array Element Assembly

Power amplification in the transmit module consists of two stages to increase the converted optical signal to the required 3.64 Watts required at each element to meet the design EIRP.

Filtering in the transmit RF modules is still at a TBD level until more refined definitions of orientation and separation of the arrays is established. The filtering is designed to help control transmit noise and spurious images in the receive band from appearing in the output and to protect the sensitive receive channel electronics from the high transmit powers. Neither filter function is expected to require difficult designs. With sufficient physical separation of the transmit and receive arrays, much of the required isolation can be achieved without filtering.

The transmit array optical-to-RF conversion is performed by an InGaAs PIN diode. This device can be grown on the same GaAs chip as the RF circuitry producing a more integrated chip. Approximately 10 mW of optical power is required at the input of the transmit module.

4.3.2 Array Element

The element for both the transmit and receive arrays must be relatively wideband, capable of circular polarization, and maintain good pattern characteristics over very wide scan angles. Several types of elements are possible candidates including spirals, helices, patches, horns, and stacked patches. The best compromise for light weight, wide angle patterns, and low cost is the stacked patch. This element has been used in arrays scanning over 70° and its characteristics are well known. The stacked patch consists of a conventional circular patch with two feed points, a low dielectric constant spacer and a circular "director" on top of the element. Although a standard patch can only achieve a bandwidth of a few percent, use of an isolated patch like a "director" can achieve more than 10% bandwidth.
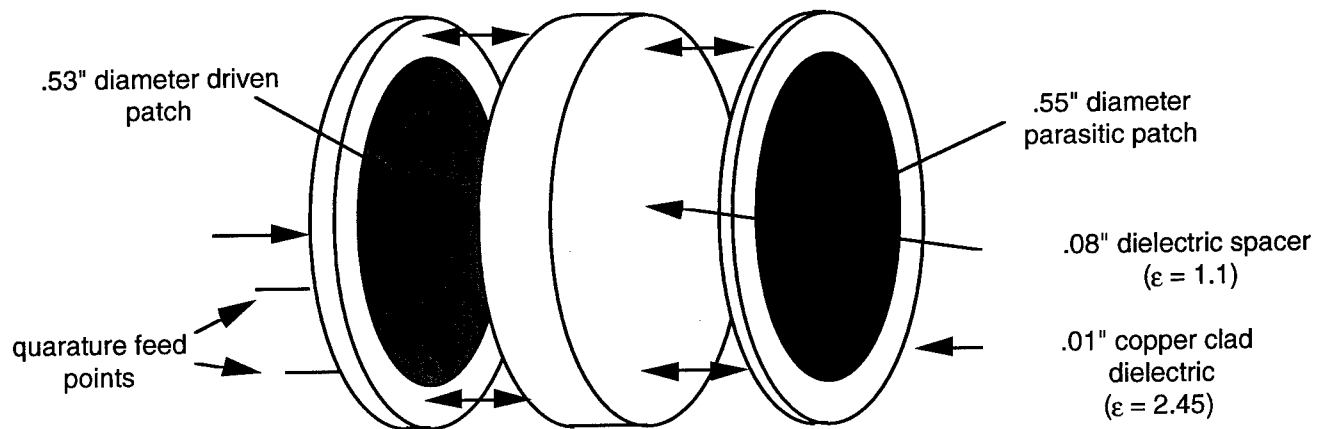
Figure 4.3.2 is a drawing of a typical element.

.53" diameter driven patch

quarature feed points

.55" diameter parasitic patch

.08" dielectric spacer ($\varepsilon = 1.1$)

.01" copper clad dielectric ($\varepsilon = 2.45$)

Figure 4.3.2 Stacked Patch Array Element
(typical X-band dimensions)

4.3.3 Beamformer

The beamformer is a four-bit, 16 element version based on the example discussion in the previous section. As remarked in Section 2, at least 14 beams are required in each plane to produce ±75° scan with 3 dB cross-overs. Therefore 4-bits are required in the beamformer. To achieve the coverage and cross-over, the command

angles are spaced equally in sine space. This results in beams in the following directions:

$$\pm 3.7°$$
$$\pm 11.1°$$
$$\pm 18.7°$$
$$+26.8°$$
$$\pm 35.4°$$
$$\pm 45.1°$$
$$\pm 56.8°$$
$$\pm 75.0°.$$

Note that because there is an even number of elements, there is no boresight beam. Figure 4.3.3-1 is a plot of the 3.7 and 75.0 degree scan plots. Plots of all beam positions to one side of normal are shown in Appendix C.
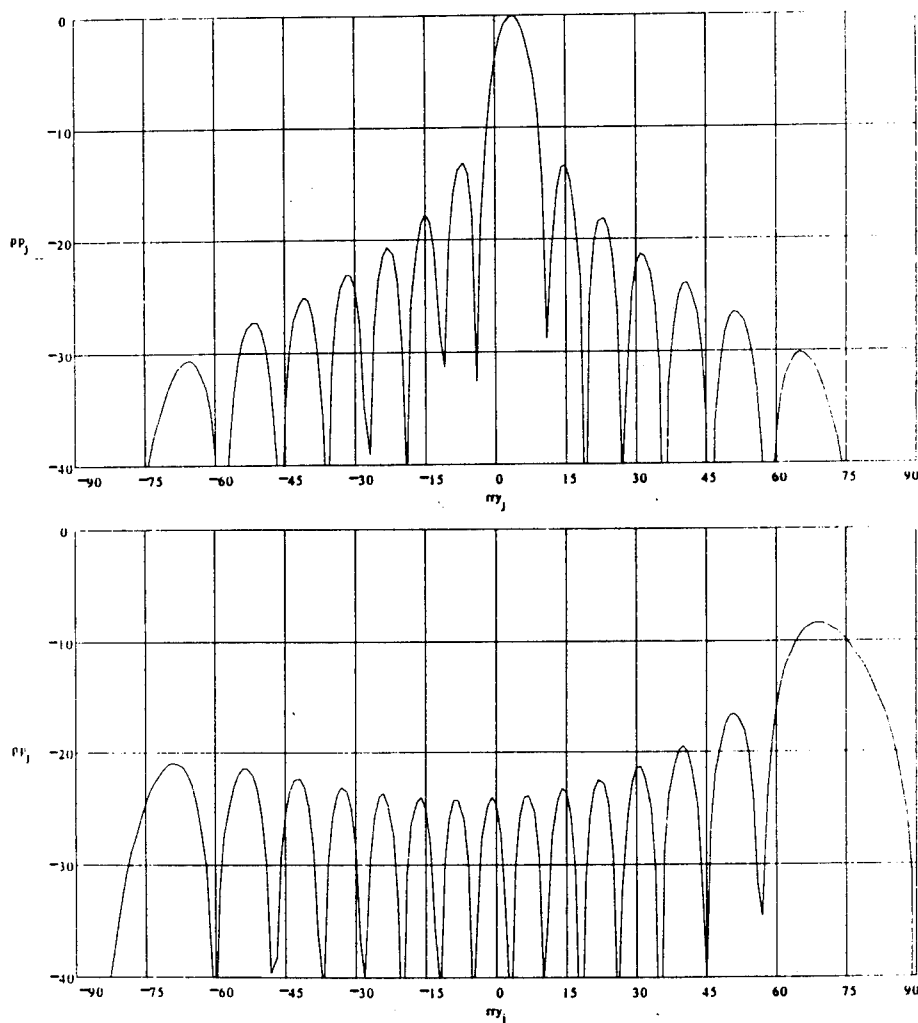

Figure 4.3.3-1   Airborne Array Scan Patterns at 3.7 and 75 Degrees

Sixteen beamformers are required for azimuth summation and a single, identical beamformer is used for elevation combining. The receive and transmit versions are identical in architecture. The receive and transmit delays are different because of the frequency difference.

Figure 4.3.3-2 shows the subassemblies of each identical 16 element beamformer. Each beamformer contains the same 8 different dual delay networks connected to a 16-way combiner/divider.
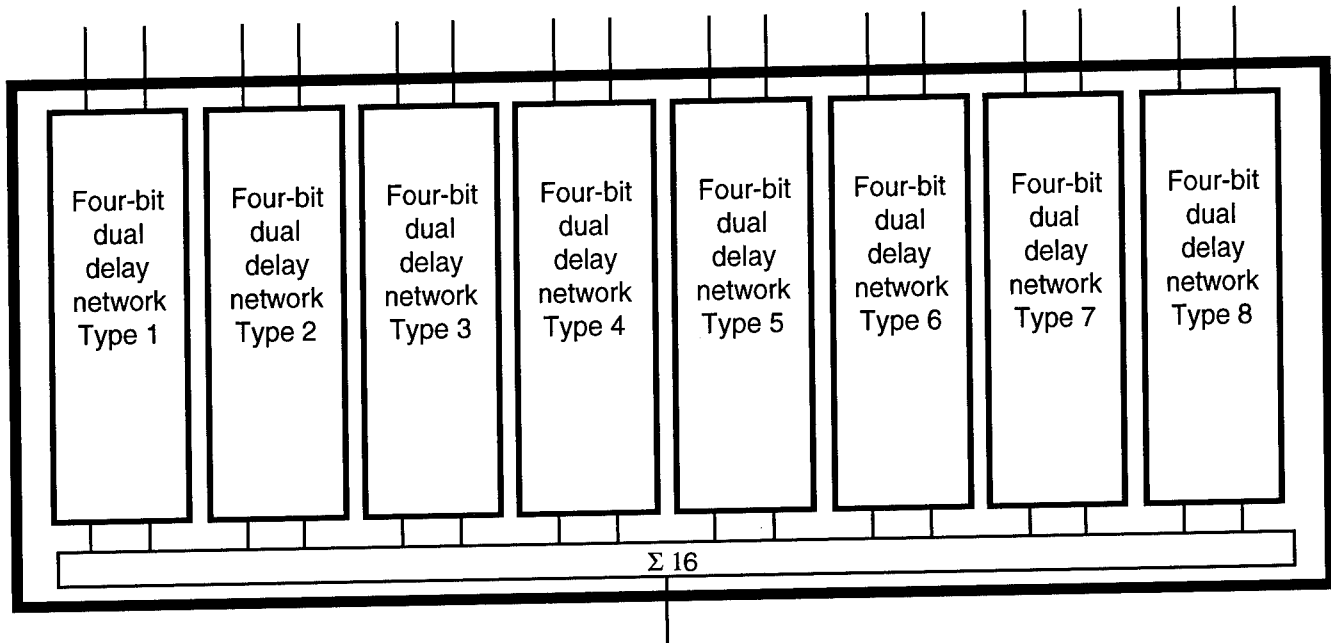

Figure 4.3.3-2   Airborne Array Beamformer

Each four-bit dual delay network is controlled by a four bit signal as shown in Figure 4.3.3-3.
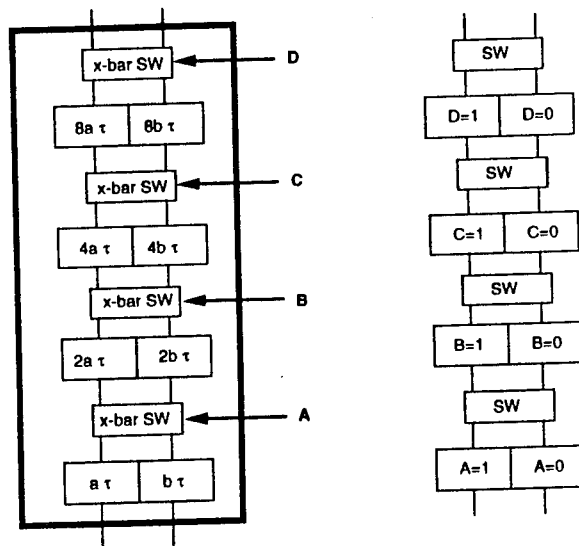
Figure 4.3.3-3   Airborne Array Four-Bit Dual Delay Network

The cross-bar switch used in the beamformers is actually only a set of four single-pole, single-throw switches. Figure 4.3.3-4 shows the assembly in both of its control states.
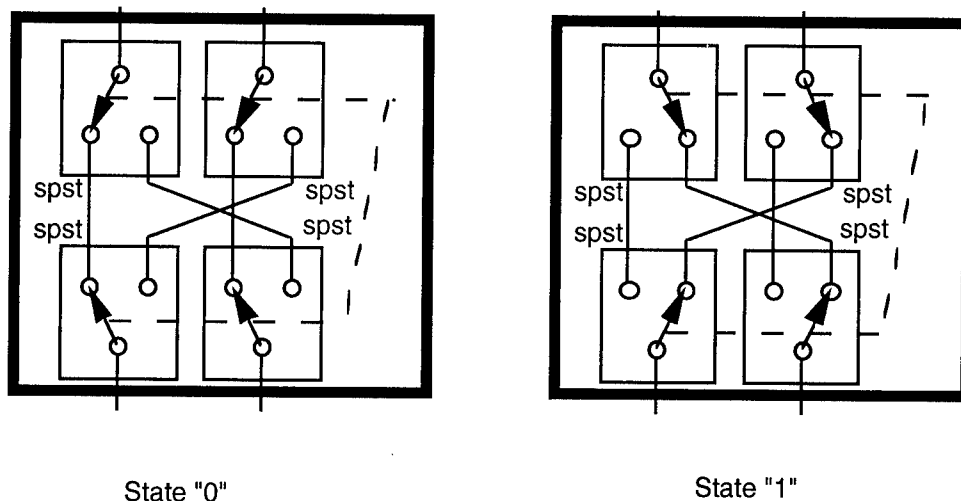

State "0"   State "1"

Figure 4.3.3-4   Two-Element Cross-Bar Switch

A 16-element beamformer with the required delays is shown in Figure 4.3.3-5. The value of tau, the smallest delay step size, is determined by the maximum delay required. At 75° scan, the maximum delay across a 12.4 inch aperture is 11.98 inches. The maximum delay in the matrix is 225 tau. Therefore, tau is 0.053 inches. For the transmit array, tau is 0.049 inches.
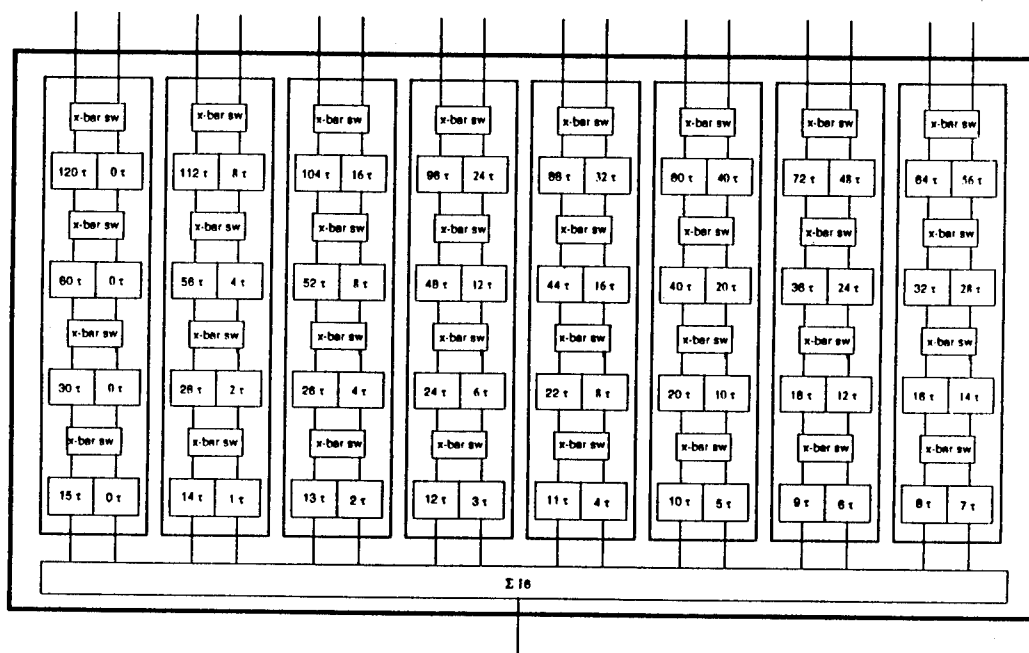

Figure 4.3.3-5   Airborne Array Beamformer

4-15

4.3.4 Controller

Because of the inherent symmetry of the airborne array beamformer, the array controller becomes very simple. Only 10 parallel wires are required to set the delays since all of the element delay networks has the same switch settings at every beam position.

Processing to determine the beam location required is also fairly easy since the host vehicle is relatively low-dynamic and the wide beamwidth means fewer switch changes. Inputs from the host vehicle will include the DSCS satellite location and the aircraft altitude, location, and attitude from the airframe GPS and INS.

4.4 Conceptual Design

The final step in the airborne array activity was to present a conceptual design of the airborne arrays using constraints relevant to a production design. Specifically, the following assumptions were made:

- subsonic aircraft
- arrays symmetrically mounted along fuselage centerline
- array face is flat and integrated into airframe skin
- operational with full solar loading while on the ground

The most significant impact on the array mechanical design is the need for external cooling. Even without full solar loading, the density of the elements and their relatively high element power demands active cooling to maintain moderate temperatures required for long life.

4.4.1 Loss Budgets

Simplified power-loss-noise figure budgets are shown in Figures 4.4.1-1 and 4.4.1-2.
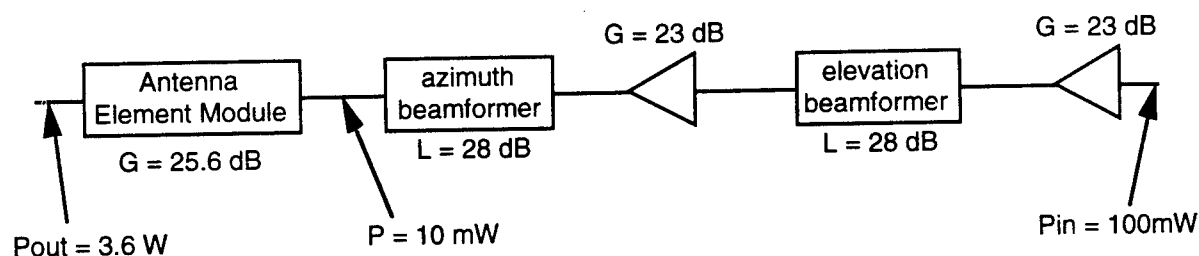

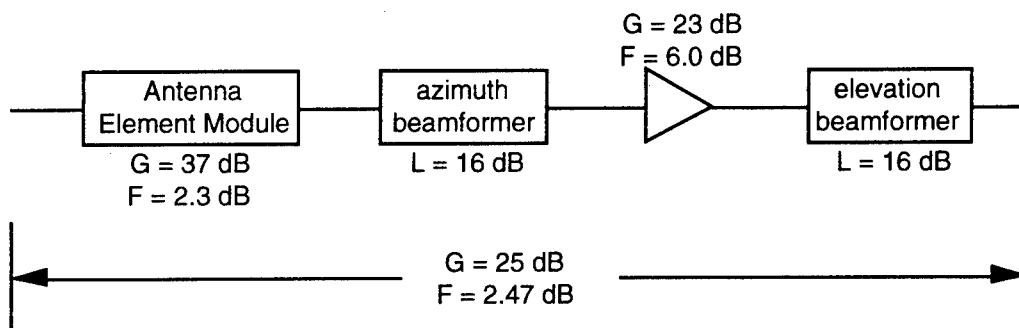Figure 4.4.1-1 Airborne Transmit Array Signal Flow Diagram

G = 23 dB
F = 6.0 dB

```
           ┌──────────────┐     ┌──────────────┐              ┌──────────────┐
───────────│   Antenna    │─────│   azimuth    │────▷─────────│  elevation   │───────
           │Element Module│     │ beamformer   │              │ beamformer   │
           └──────────────┘     └──────────────┘              └──────────────┘
              G = 37 dB            L = 16 dB                      L = 16 dB
              F = 2.3 dB
```

G = 25 dB
F = 2.47 dB

Figure 4.4.1-2   Airborne Receive Array Signal Flow Diagram

The transmit budget is relatively straight-forward with no particularly difficult requirements being levied on any of the components.

The receive budget is shown with only one level of optical amplification. This configuration results in fairly high values of gain in the antenna element module because the optical conversion losses are followed by the azimuth beamformer losses. This could easily be remedied with an optical amplifier between the AEM and the azimuth beamformer. However, the multiplication effect of the array means 256 optical amplifiers would be required at that position in the receive chain. This decision must be made with care because it has significant effects on the array size and weight. Further trades in this portion of the design will be continued in the next phase.

4.2.2 Mechanical Description

CAD drawings of the airborne arrays have been produced to illustrate how a typical final assembly might look. Since the two arrays have the same architecture and layout, only the transmit array is shown. The receive array might be somewhat smaller since it will not require as much cooling.

In Figure 4.4.2-1, the front view of the transmit array showing the array grid and overall dimensions.
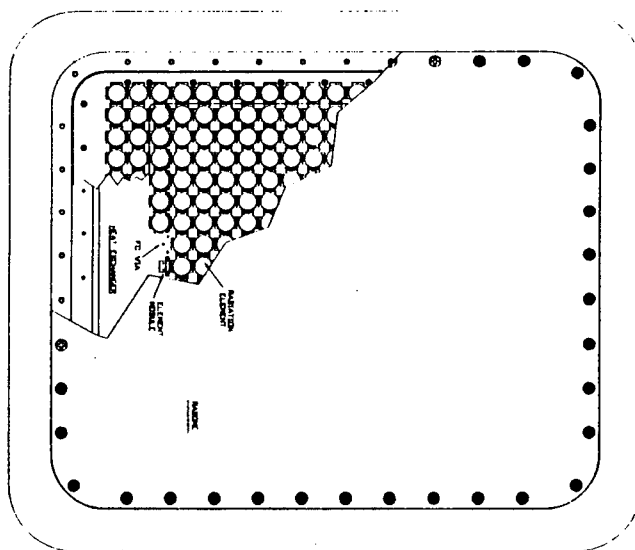

Figure 4.4.2-1   Airborne Transmit Array Front View

Figure 4.4.2-2 shows a side view with the modules and beamformer integration. A heat exchanger is placed between the element modules and the photonic beamformers to direct the coolant as close the heat sources as possible.
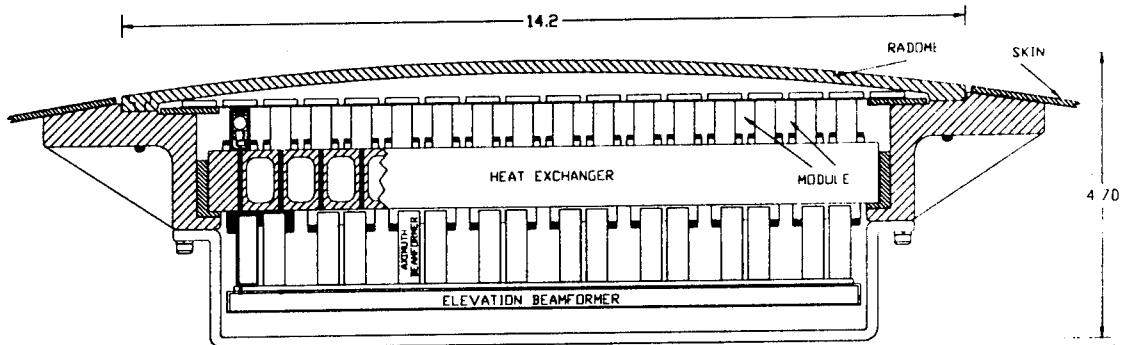

Figure 4.4.2-2   Airborne Transmit Array Side View

The array rear view in Figure 4.4.2-3 shows more detail of the beamformer integration while Figure 4.4.2-4 shows the outside details of one beamformer.
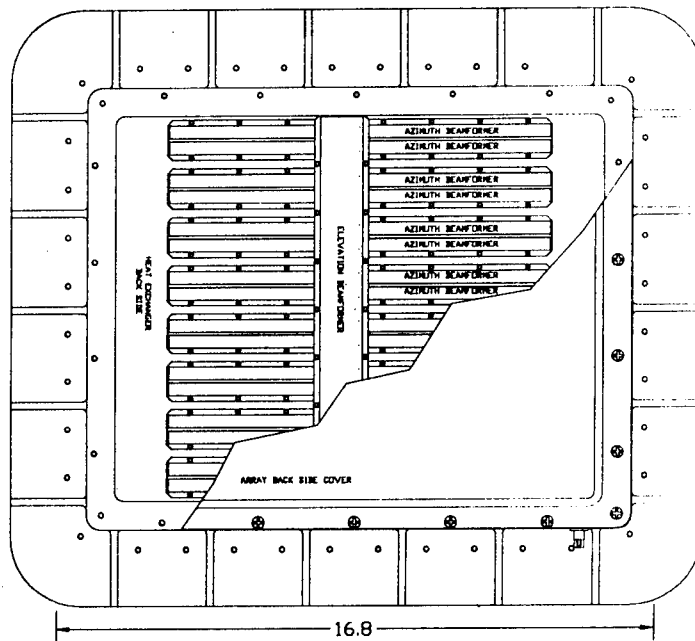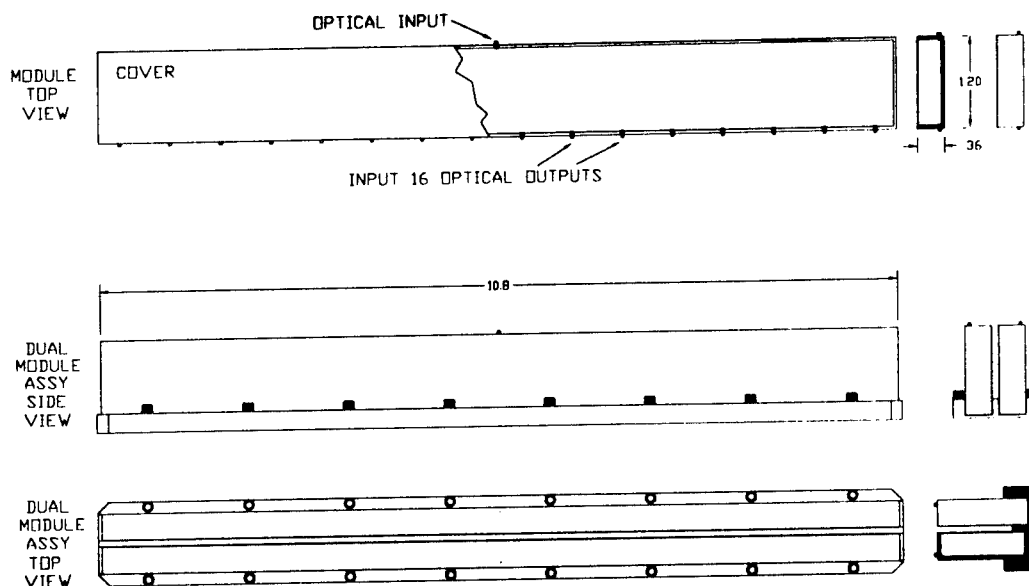

Figure 4.4.2-3   Airborne Transmit Array Rear View

Figure 4.4.2-4   Airborne Transmit Array 16-Element Beamformer

Figure 4.4.2-5 shows the integrated array element module and its assemblies. One assumption to note here is that the size of the filter assumed for this layout is relatively modest. The implied assumption is that the amount of filtering required in either transmit or receive arrays is not extraordinary. A more complex filter would make the element module get longer and therefore the array package would get thicker.
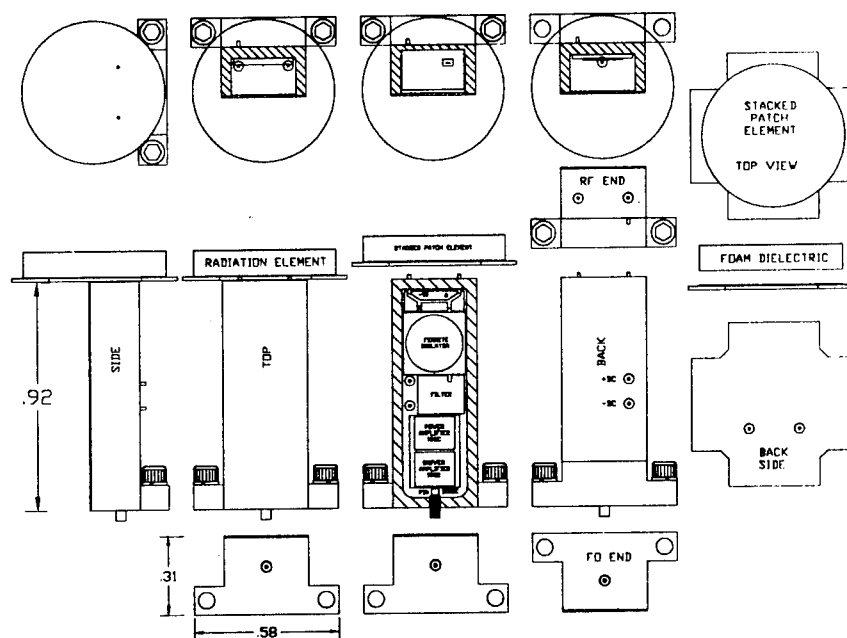

Figure 4.4.2-5   Airborne Transmit Array Element Module

Some experimentation has also been done on the impact of remoting the beamformers from the active aperture. The outer configuration is shown in Figure 4.4.2-6.
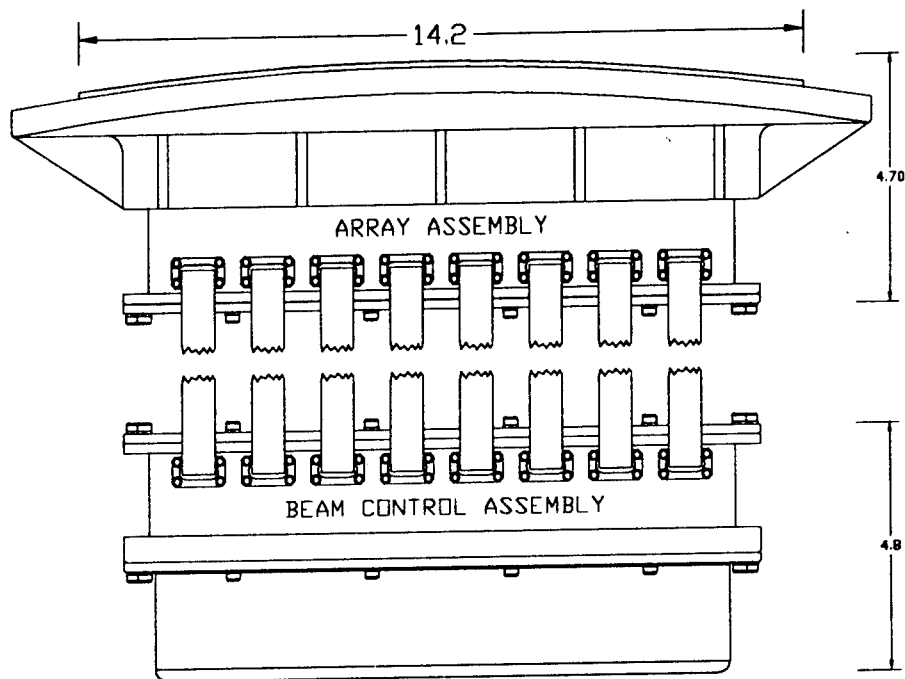
Figure 4.4.2-6   Remote Airborne Transmit Array Configuration

Figure 4.4.2-7 shows a rear and side view of an assembly where the 256 fibers are bundled into 8 connectorized bundles. It is necessary to subdivide so that one huge 256 fiber bundle cannot be bent into an arc easily. Figure 4.4.2-8 shows the cross-section view with the fiber interconnects.
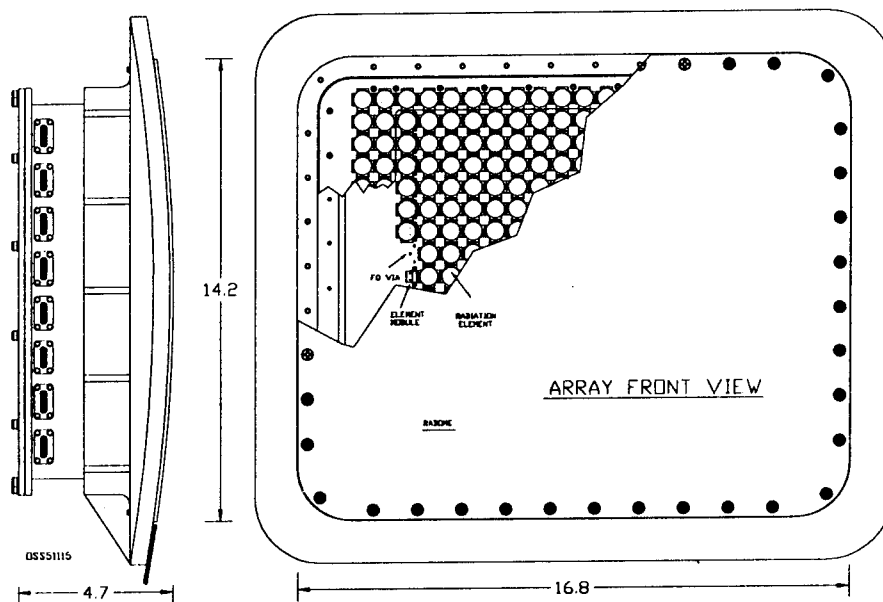

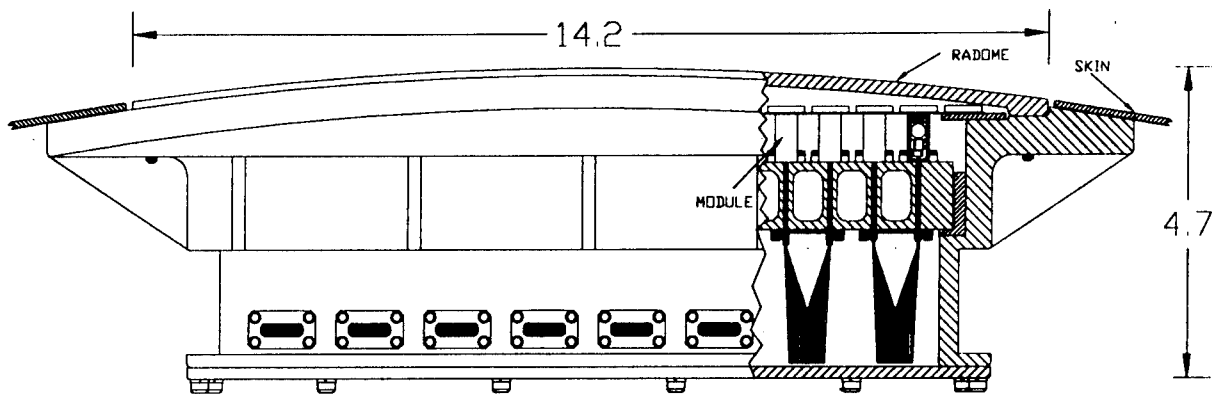Figure 4.4.2-7   Remote Airborne Transmit Array Side and End Views

Figure 4.4.2-8   Remote Airborne Transmit Array Cross-Section View

The inside hardware contains the photonic beamformer assemblies. Its layout is shown in Figure 4.4.2-9
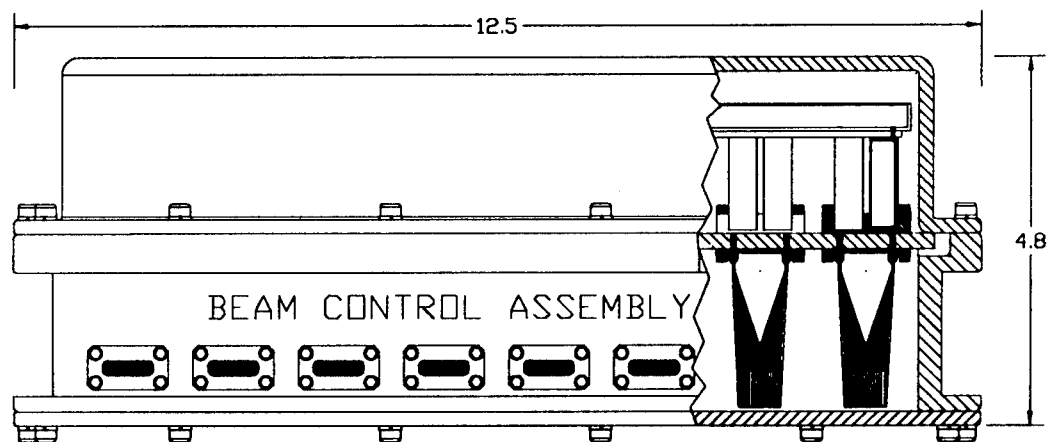

Figure 4.4.2-9   Remote Airborne Transmit Array Beam Control Cross-Section View

4.5   Risk Assessments

A key ingredient in the definition of EDM hardware is a careful, realistic examination of all risks. The following subparagraphs define perceived risks at this time in areas of mechanical design, electrical design, cost, and certification of the system.

4.5.1 Mechanical Risks

The mechanical risks in the system fall into three categories; vibration, size, weight, and thermal management.

Vibration in an airborne system can be quite severe both in short and long term perspectives. Material brittleness of conventional optical materials, alignment of any free space optics, and use of butt connections between components are all contributors to possible failures due to vibration.

Although size and weight advantages of photonics over conventional RF feed systems has been touted over the years, the development of MMIC RF hardware over the last ten years has removed many photonic size advantages in basic array building blocks like phase shifters. Only through large scale integration of optical networks can a photonic feed compete with existing high density RF packaging techniques.

Probably the highest risk to the proposed systems is in the area of thermal management. Because the array is constrained to 256 elements, each element must provide significant RF power at the output. Inherent inefficiencies of RF to optical conversion means more gain must be provided at the element. The high density of the elements means large amounts of heat must be removed. Additional measures to provide cooling, such as liquid heat exchangers increase the size and weight of the array considerably.

Additionally, the materials used in photonic hardware such as gallium arsenide, indium phosphide, and Lithium Niobate have different coefficients of expansion. This compounds the thermal problem because the materials must be held to lower temperatures to avoid interface failures.

4.5.2 Electrical Risks

The electrical risks to the airborne array design include airframe interference, wide angle scan array design, and specific component characteristics required to achieve the performance.

As is the case with nearly all antennas on airplanes, achieving the desired coverage is compromised by the shape of the airframe. Generally speaking, especially in existing airframes, the selection of the array location is limited mechanical to a small set of possibilities. The array system must live with the coverage available at the possible locations. Trying to fit the array at the best possible locations is fraught with cost impacts. The generally accepted rule is "what you get is whatever is available". Because the arrays are full duplex, the receive-transmit isolation is an important parameter in locating the arrays. The more isolation between the two arrays the easier the module designs become because the filtering requirements are eased. The coverage difficulty is compounded by the rotodome as was shown in the pattern simulations.

Requiring the array to scan to 75° adds risk in two manners. First, only a location on the aircraft rotodome will be compatible with clear views over the wide angle scan. Secondly, achieving the wide scan with a fixed element count means closely spaced elements and large amounts of gain roll-off at maximum scan angles.

During the current study, two components have been defined as critical to the proposed design. A low loss cross-bar switch is key to the beamformer architecture. Also, improved optical amplifiers for both the transmit and receive beamformers are required to achieve realistic gain/loss budgets.

4.5.3 Cost Risks

For any array, the risk of high costs plays an important role in achieving hardware that can be put into production. The hardware must be designed into a minimum number of building blocks and with a minimum number of unique parts. The proposed architecture uses a unique beamformer design that minimizes the amount of hardware (compression). In order to create a small number of beamformer building blocks , a square array lattice is used so that elevation and azimuth beamformers are identical. It is claimed that the denser packaging will offset the increased number of elements with a highly symmetrical design.

4.5.4 DSCS Non-Certification Risks

As pointed out in the system requirements discussion in the study, the airborne arrays as specified in the SOW are too small to meet the DSCS terminal certification requirements. The small array has a beamwidth 4 times wider than the system certification specifications. The options in the design is to increase the size of the array (much higher cost and more airframe real estate) or work within the system with appropriate waivers in the certification requirements.

Achieving waivers could result in limited access, increased cost to operate, or limited power. The airborne user may only be able to access DSCS when there are a smaller number of users on the network. Alternatively, a higher cost would result if resources on other satellites that would be jammed must be rented to protect other users. Another technique to reduce jamming by an uncertified user is to reduce the EIRP allowed into the system.

5.0   Satellite Array Design

Several assumptions have been made in the initial definition of the satellite arrays:

- The architecture of the receive and transmit arrays are assumed to be the same.
- The arrays have hexagonal lattices.
- At least one ring of elements will be placed around the active array.
- The spacing between the transmit and receive array is TBD.
- The focal length of the array is its altitude, 25,844 miles.
- The diameter of one 2° beam on the earth is 1050 miles.

The primary goal of the satellite array design is to develop a design with minimum hardware growth as the number of beams is increased. Figure 5.0 is a top level block diagram of the satellite arrays showing the external interfaces to radiated free space, the satellite vehicle (SV) DSCS terminal, the SV mechanical interface for structural integrity and thermal management, and the SV power sources. During normal operation, the arrays are controlled from the ground for selection of origination and destination of each user. Because of the independence of the two arrays, slaved beam pointing is not an option for the satellite arrays.

DSCS Ground and Airborne Terminals
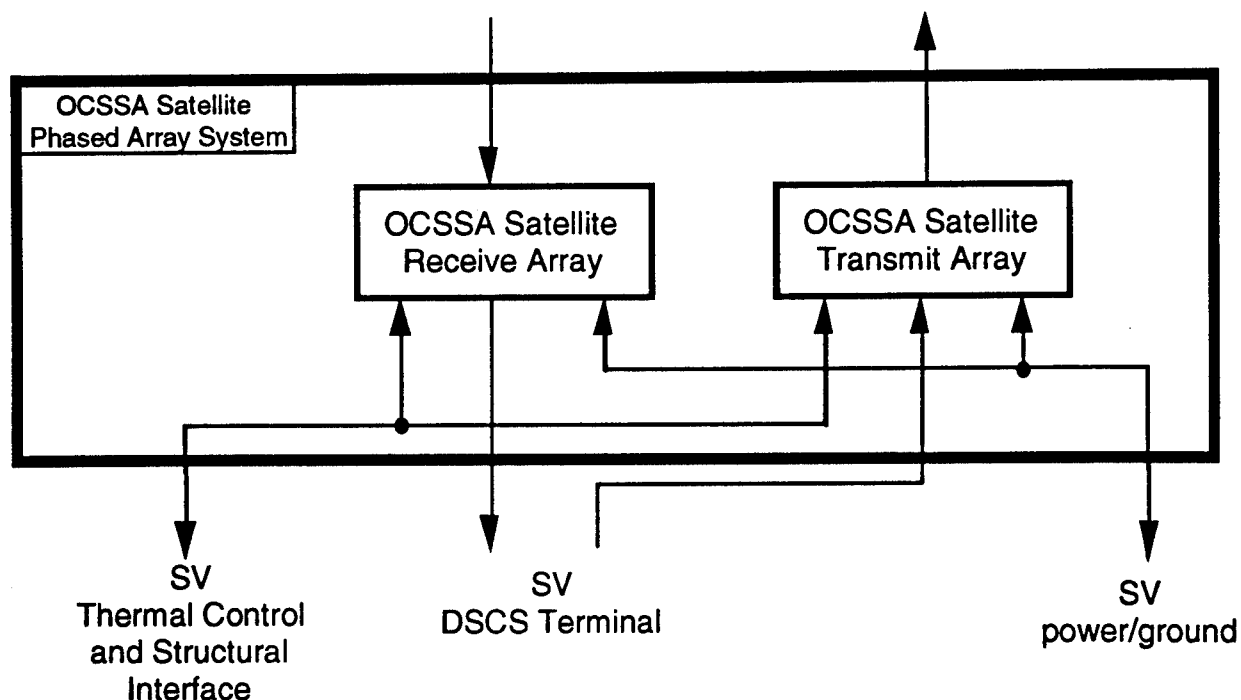
Figure 5.0   OCSSA Satellite Array System

5-1

5.1 Architecture Trades

The three driving trades to be made on the satellite arrays are multiple beam techniques, adaptive techniques, and limited scan techniques

5.1.1 Multiple Beam Trades

Three techniques can be used to form multiple beams with an array: Butler matrices, channel division, and lens techniques.

- **Butler Matrices**

A Butler matrix feed is a fixed, hybrid network designed to allow an N element array scan to M possible beam positions. There is an input port for each beam position and an output port for each array element. A single beam array is obtained by putting a M-way switch to the input ports. To obtain multiple beams requires a more complicated switch matrix that allows any user to select any beam. Each beam position is hard-wired to an input. This technique is most applicable when the number of beams is roughly the same as the number of elements.

Although this type of network can be built optically, the hardware quantity and complexity makes its selection probability remote.

- **Channel Division**

If the number of beams is significantly less than the number of elements, a channel division feed can produce multiple beams efficiently. Multiple beams are formed by performing a channel division between the element amplifiers and the corporate combiner. For M-beams, a M-way combiner/divider is inserted between the amplifier and phase shifter. Then M phase shifters are added to each channel. For a N-element array, there M x N phase shifters. M N-way power combiners/dividers form beams by attaching to one phase shifter at each element. The result is M parallel channels.

For the satellite array, channel division is a candidate because there are 256 elements and only four beams. However, the hardware multiplication when additional beams are added makes packaging difficult.

- **Lens Techniques**

A lens technique, either at RF or optical frequencies, uses a reflector or lens to form multiple main beams. This is a very wideband technique in which beam position is related to a position of the lens' focal plane. A limitation of reflector versions of this approach is than the maximum scan is limited.

For the purposes of achieving multiple beams with a minimum of hardware multiplication, this approach is the best option.

5.1.2 Adaptive Trades

Selection of an adaptive technique is based on four parameters: threat, hardware architecture, adaptive algorithm and required nulling performance.

The threat to the DSCS system can be a powerful, fixed jammer located either in the sidelobes or in the main beam. The OCSSA requirements identified up to three simultaneous jammers total.

Adaptive antenna architectures include:

- fully adaptive arrays where all array elements are weighted by the adaptive controller
- partially adaptive arrays where only a few array elements are weighted
- adaptive beam arrays where a dedicated beam is steered toward a jammer, weighted to the desired signal pattern in the same direction and subtracted to form a null.

Adaptive null algorithms include:

- search - dithering the weights to try different combinations. Has very simple hardware
- LMS - most common, rapid one jammer nulling, generally expensive hardware
- direct - matrix inversion, very fast, computationally intensive
- PSF^{tm} - hardware like search algorithms, performance like LMS
- beamspace - subtracting a jammer beam from the signal beam

Adaptive nulling done with a beamspace algorithm appears to be a quality approach for this application. A finder beam is used to peak up on the jammer. Then those steering vectors are used to formulate a beam in the jammer direction. The jammer beam is weighted and subtracted from the main signal pattern. By using the full aperture of the array to make the jammer beam, its effect on the signal beam is minimized because the jammer beam is as narrow as the main beam. Beamforming hardware grows to make enough beams to point at the signals and at the jammers. This approach is a natural to a beamformer that does not have large multipliers for additional beam capability.

5.1.3 Limited Scan Trades

Although the OCSSA satellite array design was specified as an array of elements spaced two wavelengths apart, a cursory look at alternative techniques was made to see if there might be a strong benefit to consider another approach. Limited scan techniques include:

- arrays of subarrays or high gain elements (OCSSA baseline)
- overlapped subarrays
- aperiodic arrays
- array/reflector/lens hybrids

These candidates do have potential benefits for the array. However, the design derived in this study has a very attractive mechanical package. Use of these other techniques would appear to add either complexity or physical size.

5.2 Photonic Beamformer

Selection of the beamformer for the satellite arrays is based primarily on reducing the hardware multiplication of multibeam arrays. This approach rules out any conventional, low risk corporate feed technique using either phase shifters or time delays. The approach was to commit to some type of spatial Fourier transformation to produce multiple beams.

The approach selected uses frequency multiplexing to create multiple beams, spatial offsets to determine the beam direction, and a SLM mask to shape the desired pattern. Either the signal or the LO could be used to create the pattern shape through the SLM while the other is a point source. With no real advantage to one or the other, the LO was selected to be the point source. The multiplexed frequencies for each beam are set by a frequency offset from a locked dual frequency laser pair. Crosstalk is avoided between beams by selecting the center frequencies of the laser pairs sufficiently far apart to force the cross terms (interference between different LO/SLM pairs) out of the reception band of the photodetectors.

The beamforming concept is shown in Figure 5.2. Each LO is a point source. Each signal is its own mask defining the pattern coverage on the earth. Through the Fourier lens, they define a set of element excitations to create the beam defined in the mask. Pattern shaping and adaptive nulling are done by weighting the multiple images in the mask and by creating a dedicated beam for a jammer using the same LO.
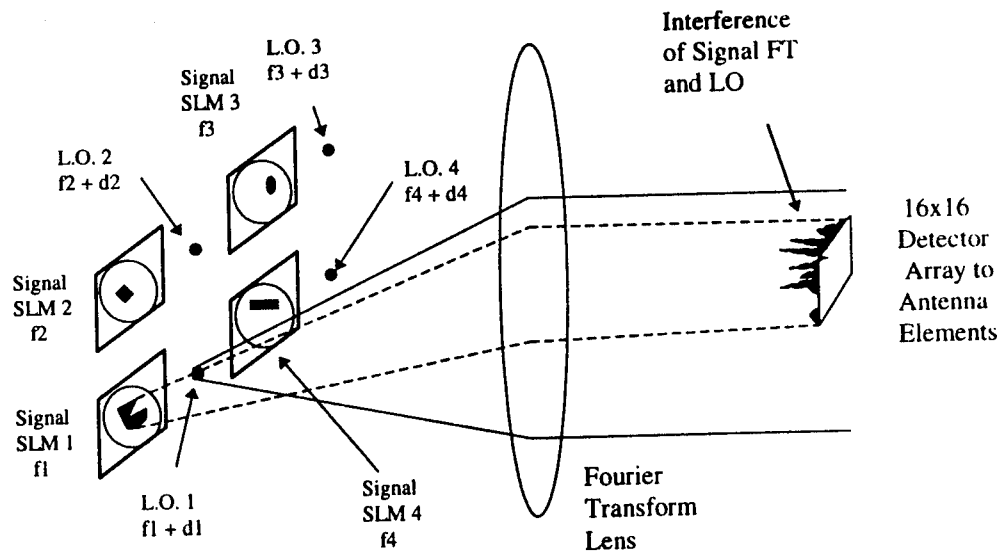
The beam angle is determined by the angular offset of the local oscillator and the signal SLM.

Figure 5.2   Satellite Array Photonic Beamformer

5.3 Baseline Definition

The baseline satellite architecture was selected to minimize the hardware especially as the number of simultaneous, independent beams are increased. The

configuration is amenable to adaptive nulling either through dedicated jammer beams in "beam space" or through footprint weighting in the SLM.

The lattice used in the satellite arrays is a conventional hexagonal array grid. For 256 elements and two wavelength spacing, this gives the minimum beamwidth. Because the beamformer for the satellite array is entirely different than the airborne array, use of a square grid offers no symmetry advantages.

Figure 5.3 shows the hardware definition and architecture of the receive and transmit satellite arrays. Highlighted in the figure are the array element modules (AEM), the Fourier transformers, and the pattern image generators.
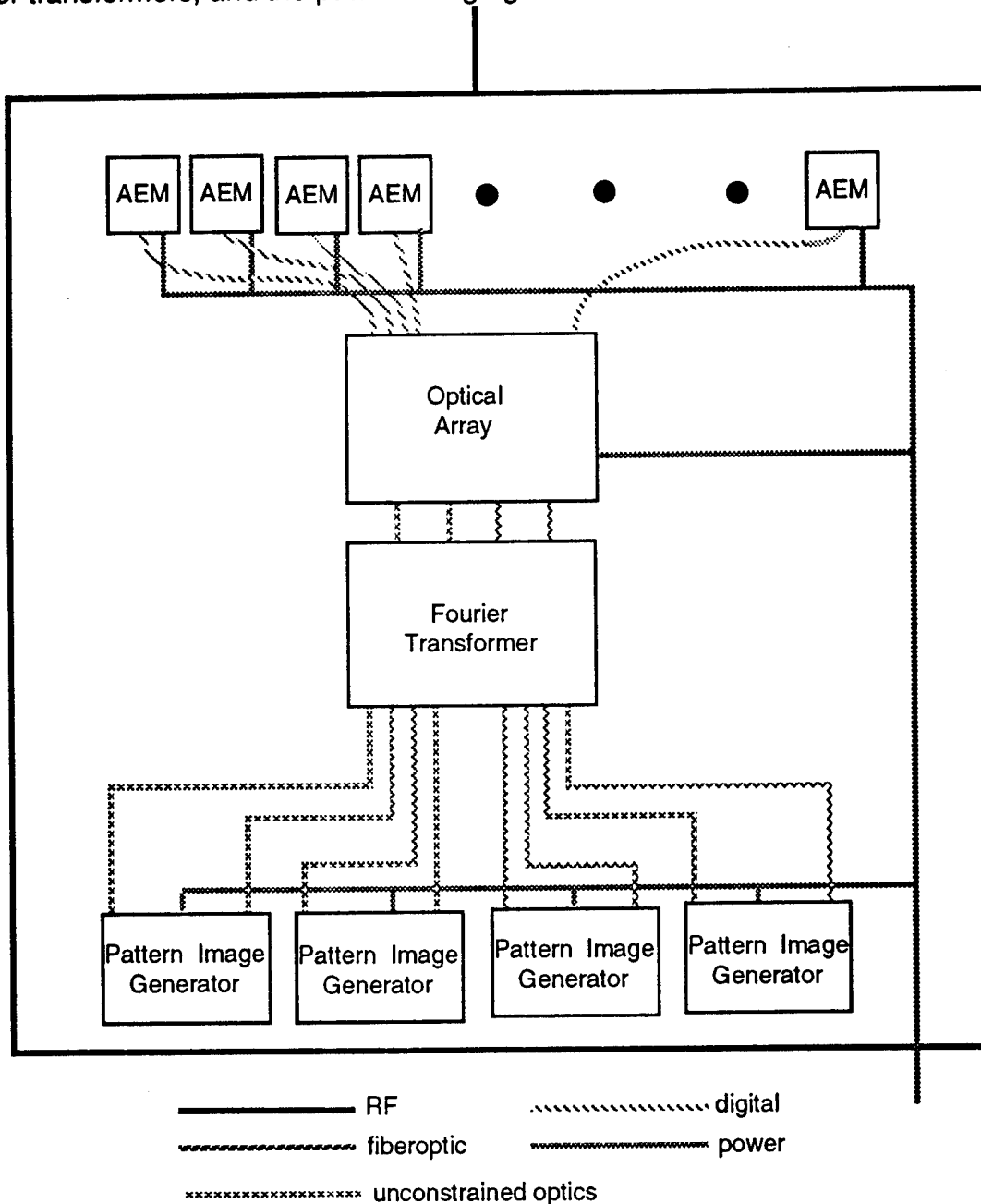
Figure 5.3   Satellite Array Baseline Block Diagram

Just like the airborne arrays, there are no phasors in the antenna element modules.

The feed for the array uses unconstrained optics with a lens in order to illuminate the phased arrays. Photonic conversion occurs right before/after the amplifiers in the element assemblies. This achieves maximum photonic integration. Improving RF technologies have made very low-noise amplifiers and moderate output power amplifiers easily achievable for the element level conversion from optics to RF. The beamforming is done entirely with weighted laser beams and a Fourier lens..

5.3.1 Array Element Assemblies

The array element assemblies are the building blocks for the satellite arrays. These assemblies are the array cost drivers because of their cost multiplication by the number of elements. Critical importance must be placed on the low-cost and small size of all the parts in these assemblies.

At each transmit array element, there is a RF transmit module containing RF conditioning and optical/RF conversion circuitry. Figure 5.3.1-1 is the definition of the transmit array element. assemblies. The diagram is the same as the receive array except for the photonic conversion and the amplifiers.

Power amplification in the transmit array element module consists of two stages to increase the converted optical signal to the required 0.07 Watts required at each element to meet the design EIRP.

Filtering in the transmit RF modules is at a TBD level until mature definitions of orientation and separation of the arrays is established. The filtering is designed to help control transmit noise and spurious images in the receive band from appearing in the output and to protect the sensitive receive channel electronics from the high transmit powers.

Only a single feed is required for the satellite array element (see next subsection).

The transmit array optical-to RF conversion is performed by the same type of hardware as the airborne array.
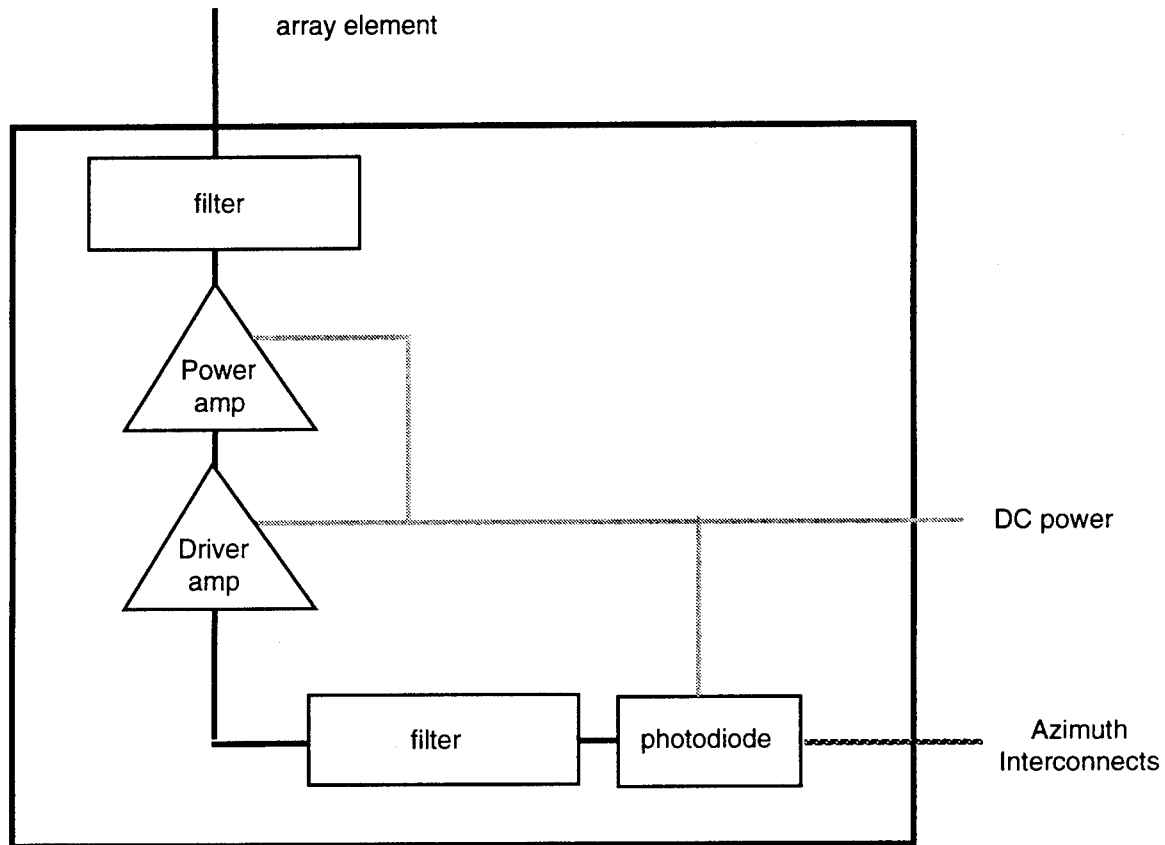
Figure 5.3.1-1   Satellite Transmit Array Element Module

The satellite receive array element modules have one important difference with the airborne array equivalent. Functionally, each module contains RF conditioning and optical/RF conversion circuitry just like the airborne array. However, the receive satellite array also contains one RF output port in which the received signals are combined. The block diagram of the satellite array receive module is shown in Figure 5.3.1-2
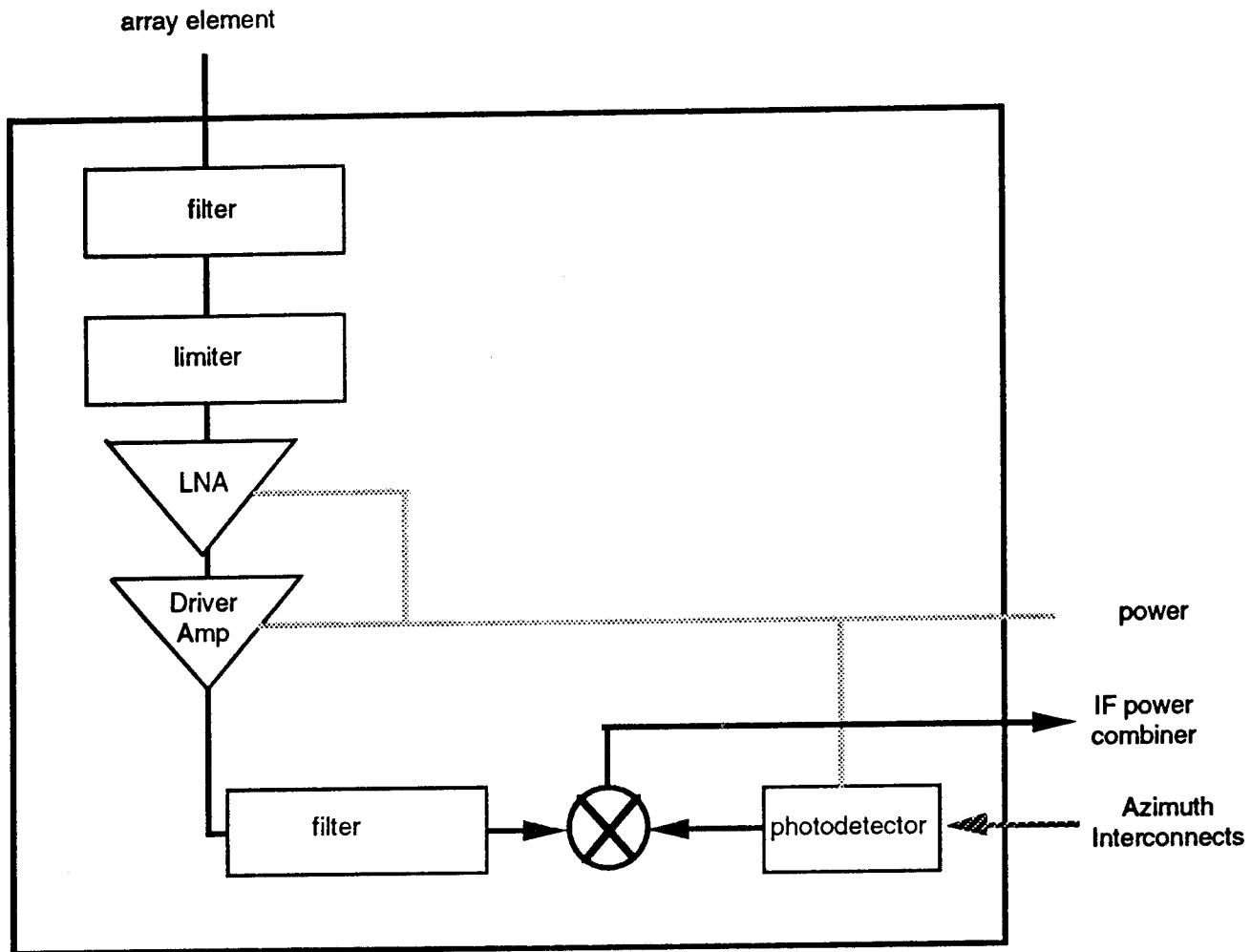
Figure 5.3.1-2   Satellite Receive Array Element Module

The receive path RF amplification consists of components with performance similar to the airborne array.

Filtering in the satellite RF modules takes on a slightly different function with the frequency multiplexed signals at a single output. Besides providing transmit isolation, the filtering must control the frequency plan of the satellite receive array.

The receive array RF-to- optical conversion is performed by the same type of hardware as the airborne array.

Initial reaction to using RF to combine the beams was somewhat negative because the elegance of a completely photonic beamformer was lost. However, upon consideration of the array's use in the DSCS satellite, the conversion is not nearly as inconvenient as may be thought.

The transponders in the DSCS satellite have typically about 100 dB of gain between the receive antenna and the transmit antenna. This amount of gain in photonic components would be hard to achieve while it is pretty easy at RF. Since the receive array converts its output to RF, large amplification can be obtained and then converted back to optics at the transmit array.

5.3.2 Array Element

The element for both the transmit and receive arrays must be relatively wideband, capable of circular polarization, and have sufficient gain to efficiently capture the energy over its two-wavelength diameter.. Several types of elements are possible candidates including spirals, helices, stacked patch subarrays, and horns. The best compromise for light weight, moderate gain and good axial ratio is the multi-turn helix. This element has been used in satellite arrays many times and its characteristics are well known. The helix consists of a single wire formed to make about eight turns over approximately a two wavelength axis. With multiple turns, acceptable axial ratio and pattern performance can be maintained. An additional advantage of the single wiring helix is that no hybrid coupler is required to make circular polarization.
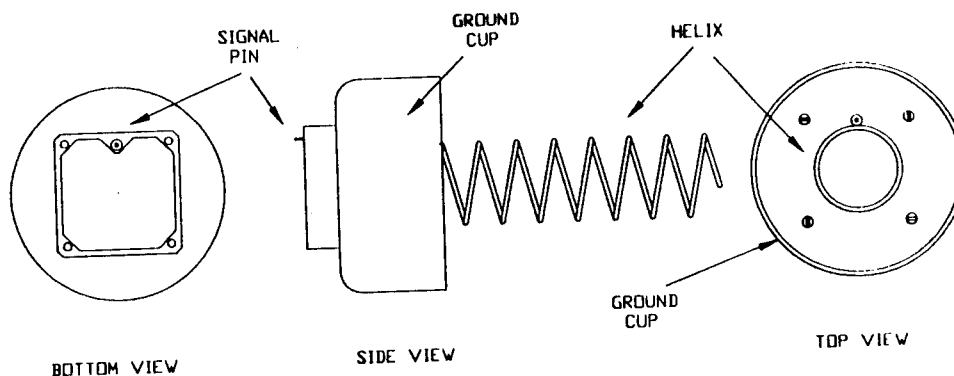
Figure 5.3.2 Satellite Array Helical Element

5.3.3 Beamformer

The beamformer approach selected for the satellite arrays must meet two basic criteria. First, it must be able to create a beam in less volume than for a RF approach. Second, it must be able to add more beams to its capability without the hardware multiplication associated with RF approaches.

The proposed beamformer meets those criteria with architectures of the transmit and receive arrays virtually identical. Figure 5.3.3 shows the optical configuration for one single beam. On the transmit array, the DSCS signals are injected into optical modulators. On the receive array, there are no modulators and the FDM signal outputs from each module are combined at RF with a 256-way combiner.

LO

Fourier
transform
lens

fiber
bundle

phased
array
beamformer
and
aperture

source → modulator → signal mask

beam
shape
control

array
controller

SV
Power

signal
(transmit)

SV
Controller

signal
(receive)

———— RF   ////////// digital   ▨▨▨▨ power   ———— optics
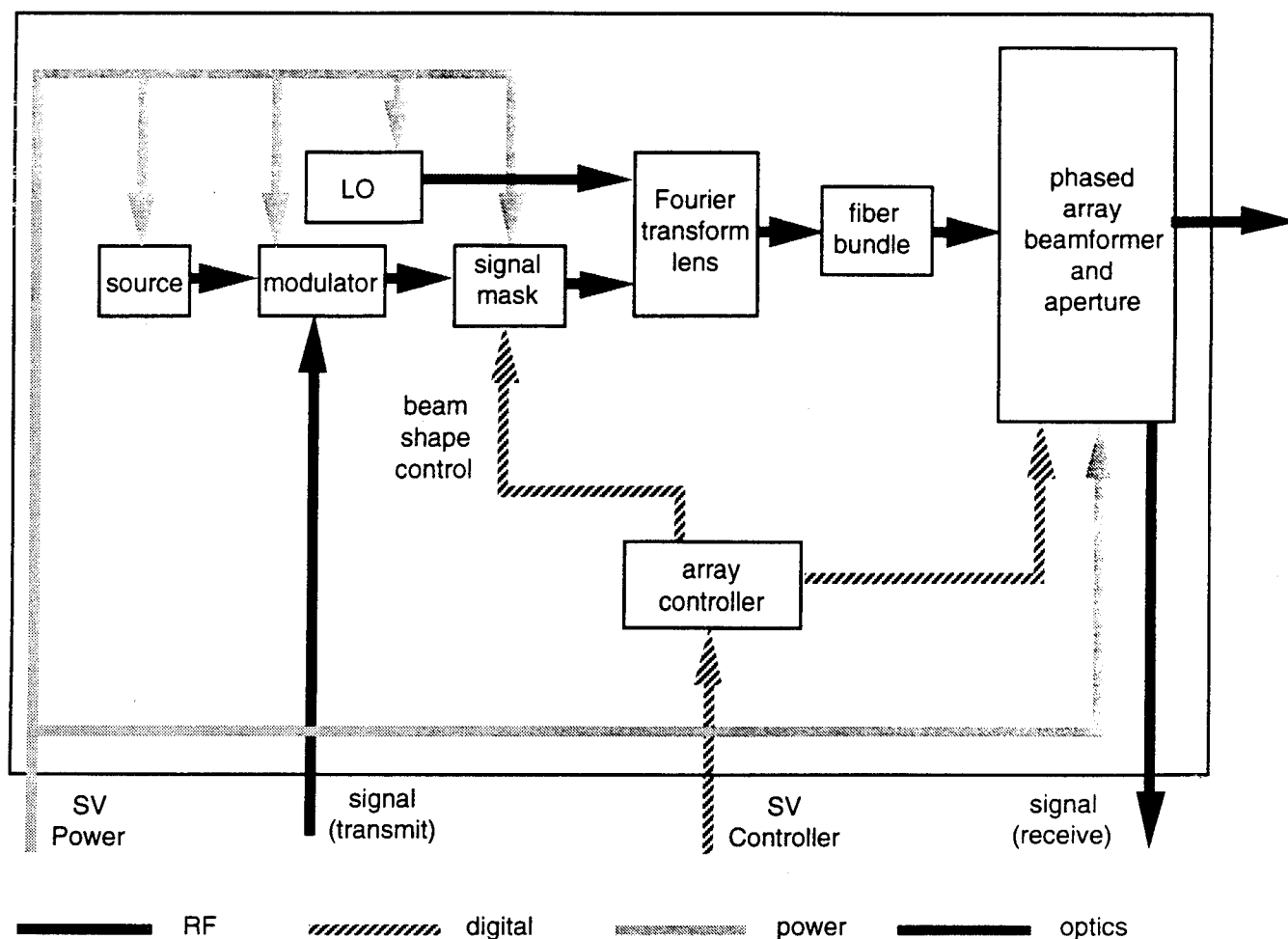
Figure 5.3.3   Satellite Array Optical Beamformer

The basic approach is to use a SLM with one cell per beam position and a point source LO for each beam. The beam scan position is set by the separation between the signal point source on the SLM and the LO source. The multiple beams are separated by using different LO frequency offsets for each beam.

Beam shape customization can be done with scaled amplitudes of the various SLM pixels.

At this point in the development of the satellite array design, the downselection of the SLM technology is the next critical step. Although there are many possible SLM technologies, there has been essentially no activities at 1.3 mm infrared wavelengths. Most work on LCD's for example have been at visible wavelengths to support video screens.

The selection of an appropriate SLM technology can be based on a comparison of factors of merit as defined for the OCSSA application. The following list of quality factors are considered appropriate:

1. contrast ratio amplitude ratio of the SLM pixel in the ON state compared to the pixel in
            the OFF state

2. spatial resolution   the smallest resolvable dimension of the SLM (not necessarily pixel size)

3. framing speed   the rate at which the SLM can be updated

4. switching energy per pixel   the energy required to change a pixel state from OFF to ON

5. space-bandwidth product   the number of pixels

6. gray-scale dynamic range   used in amplitude weighting and typically given in bits

7. storage time   measure of the image persistence after the drive signal is removed

These quality factors all need to be considered in accessing the applicability of the following technologies:

1. electro-optic SLM   uses an electric field-induced change in a material's refractive index

2. photorefractive SLM uses an optical field-induced change in a material's refractive index

3. liquid crystal SLM   uses a field-induced molecular realignment

4. deformable mirror SLM   uses mechanical motion to change wavefront

5. magneto-optic SLM   uses Faraday rotation to change light polarization

6. electro-absorptive SLM   uses variable absorption to modify wavefront
(typically with multiple quantum well devices)

As an example, a preliminary qualitative comparison is shown in Table 5.3. Although incomplete at this time, the table does point to some preliminary candidates. If one uses the selection criteria of the most universally applied technologies, liquid crystal and acousto-optic SLM's might be the most promising. The first step in converging to a solution would be a more comprehensive search for data at 1.3 μm. If insufficient data is found, a method for funding new IRAD activities is appropriate.

Table 5.3 Preliminary SLM Technology Comparison

SLM technology	Physics	Advantages	Disadvantages	Speed
magneto-optic	Faraday	solid state	larger magnetic fields at higher frequencies	1 msec.
acousto-optic		high contrast		1 msec.
liquid crystal	molecular rotation	widely used commercially	unproven at 1.3 μm	10 μsec.
PLZT/SOS	electro-optic	solid state	larger electric fields at higher frequencies	< 1 μsec.
multiple quantum well			absorptive	

5-11

5.3.4 Controller

The controller for the satellite arrays must handle four simultaneous signal beams. Four simultaneous beams each with its own customized footprint are formed toward specified ground stations and sea or airborne platforms. If given constraints, the controller shapes the footprint of the pattern. Each of the SLM's receives its own input specifying which pixels to be set at specified levels. These commands form the mask used by the signals to shape their beams. Adaptive channels will add additional beams with their own SLM.

5.4   Conceptual Design

The conceptual design of the satellite arrays is described in two stages: optical and mechanical implementation

Figure 5.4 is a block diagram of the transmit array showing the four parallel networks for the four beams.
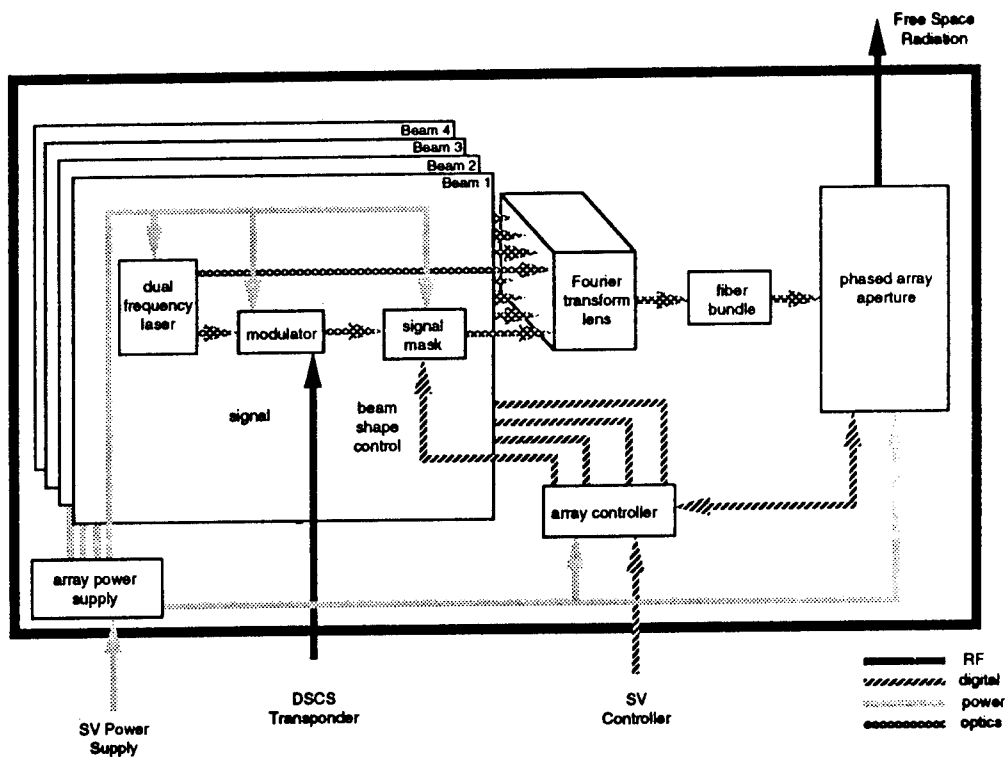
Figure 5.4   Satellite Transmit Array Block Diagram

5.4.1 Optical Implementation

The development of the physical sizing of the array optics is summarized in Figures 5.4.1-1 to 5.4.1-4. The fiber bundle size is based on the arrangement of the fibers into a lattice like the array aperture. The SLM sizing is based on the number of beams required to cover the earth (61). The Fourier lens sizing is based on an

assumed f/D ratio of 3.0. The SLM - LO pixel spacing image plane dimensions are based on lens focal lengths and fiber core diameters.

sheath

125 μm cladding

8 μ core
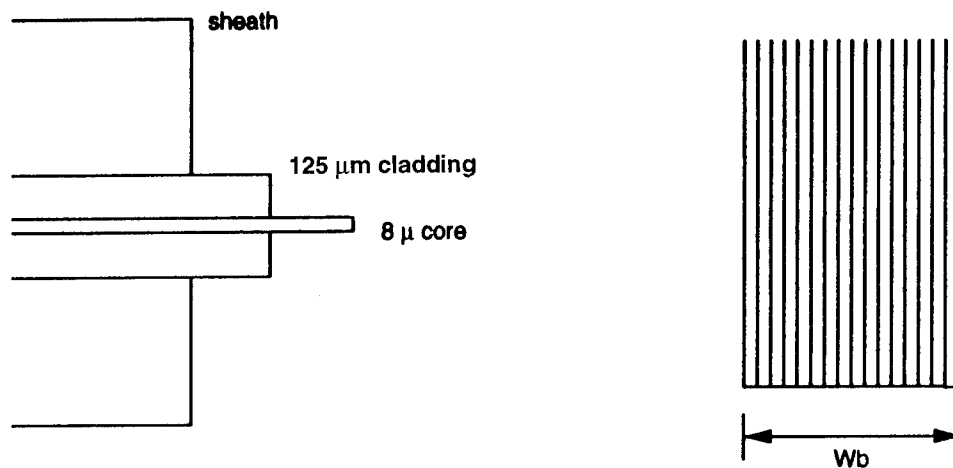
assume fiber bundle packing of core cladding in hexagonal pattern with a maximum of 17 fibers across

Wb

$Wb = 17 (125 μ) = 2.12 mm$

Figure 5.4.1-1   Satellite Transmit Array Fiber Bundle Sizing

Wp
(one pixel)
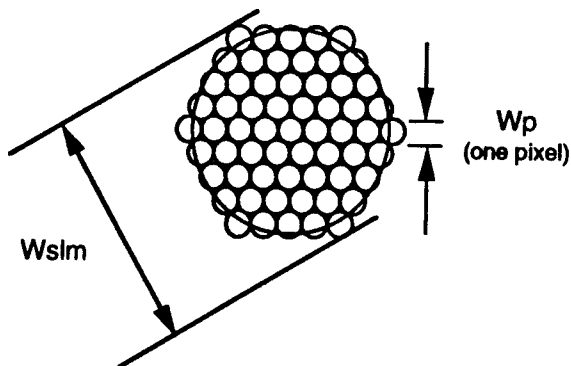
Wslm

$$\frac{Wslm}{\lambda f} = \frac{1}{wfb}$$

$$\frac{Wslm}{f} = \frac{\lambda}{wfb} = \frac{1.3 \, \mu}{2.12 \, mm}$$

$$\frac{Wslm}{f} = 6.1 \times 10^{-4}$$

Assume Wp = 25 μ

Wslm = 9Wp = 225 μ

Figure 5.4.1-2   Satellite Transmit Array SLM Sizing

5-13
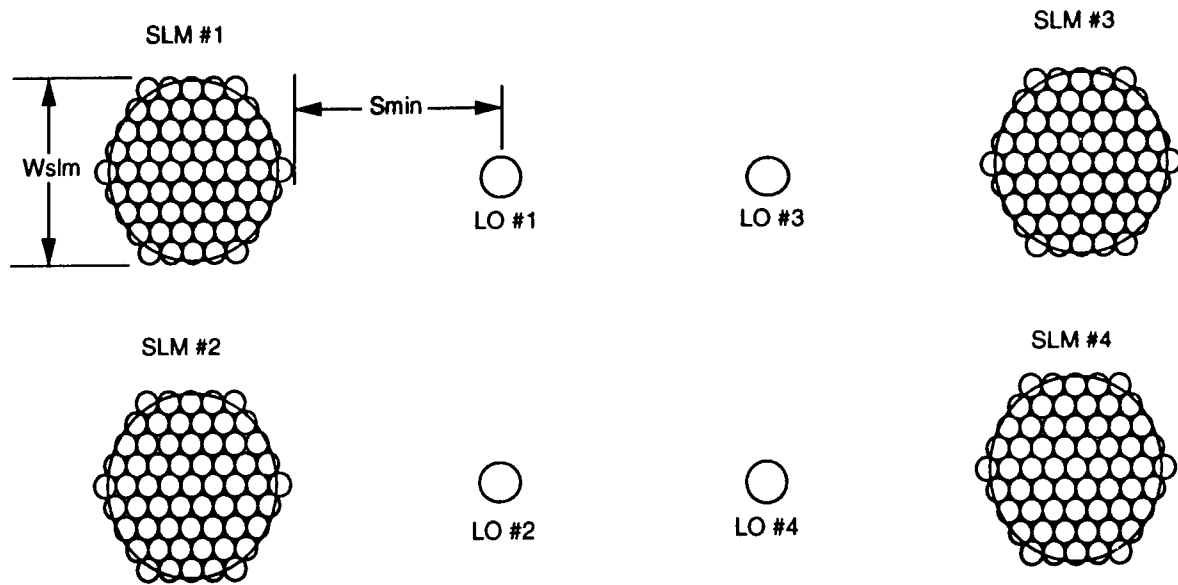
Figure 5.4.1-3   Satellite Transmit Array SLM Image Plane Geometry
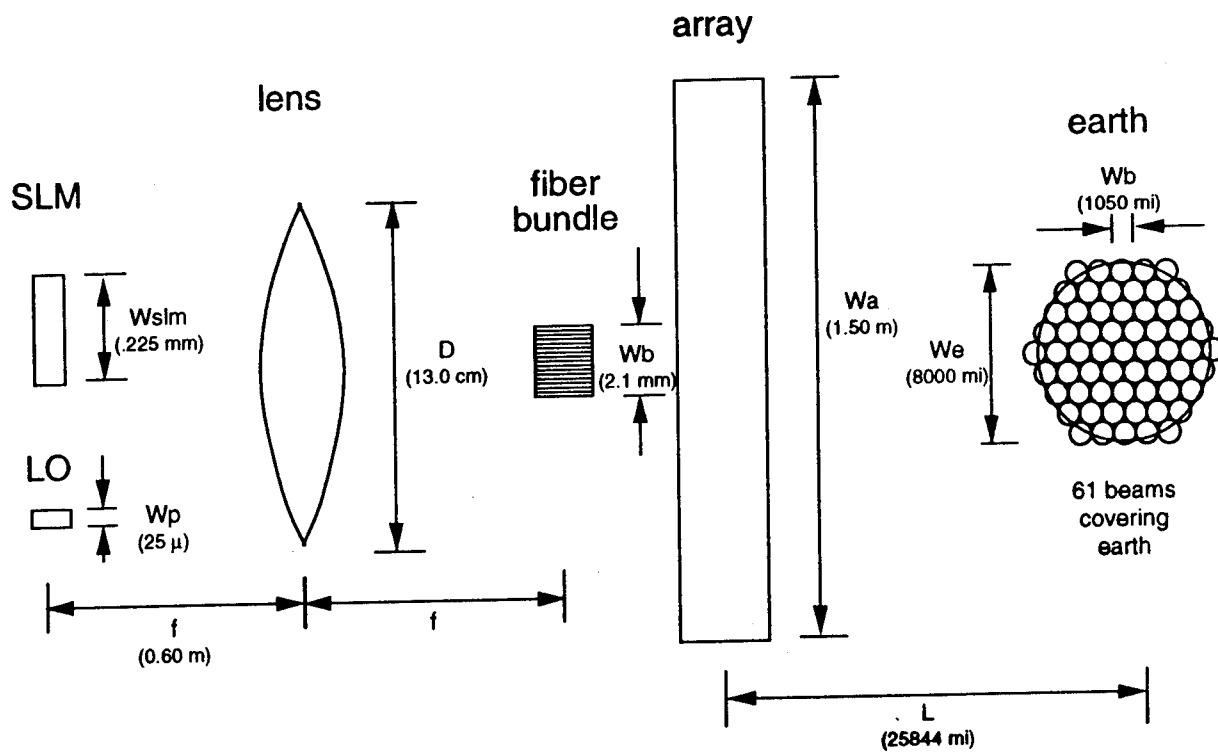
Figure 5.4.1-4   Satellite Transmit Array Optical Dimensions

The calculations for the receive array are quite similar. Figure 5.4.1-5 shows the block diagram. Note there is no signal interface or modulator at the beam signal mask. There is a 256-way RF power combiner to sum the frequency multiplexed aperture output. The only difference in the optics dimensions is the array diameter which is smaller on receive (1.39 meters versus 1.50 meters on transmit) because of the receive arrays higher frequency.
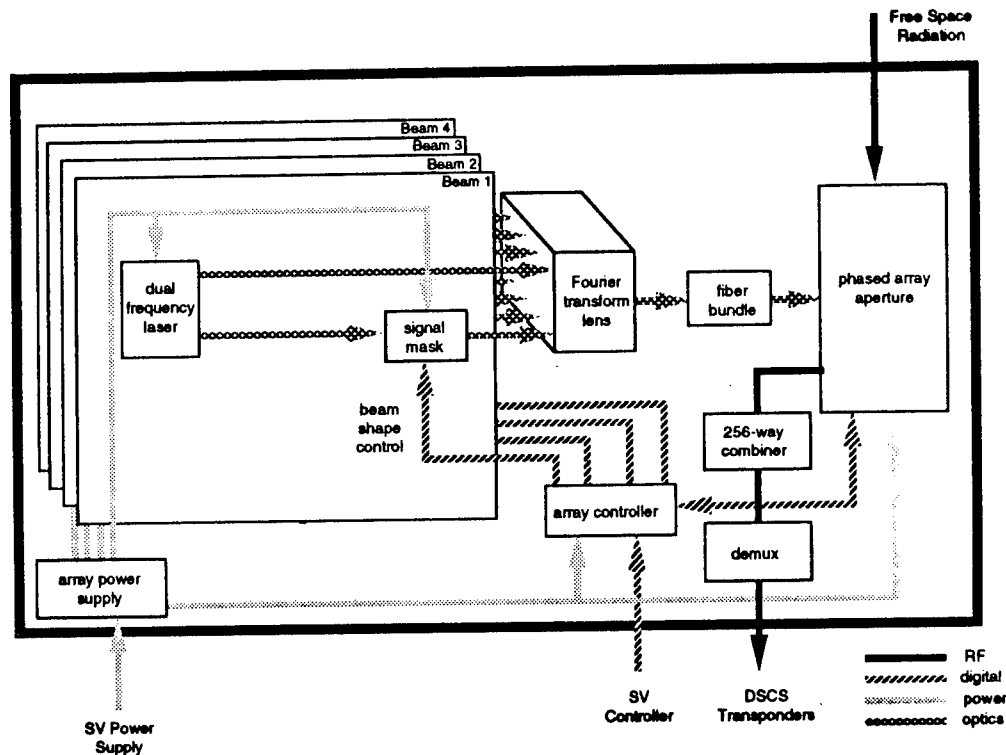
Figure 5.4.1-5   Satellite Receive Array Block Diagram

At the final oral review, when the receive array architecture was first presented, it was noted that the frequency plan to incorporate multiple LO's had not been examined to determine the risk of spurs in the downconversion and separation of the multiple beams. Since that time, initial evaluation has been done including simulation and bench measurements. Can the product terms with multiple LO's be controlled?

The problem is defined in Figure 5.4.1-6. The photodetector accepts four different laser frequencies, each with a unique offset. Those offset frequencies, when mixed with the receive band input create four IF bands that are combined and demultiplexed. Note that the frequencies shown in the figure are examples and are not intended to be the optimum choice.
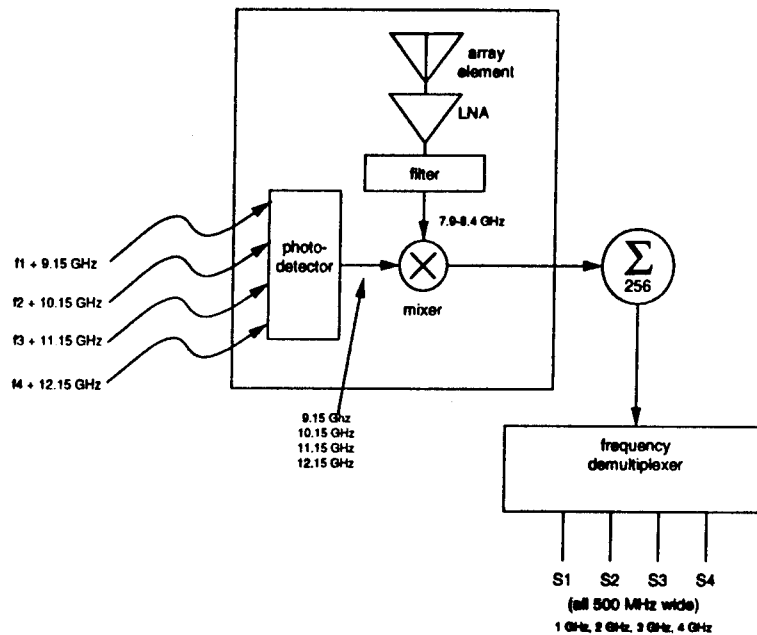
Figure 5.4.1-6   Satellite Receive Array Example Frequency Plan

The results of the examination are discussed in Appendix D.   Briefly, the conclusions are:

- The problem is a difficult one but it is not insurmountable.
- The degree of difficulty is tied to the suppression of spurious tones required by the system.
- The problem of spurs due to multiple LO's is an uncommon problem for mixer design and device technologies. The optimum mixer for this system may be a type totally unsuitable for conventional systems.

Simplified power-loss-noise figure budgets are shown in Figures 5.4.1-7 and 5.4.1-8.
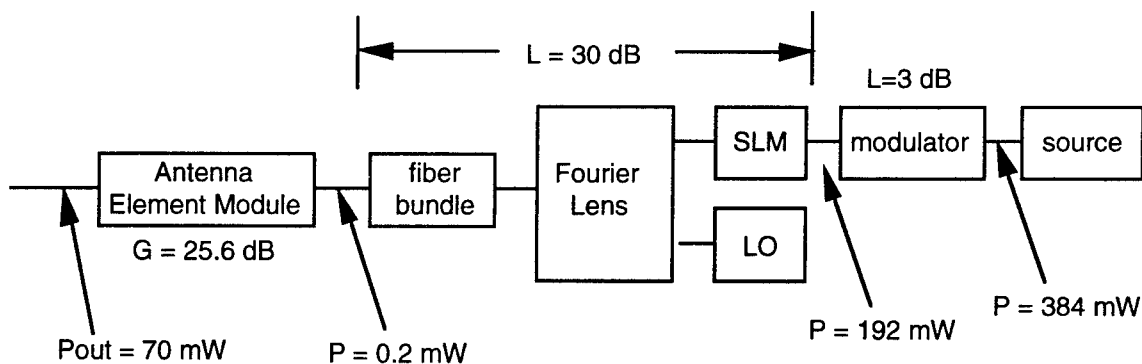
Figure 5.4.1-7   Satellite Transmit Array Signal Flow Diagram
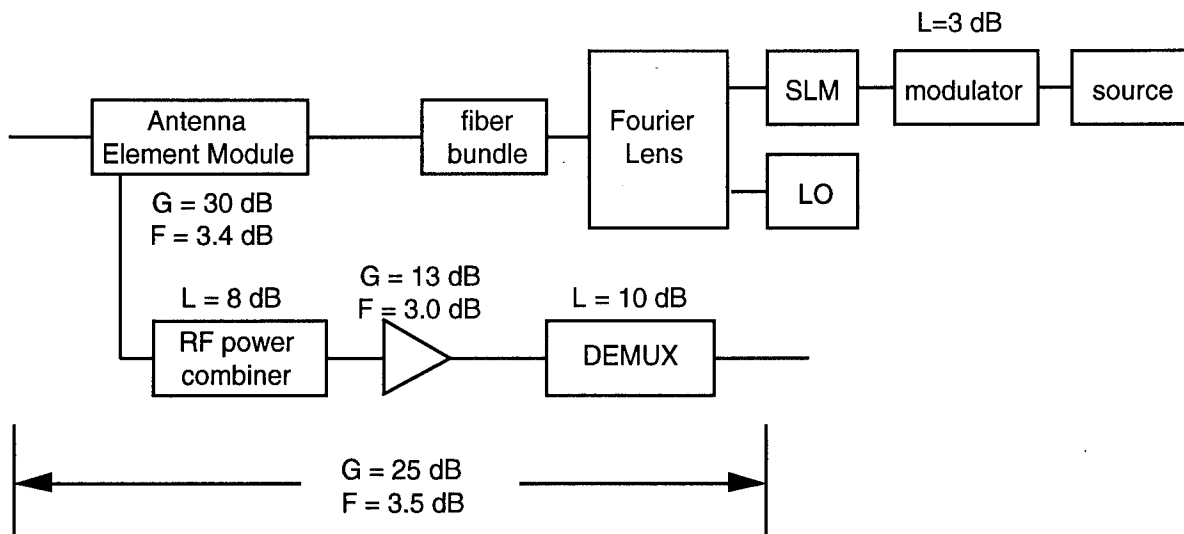
Figure 5.4.1-8   Satellite Receive Array Signal Flow Diagram

Both budgets are based on a loss of about 30 dB through the Fourier lens and into the fiber bundle. Use of Grin lenses on the fiber bundle has been assumed. The transmit budget results in component values that should pose no significant problem. No additional optical amplification appears to be required. The receive budget is somewhat unique because the received signals are processed in RF. The optical budgets affect levels required to perform the conversion.

5.4.2   Mechanical Implementation

A preliminary cut has been taken on the physical implementation of the OCSSA satellite arrays. It should be noted that this exercise was limited to the physical description of the array without consideration of making the array for on-orbit deployment. That issue is better served later when closer to FSD and launch vehicle constraints are identified.

Figure 5.4.2-1 shows the transmit array front and side views. The RF modules are imbedded in the honeycomb structure. The fibers between the modules and the beamformer are shown dressed toward one side for wrap-around to the back of the array.
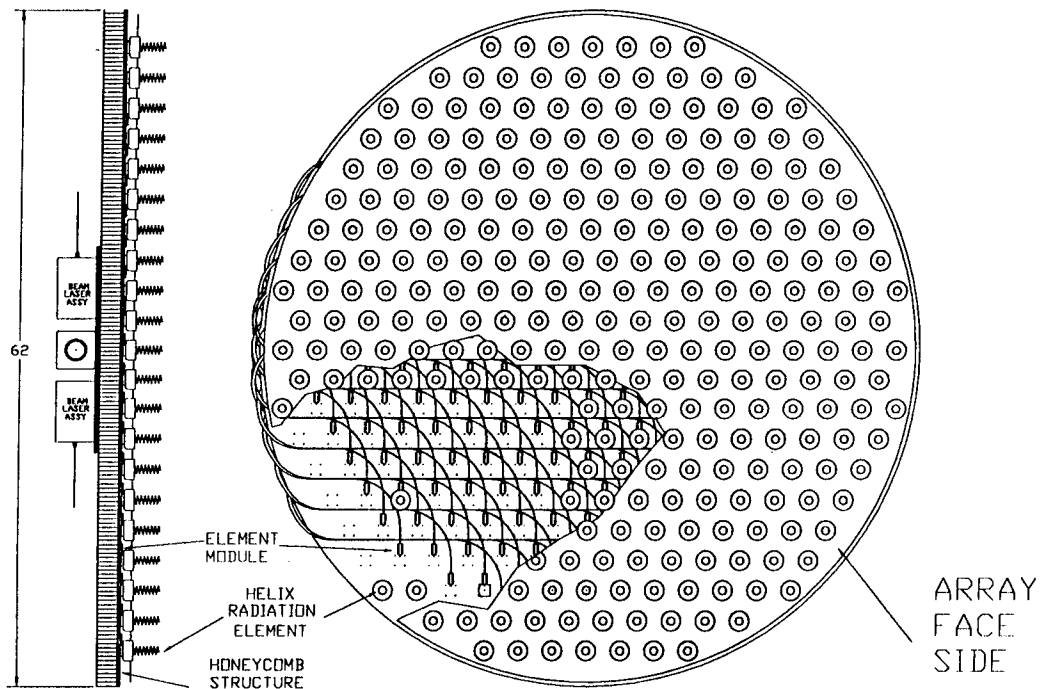
Figure 5.4.2-1   Satellite Transmit Array Front and Side Views

Figure 5.4.2-2 shows the rear view of the satellite array including the beam control assembly. The small size potential of the photonic beamformer is apparent. Addition of more beams in the array means adding a dual laser assembly and an SLM for each new beam inside the Fourier Transform Assembly. Hardware growth for additional beams is minimized to perhaps less than a 10% increase per beam.
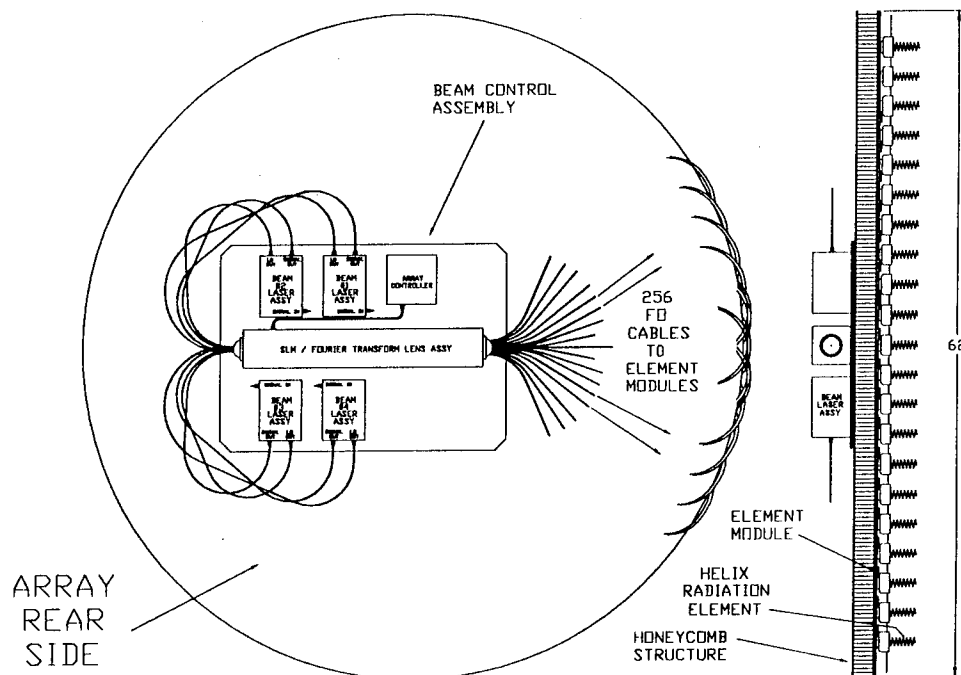
Figure 5.4.2-2   Satellite Transmit Array Rear and Side Views

Figures 5.4.2-3, -4, and -5 show more detail of the beamformer assembly, the feed geometry, and the quad SLM assembly.
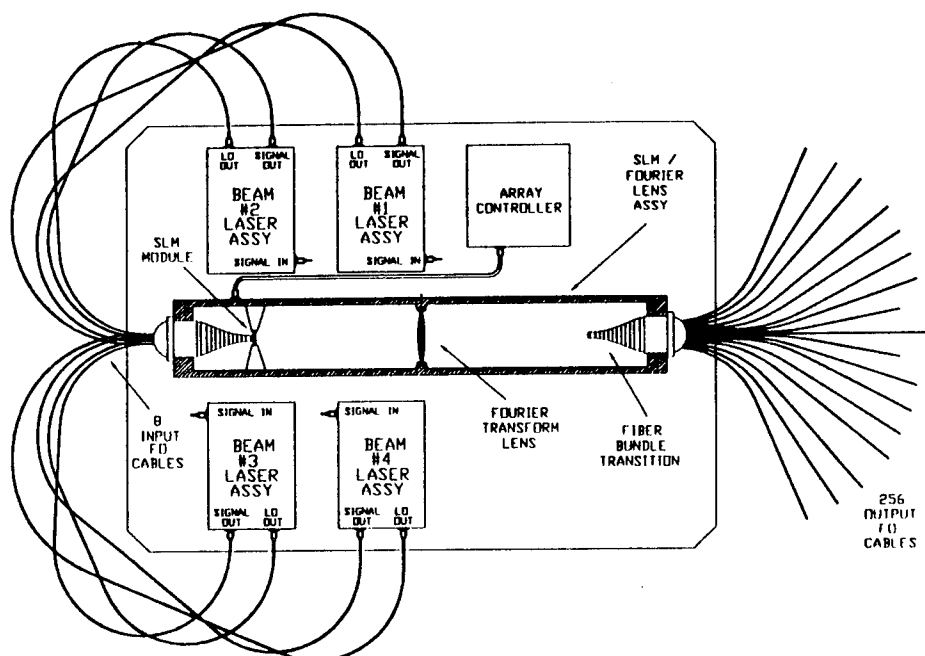
Figure 5.4.2-3   Satellite Transmit Array Multiple Beamformer
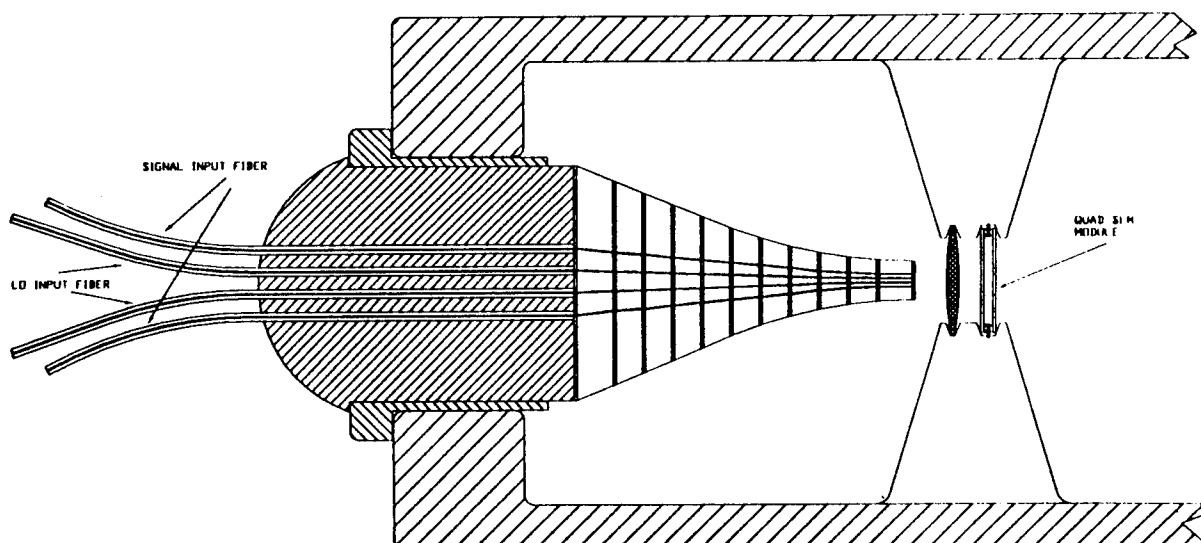
Figure 5.4.2-4   Satellite Transmit Array Feed Geometry
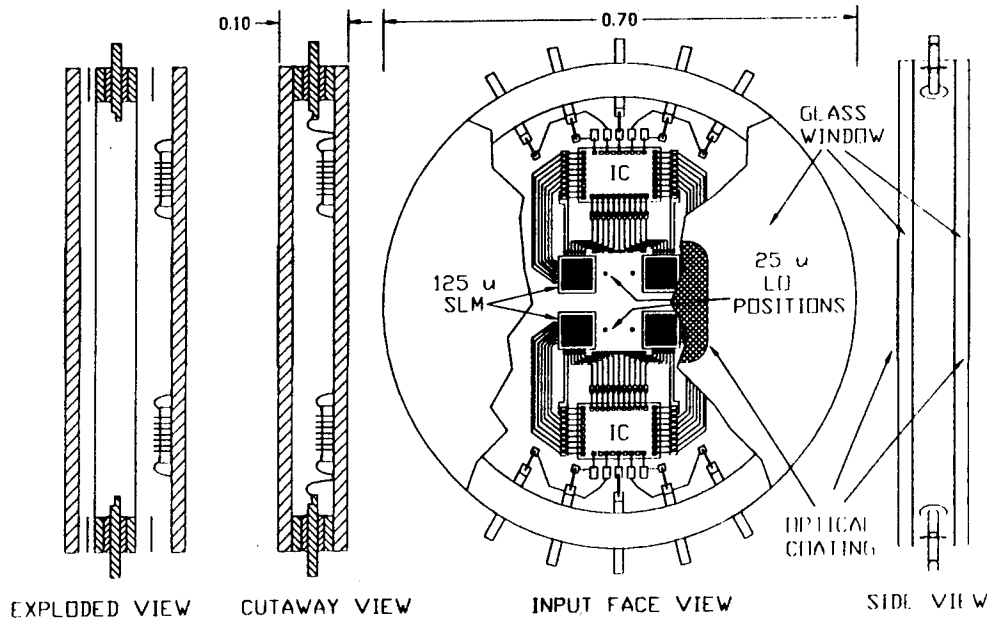
Figure 5.4.2-5 Satellite Transmit Array Quad SLM

For the receive array, only the dimensions of the aperture and the addition of an RF combiner and demultiplexer are different from the transmit array. Figure 5.4.2-6 shows the rear and side views with the impact of the changes.
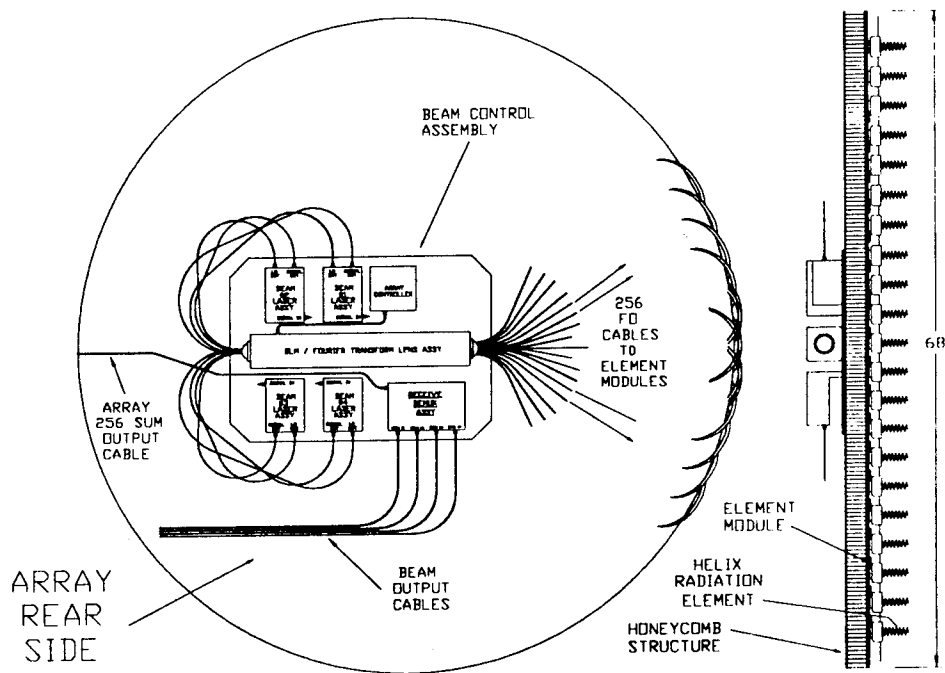
Figure 5.4.2-6 Satellite Receive Array Rear and Side Views

5.5 Risk Assessment

As for the airborne arrays, the definition of risks in the proposed satellite array designs is paramount to development of a logically organized EDM-ADM-flight hardware development. As mentioned in paragraph 5.0, the design challenges for the satellite array are significantly more difficult than for the airborne array. To achieve a level of competitiveness with conventional RF phased arrays, a photonic-based satellite phased array must show at least parity.

At an early stage of the initial study program, a satellite array was configured that achieves significant weight and size reductions compared with conventional multiple beam arrays. The cost of achieving these goals is improved technologies in SLM's and mask generation.

5.5.1 Mechanical Risks

The expected mechanical risks in the satellite arrays are fundamentally the same as for conventional approaches:
- size/weight
- low power consumption
- thermal management
- radiation hardness

Solutions to all of the mechanical risks can be found in existing space-qualified satellite arrays.

The most radiation sensitive component in the design is the SLM. However some compromises in shielding designs can be achieved as long as the overall array weight is less. The small size of the SLM hardware helps make the additional shielding weight tolerable.

5.5.2 Electrical Risks

The electrical risks to the satellite array designs are quite high. The benefits to the array built with the proposed design are also quite high.

The most fundamental area of risk is in the spatial light modulator defined in the array architecture. Defining one beam per SLM element, the amount of amplitude control over each pixel and control of phase changes versus amplitude level must be improved over existing designs. Also, devices at the specified 1.3 micron wavelength have not been studied to great depth at this point in the technology history.

A second risk is how the SLM excitation is best determined especially when nulling jammers and creating a custom beam shape on the earth surface.

The frequency plans including LO offset frequencies for each laser beam and subsequent downconversion of multiple beams into a one FDM signal at the RF module output needs further analysis and experimentation.

The design of the aperture with wide spacing and high gain array elements should be characterized more completely insuring proper control of grating lobes.

5.5.3 Cost Risks

The cost risk in a design based on expanded technology components is apparent to everyone. The solution to this cost risk is a concentrated R&D to define and fabricate

the components off-line to the primary development program. Because the application of photonic technology to a DSCS satellite must wait for the next generation of satellites, there is calendar time to solve the component design challenges before commitment to a system development.

6.0 Hardware Demonstration

Generation of multiple, simultaneous beams for the satellite array is a task more efficiently performed with light than microwaves. Taking advantage of the non-interaction of light and the Fourier transforming properties of an optical lens enables a single feed network to drive the array elements regardless of the number of simultaneous beams. Optical superheterodyne techniques are used to produce the antenna's RF transmit frequencies and reduce optical crosstalk at the detector The hardware demonstration was designed to demonstrate two aspects of the proposed four-simultaneous-beam satellite array; 1) the non-interference of beams with different laser offset frequencies and 2) the spatial light modulator (SLM) requirements for sixty-one beam locations (earth coverage).

6.1 Demonstration Selection

The proposed optical system for the simultaneous-beam satellite array is shown in Figure 6.1. Each beam is generated by a local oscillator (LO.)/signal spatial light modulator (SLM) pair. Each pair is illuminated by a single laser (of frequency f), however, the light through one element of the pair is frequency offset by the RF transmit frequency (d) desired for the beam. The four local oscillators and signal SLMs are located in the front focal plane of a Fourier transform lens. An array of 256 photodetectors or optical fibers leading to photodetectors is located in the back focal plane (the Fourier transform plane) of the lens. The photodetectors, one per antenna array element, are ac-coupled to remove any bias and low-pass filtered to remove any frequency terms that are above the antenna transmit frequency.
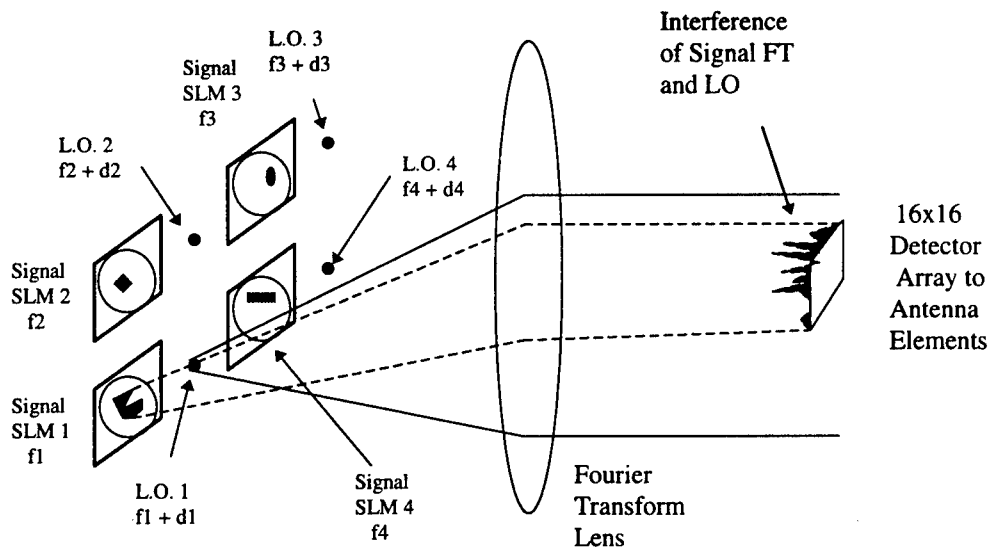
The beam angle is determined by the angular offset of the local oscillator and the signal SLM.

Figure 6.1. The proposed multiple-beam satellite array beam generation optical system.

The pattern superimposed on a given laser beam by an SLM represents the beam shape radiated by the antenna onto the target (earth). The optical pattern is Fourier transformed by the lens onto the photodetectors where it interferes with its local oscillator to form a spatial fringe pattern determined by the spatial offset of the local oscillator from the SLM in the front focal plane and is weighted by the SLM Fourier transform. This spatial fringe pattern will not be stationary on the detectors but swept across them at the offset frequency, d. Each detector represents one pixel of the Fourier transform whose amplitude is modulated at the antenna transmit frequency. Interference between elements of different LO/SLM pairs will be at frequencies beyond the range of the photodetectors (assuming proper laser frequency selection) and this crosstalk will be suppressed or eliminated.

6.2 Hardware Description

The experimental demonstration of the optical multiple-beam generation system was limited by the availability of only one suitable laser source. Frequency offsets as well as spatial separations were generated using a pair of acousto-optic Bragg cells. A silicon camera was used in the Fourier transform plane to simulate the optical fiber and detector array. The demonstration system is shown in Figure 6.2-1.
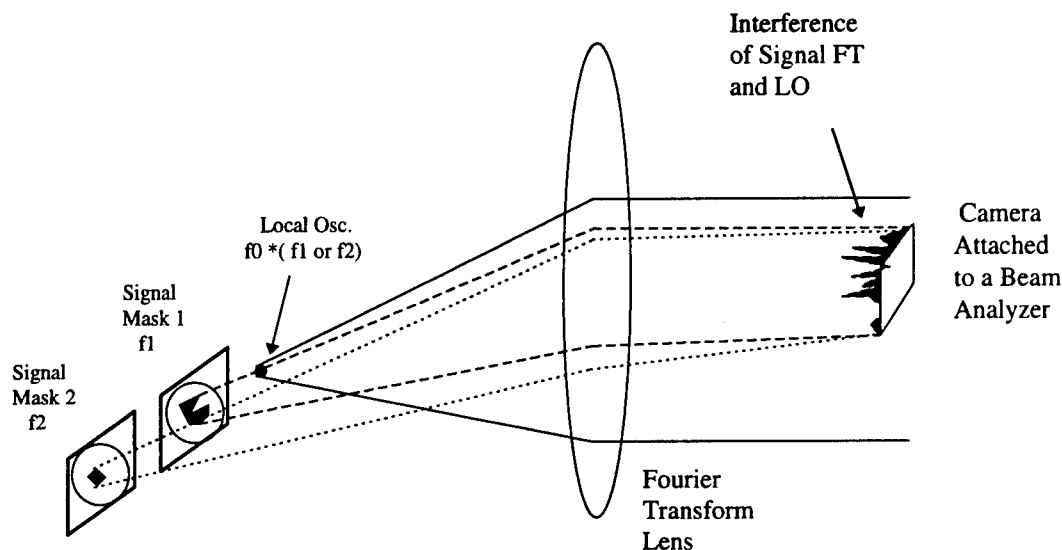
The beam angles are different in this experiment as we trade spatial freq. for temporal freq. to facilitate detection.

Figure 6.2-1. Multiple-beam generation for the laboratory demonstration.

This system is capable of achieving both of the demonstration goals. The single local oscillator was locked to the frequency of one signal mask at a time with an offset frequency in both cases of 0. This caused the interference pattern between the local oscillator and the selected mask to be stationary on the

camera while the interference patterns due to all other signals traversed the camera aperture at some non-zero rate and appeared as a background signal. Because the lateral separation between the LO and the first SLM is different from the separation between the LO and the second SLM, the standing fringe pattern on the camera has a different period depending on which SLM is locked to the LO. The spatial separations would be identical in the real system to ensure that the broadcast antenna patterns from the different LO/SLM pairs overlapped at the target. The demonstration system merely trades the temporal frequency used for transmission in the real array for a spatial frequency that is easy to observe in the demonstration.

The second demonstration goal of gaining insight into the SLM requirements was accomplished by locking the LO to the frequency of one of the SLMs. The frequency of the locking signal was then scanned to emulate the selection of different elements across the SLM. The requirement that the antenna be capable of pointing to sixty-one individual beam locations on the target results in an SLM with sixty-one elements in a circular arrangement. The SLM would then be nine elements across at its widest point. Generating nine linear, non-overlapping beams in the antenna's far-field requires that the fringe pattern formed by the LO and one of the SLM elements increase by one fringe for each SLM element. Therefore, the fringe pattern formed by the furthest SLM element from the LO and the LO has nine more fringes in the pattern than that formed by the nearest SLM element to the LO and the LO.

The electrical and optical setups used in the demonstration are shown in Figures 6.2-2 and 6.2-3. The first Bragg cell has an operating frequency of 400 MHz and the second Bragg cell operates in the 30-80 MHz range. A pulse generator and mixer is required to lock the LO (generated by the first Bragg cell) to one of the SLM signals (generated by the second Bragg cell). In the optical setup, a HeNe laser illuminates the first Bragg cell that is driven by a 400 MHz sine wave under a square-wave envelope at the frequency of one of the SLM signals. The first diffracted order from the first Bragg cell enters the second Bragg cell which generates the three beams; the LO (the undiffracted light) and the two SLM beams (modulated at frequencies f1 and f2).
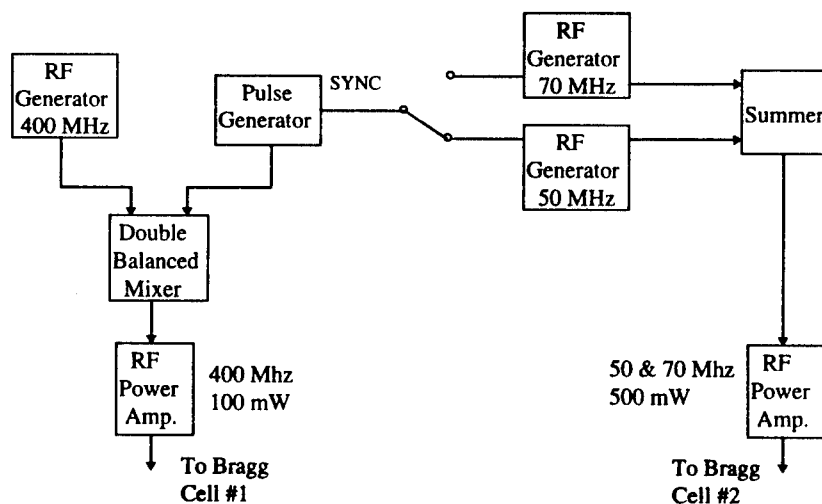
Figure 6.2-2. Electrical setup for demonstration of simultaneous beam generation.
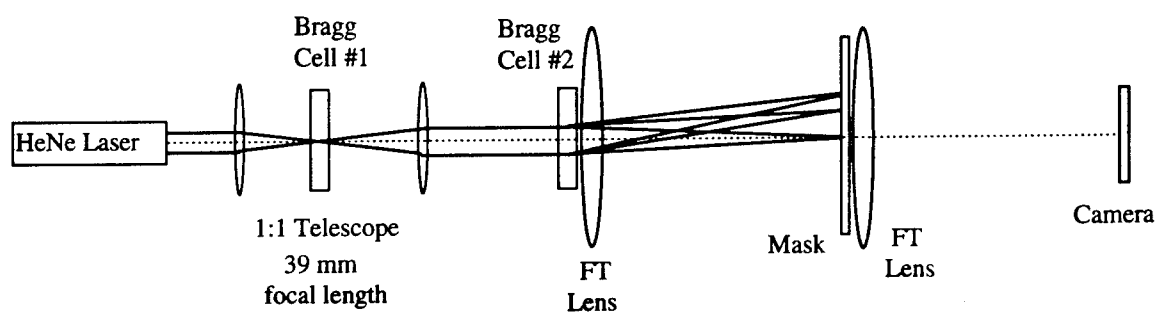
Figure 6.2-3. Optical setup for demonstration of simultaneous beam generation.

The LO forms interference patterns with both SLM beams at the camera aperture. The SLM beams that is frequency locked to the LO forms a stationary fringe pattern with the LO while the other SLM/LO interference pattern sweeps across the camera aperture. The rate at which the second fringe pattern sweeps across the camera is determined by the difference in the two SLM frequencies and the relative, perhaps varying, phase between them.

6.3 Test Results

Several optical masks were generated to serve as the SLMs for the demonstration. Unfortunately, the camera resolution precluded the use of all but the simplest patterns. The two signal patterns presented here are shown in Figures 6.3-1 and 6.3-2. The figures are labeled according to the output of the second Bragg cell; the LO is the 0-order beam and the diffracted beams at $f1 = 50$ MHz and $f2 = 70$ MHz represent the two signal SLM beams. Figure 6.3-1 shows the SLM beams unpatterned producing Gaussian amplitude plane-waves as the SLM signals. Figure 6.3-2 shows patterns similar to those in Figure 6.3-1, however, a knife edge has been inserted into the SLM plane to block half of the f2 signal. In both cases, the LO was focused to a spot in the SLM plane to emulate a point source LO.
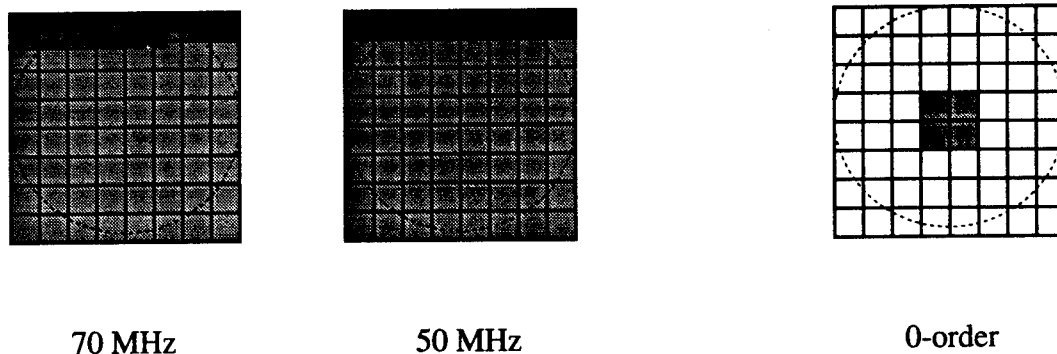
70 MHz   50 MHz   0-order

Figure 6.3-1   Plane-Wave Input Mask Plane
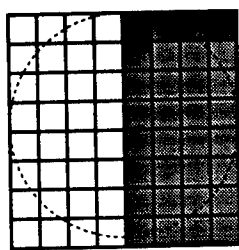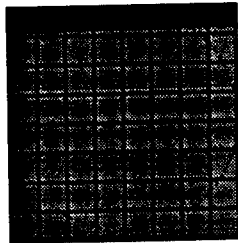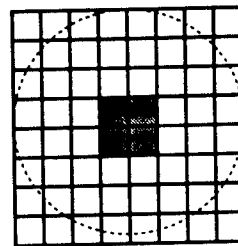
70 MHz   50 MHz   0-order

Figure 6.3-2. Knife-Edge Mask Plane.

The camera was attached to a Spiricon Laser Beam Analyzer (Model LBA-100A) that recorded the interference patterns. The patterns recorded are equivalent to the antenna excitation. Figures 6.3-3 and 6.3-4 show the patterns recorded when the LO was locked to the 50 MHz and 70 MHz plane-wave patterns, respectively. Note the difference in fringe spacing due to the difference in displacement from the LO of the two SLMs. Antenna excitation patterns for the knife-edge mask are shown in Figures 6.3-5 and 6.3-6. Several aspects of the system may be gleaned from this data. First, Figures 6.3-3 and 6.3-5 are nearly identical so that the 50 MHz signal is unaffected by the 70 MHz signal which is required if our LO/SLM pairs are to operate independently. Conversely, the 70 MHz signals shown in Figures 6.3-4 and 6.3-6 display a smearing of the antenna excitation with the insertion of the knife edge as expected from Fourier transform theory. Finally, note that there are, roughly, five more fringes displayed in Figure 6.3-4 than there are in Figure 6.3-3. Therefore, tuning the SLM frequency from 50 and 70 MHz demonstrates the equivalent of selecting, in turn, each of five elements out of the nine elements that comprise the sixty-one-element SLM's width.
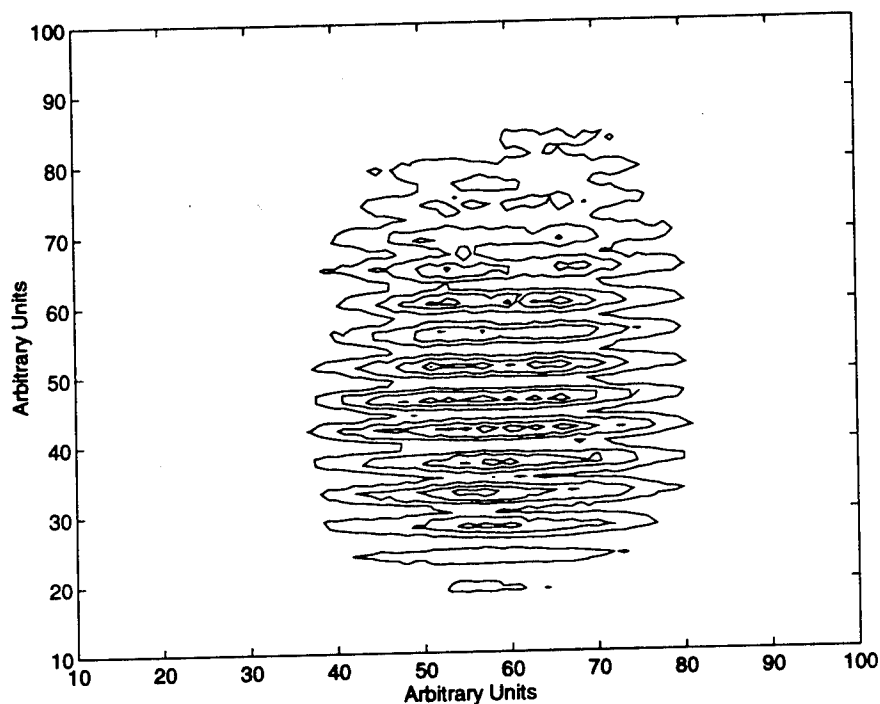
Figure 6.3-3. Contour plot of antenna excitation recorded by the Spiricon when the LO was locked to the 50 MHz plane-wave SLM.
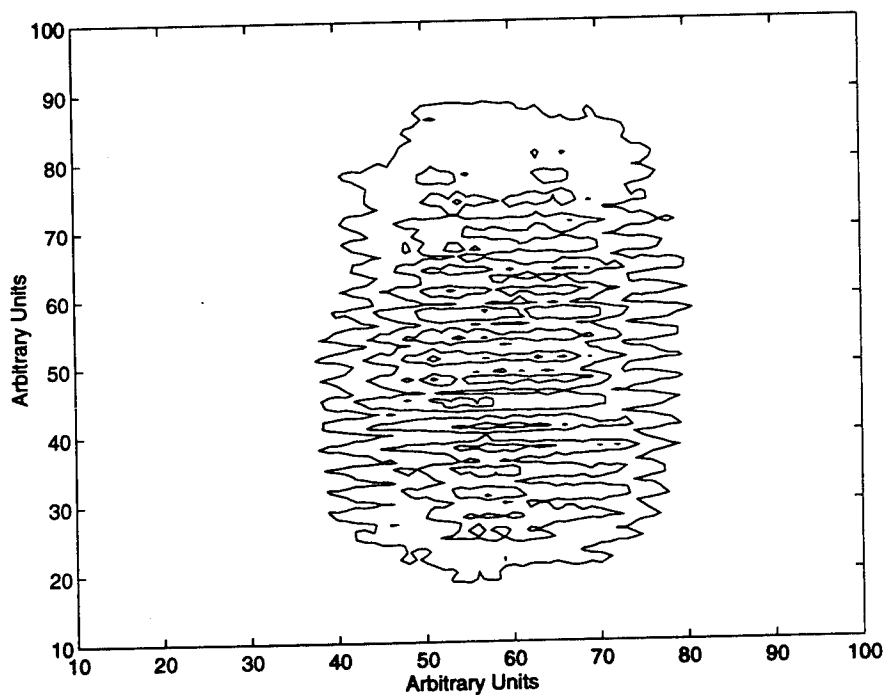
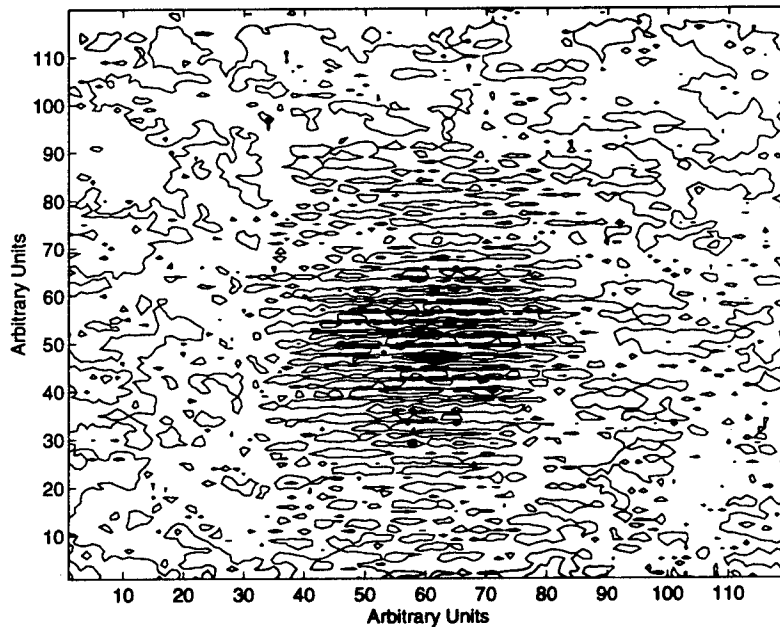**Figure 6.3-4.** Contour plot of antenna excitation recorded by the Spiricon when the LO was locked to the 70 MHz plane-wave SLM.
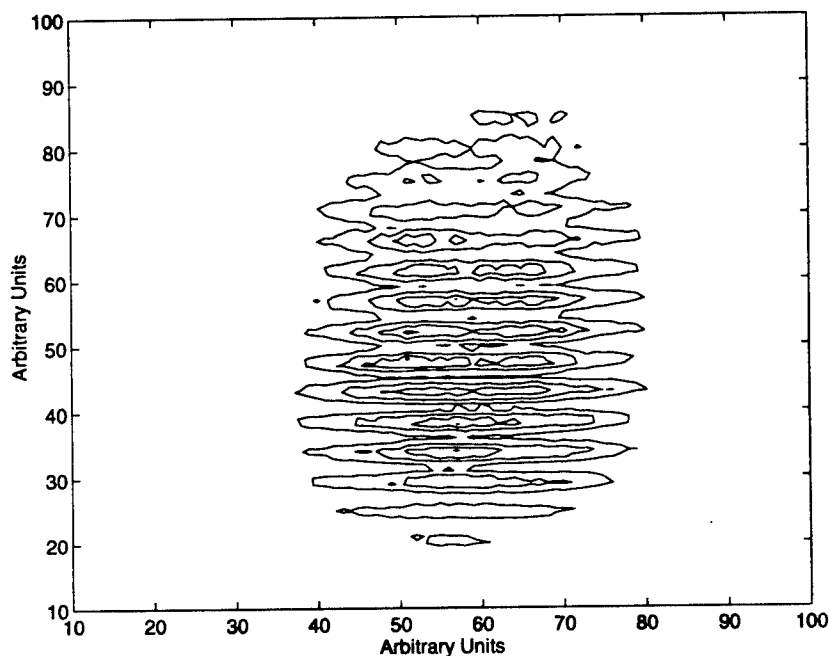
Figure 6.3-5. Contour plot of antenna excitation recorded by the Spiricon when the LO was locked to the 50 MHz knife-edge SLM.
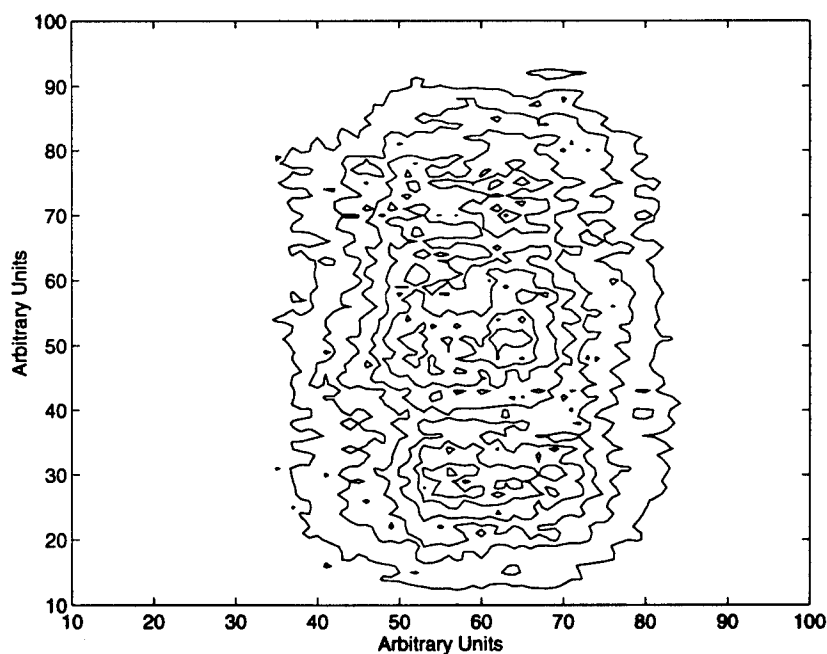
Figure 6.3-6. Contour plot of antenna excitation recorded by the Spiricon when the LO was locked to the 70 MHz knife-edge SLM.

The software package, MatLab, was used to Fourier transform these antenna excitation patterns to obtain the antenna's far-field pattern. These far-field patterns are shown in Figures 6.3-7, -8, -9 and -10. The center spot in

these figures is due to background light in the laboratory and would not be present in true satellite systems in which the detector array would be ac-coupled. The far-field spots don't overlap at the different frequencies because of the different offset distance between the LO and the two SLMs. This also will not be a problem in a true system implementation. Again, the two 50 MHz patterns are consistent, but now the knife-edge 70 MHz far-field pattern resembles a cut-off beam. To make this more evident, a 60 MHz signal was applied to the second Bragg cell and that was locked to the LO. The LO spot size in the SLM plane was reduced further to increase the contrast ratio of the interference pattern. The antenna excitation is shown in Figure 6.3-11 and the far-field pattern shown in Figure 6.3-12 and 6.3-13. The knife edge is much clearer in the 60 MHz data.
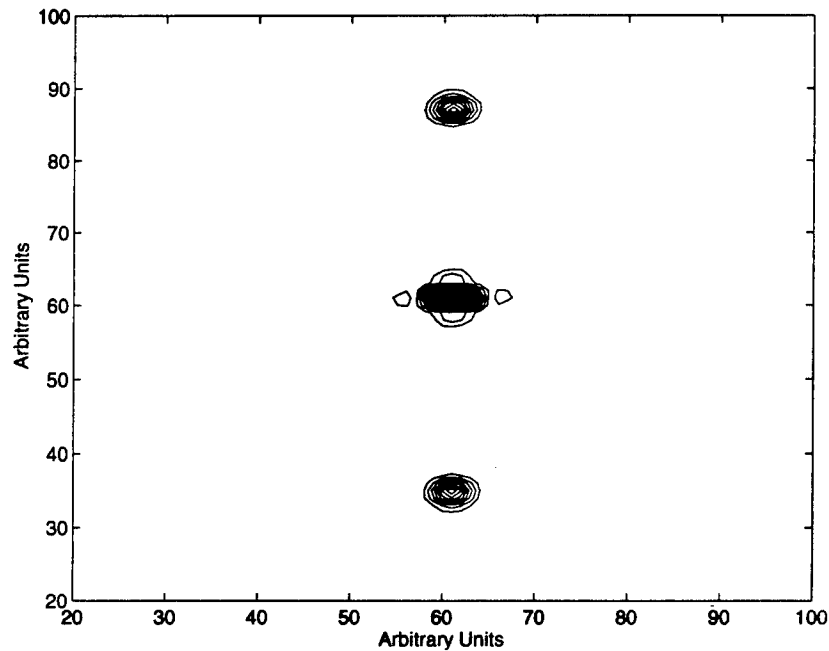
Figure 6.3-7. Fourier transform of the pattern in Figure 6.3-3 representing the antenna far-field pattern of the 50 MHz plane-wave SLM.
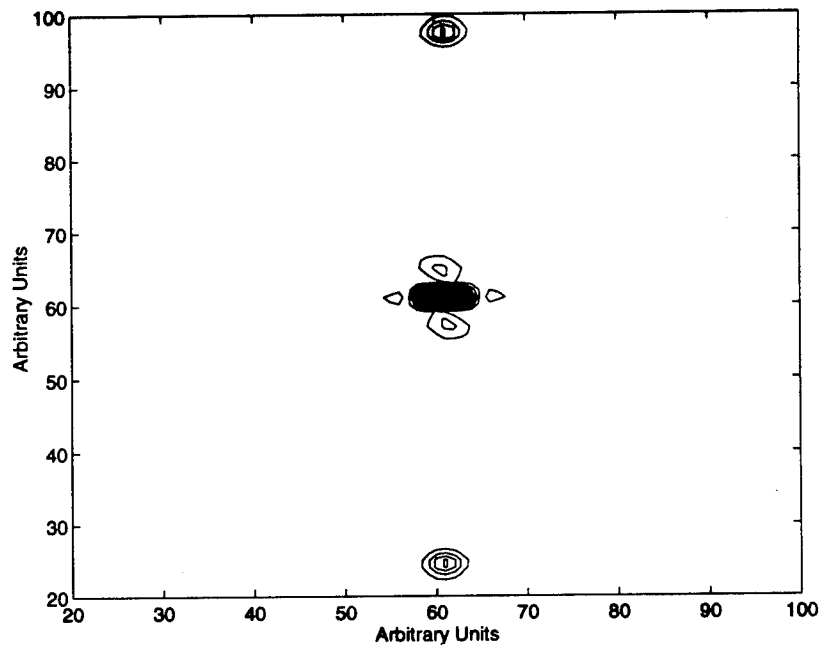
Figure 6.3-8. Fourier transform of the pattern in Figure 6.3-4 representing the antenna far-field pattern of the 70 MHz plane-wave SLM.
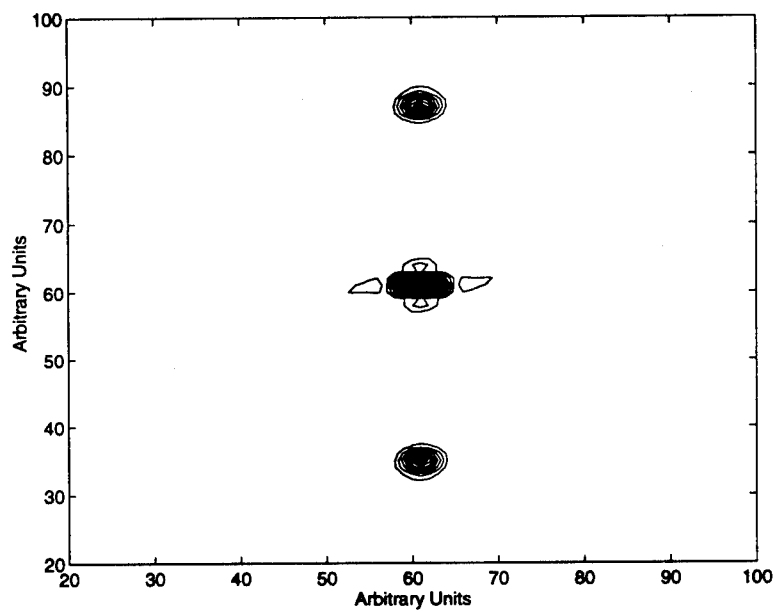
Figure 6.3-9. Fourier transform of the pattern in Figure 6.3-5 representing the antenna far-field pattern of the 50 MHz knife-edge SLM.
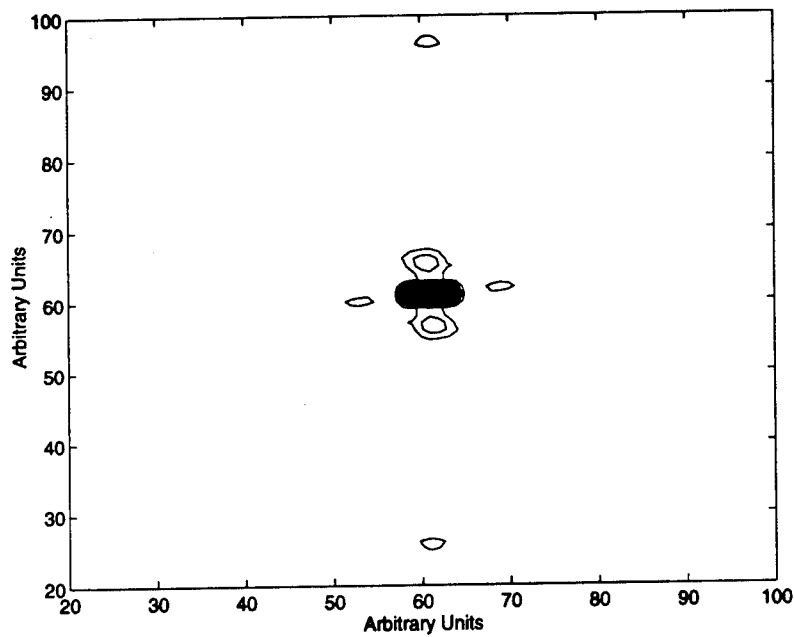
Figure 6.3-10. Fourier transform of the pattern in Figure 6.3-6 representing the antenna far-field pattern of the 70 MHz knife-edge SLM.

Figure 6.3-11. Contour plot of antenna excitation recorded by the Spiricon when the LO was locked to the 60 MHz knife-edge SLM. Image cleanliness has suffered as contrast has improved.
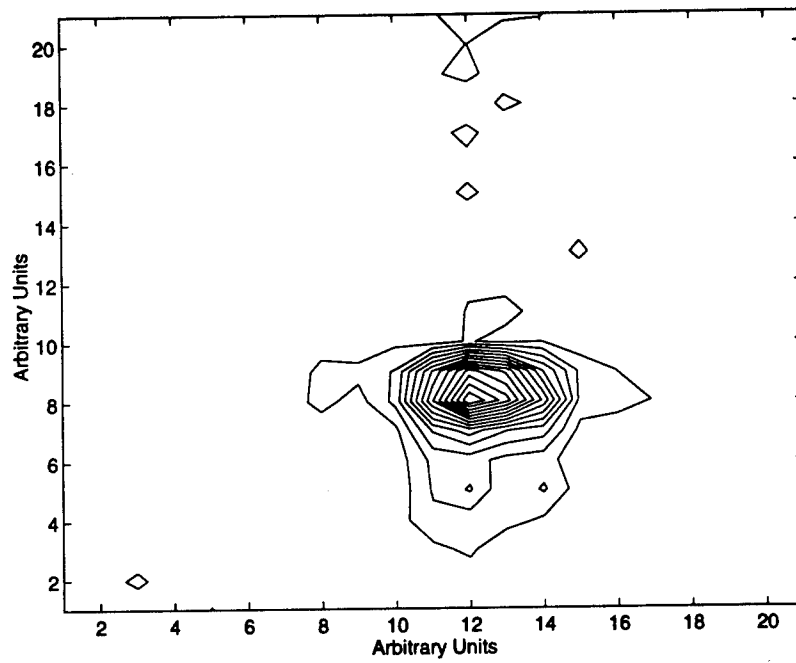
Figure 6.3-12. Fourier transform of the pattern in Figure 6.3-11 representing the antenna far-field pattern of the 60 MHz knife-edge SLM. The scale has been enlarged to show only one lobe of the pattern.
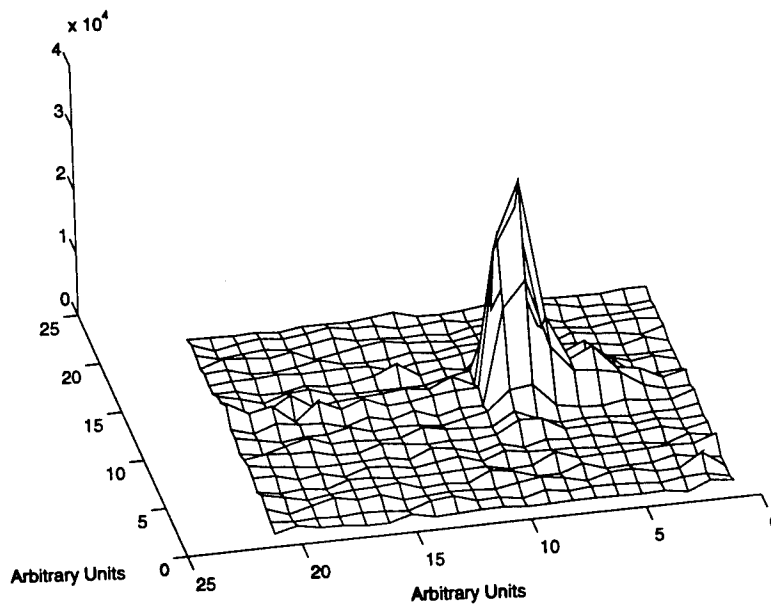
Figure 6.3-13. Surface plot of Figure 6.3-12 showing well-defined knife edge.

7.0 OCSSA Array Features and Limitations

The two array designs presented in this report are significantly different in both architecture and in feasibility within today's state-of-the-art.

The airborne array, as described in the introduction, represents a more cautious approach using technology within reach today. The goal of the airborne array exercise was to compare sizes with current RF design technologies. The airborne array as presented has a minimum number of unique building blocks. Each beamformer contains the same set of dual delay networks and all 17 beamformers for azimuth and elevation are identical. The number of bits in each dual delay network sets the number of beams in its scan plane. The control scheme for the array is elegantly simple with all azimuth beamformers operating in the same state, there is only one control line per bit in azimuth and one line per bit in elevation.

The airborne arrays use a square rather than a triangular grid lattice. Although requiring the elements to be packed more closely and not creating beams in a symmetric, conical nature to match the scan volume, the symmetry in both planes makes the delay networks and control scheme possible.

The satellite array architecture is an ambitious attempt to apply photonic technology where significant size and weight reductions can be achieved. Rather than quadrupling the hardware to achieve four beams, the satellite beamformer optics remains the same. Growth to additional beams requires an additional SLM, a dual frequency laser in both receive and transmit arrays and a filter modification in the receive array. Adaptive beamforming is added by creating unique jammer beams to subtract from the main beams.

The satellite array configuration will require technology breakthroughs in SLM technology. As discussed during the study, the maximum photonic benefit will only be achieved when SLM technology allows Fourier optical processing to be done efficiently.

Further analysis on the receive array frequency plan has been done and presented in this report. The LO multiplexing in the receive array does not appear to create a show-stopping image problem.

8.0 Development Issues

There are several areas of concern in the forecast of how well the proposed airborne and satellite arrays will transition to full scale development, to larger arrays, and to higher frequency arrays. Because they are discussed elsewhere, the issues of material and device technology growth are not repeated here. For the purpose of this discussion, it is assumed that the components and materials are available to meet expected requirements

8.1 Reliability, Maintainability, and Supportability

The reliability, maintainability, and supportability performance of the airborne array is based on three characteristics:

- distributed amplifiers at each element means graceful degradation

- modular, identical beamformer means fewer unique subassemblies

- external cooling to keep temperatures in control.

On the down side, the mechanical issues discussed in the risk discussion point to areas where mechanical failures might occur. Data on connections in fiberoptic systems is gathered every day on current avionic developments using fiberoptic signal distribution on developing airframes. The key mechanical areas of difficulty will be thermal management of dissimilar materials, the bundles of fibers inconnecting the element modules to the beamformers, and vibration.

The satellite arrays require maintainability and supportability only until placed in orbit. Then reliability becomes the driving issue. The following characteristics benefit the satellite array:

- no long-term vibration environment

- parallel nature of the beamformer and distributed amplification means graceful degradation

- relatively easy to add spare beams to the design

Mechanically, the thermal control problem appears to be no more difficult than on a RF array or the airborne OCSSA array.

8.2 Producibility and Life Cycle Costs

Designing the OCSSA arrays for producibility and low life cycle costs is achieved through the use of a minimum number of unique building blocks. In each array, this goal has been adhered to. The airborne array uses identical beamformers to take advantage of the symmetry.

It might be suggested that the same beamformer be used for both the receive and transmit functions to achieve even more commonality. However, the frequency differential makes the delay lengths unsuitable. Depending on which beamformer is used, the other array will either scan too far, creating high values of scan loss between beams, or will scan only part way, meaning additional bits would be necessary to either fill in the holes or achieve full 75° scan. In either case, use of a common beamformer does not appear to be attractive in terms of cost because half of the beamformers would have to carry superfluous hardware.

The satellite array beamformers use relatively small number of hardware pieces. Size scaling with frequency is necessary meaning common optical components are not feasible. Possibly the dual frequency lasers could be identical units each tuned to its specific frequency and offset.

8.3 Extension to Large Arrays

Extending the OCSSA arrays to more elements suggests two independent impacts.

For the airborne arrays, the best approach might be to use the 256 element array as a subarray for a larger array. This pays dividends in life cycle costs. The complexity will be increased in the dual delay networks because the narrower beamwidth of the larger array means more beams to achieve coverage. Realizing more beams means more bits of selection in each network however the use of all delays all the time will be maintained.

For the satellite arrays, extension to a larger array appears to force additional technology growth in the SLM. With more elements, there must be more pixels in each beam's SLM. All of the remaining hardware and the beamformer physical dimensions appear to have small changes as the array gets larger.

8.4 Extension to Higher Frequency Arrays

One of the clear advantages of photonics is the independence to RF bandwidth and frequencies.

In the airborne arrays, the beamformer is sized by the delays in nanoseconds across the aperture. At higher frequencies, the physical lengths of the delays will get smaller but should be achievable within the beamformer design with little difficulty. At higher frequencies, the array elements get very close together and fitting the necessary conditioning and conversion hardware behind each element and distributing to each element gets more difficult. RF connections are replaced by optical connectors or butt joints. With photonics, there is the option of radiating the optic signal if sufficient mechanical stability can be met. The real constraint in the airborne array architecture appears to be the hardware behind each element.

For the satellite arrays, where the separation is two wavelengths, achieving higher frequencies is easier because of the wider element spacing. The spacing is four times the airborne array spacing so theoretically packaging would not become a significant issue. The beamformer itself is independent of the RF frequency and is not affected by increasing frequencies. The first area

that might have difficulties as the frequencies go up may be the receive array combiner and demultiplexer.

9.0 References

1. Defense Information Systems Agency, "Defense Satellite Communications Systems (DSCS) Earth Terminal Certification Requirements", Final Version, 13 May 1993.

2. K.Noguchi, O. Mitomi, K. Kawano, and M. Yanagibashi,"Highly Efficient 40-GHz Bandwidth Ti:LiNbO3 Optical Modulator Employing Ridge Structure," IEEE Photon Photon. Technol. Lett.,vol.5, pp 52-54, 1993

3. G.K. Gopalakrishnan, C. H. Bulmer, W.K. Burns, R.W. McElhanon and A.S. Greenblatt, "40 GHz, low half-wave voltage Ti:LiNbO3 intensity modulator," Electron Lett., vol. 28 pp 826-827 1992.

4. Wilkinson, E.J., Parad, L. I., and Connerney, W. R., "An X-Band Electronically Steerable Phased Array, Microwave Journal vol. 7, February 1964, pp 43-48.

5. R. C. Hansen, editor, and J. L Butler, Microwave Scanning Antennas, Volume III, Array Systems, Penisula Publishing, 1985, pp 222-224.

Appendix A 16 Element Array Patterns on Airframe Model

16-Element Linear Array
Pitch Plane, 0° Scan
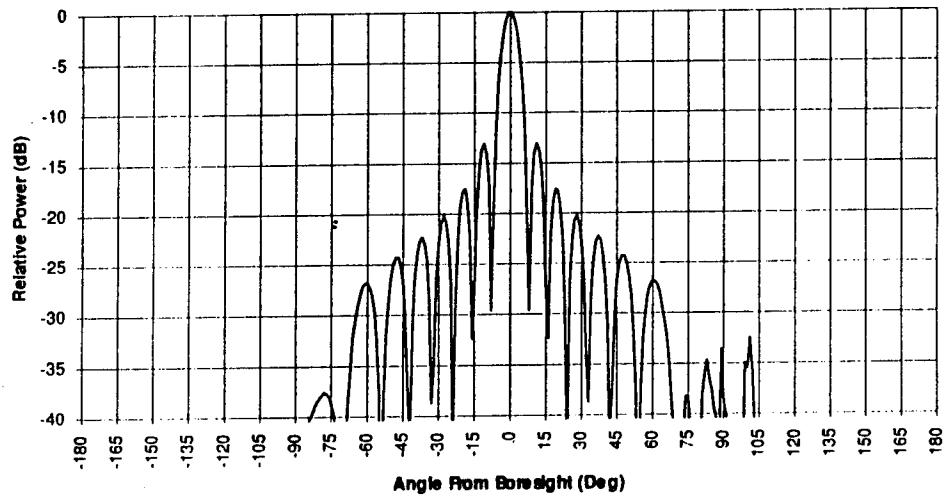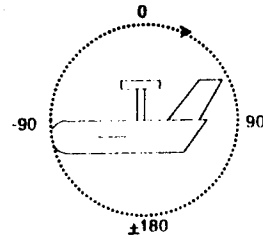
Figure A-1   Linear Array Pitch Plane Pattern, 0° Scan

16-Element Linear Array
Pitch Plane, -30° Scan
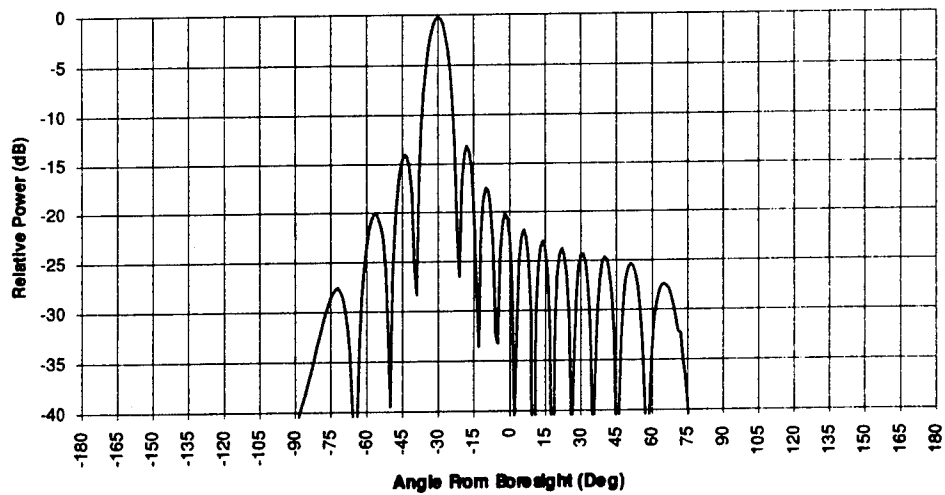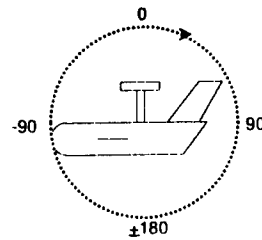
Figure A-2   Linear Array Pitch Plane Pattern, -30° Scan

16-Element Linear Array
Pitch Plane, -60° Scan
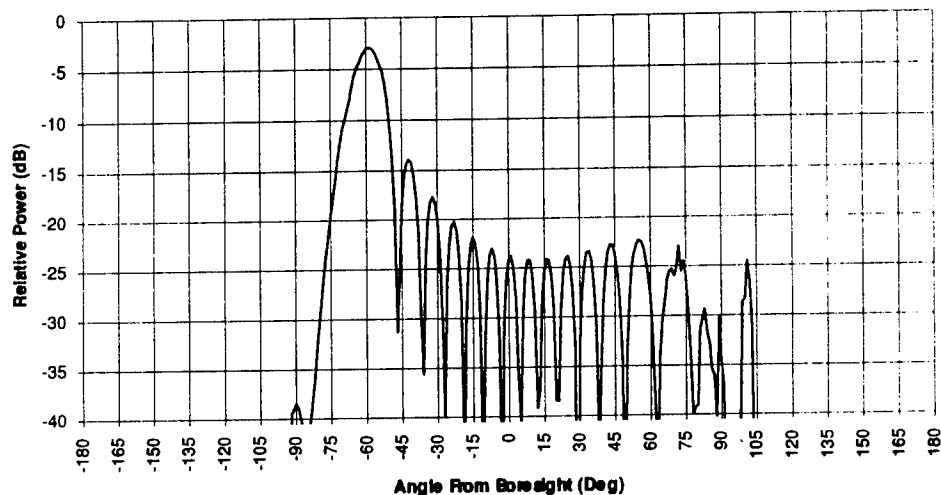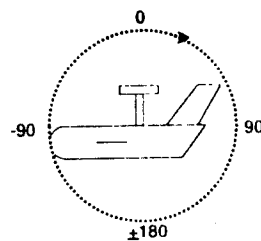
Figure A-3   Linear Array Pitch Plane Pattern, -60° Scan

16-Element Linear Array
Pitch Plane, -75° Scan
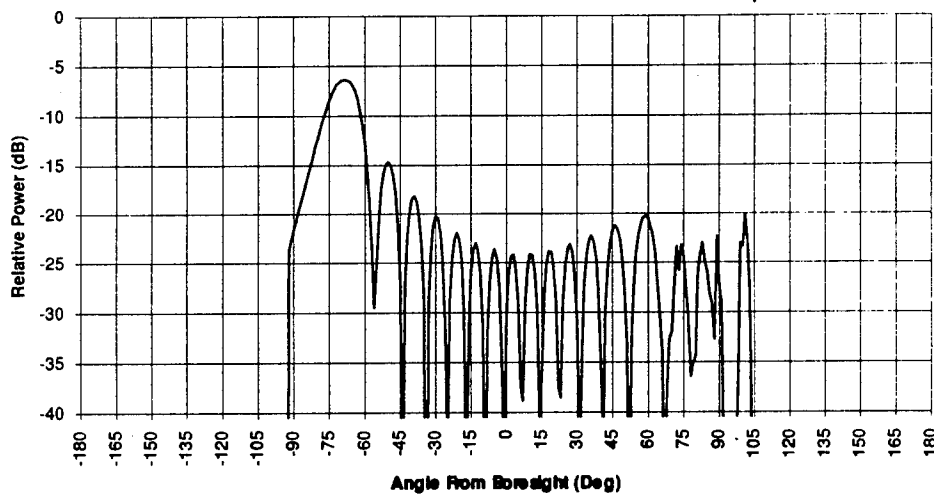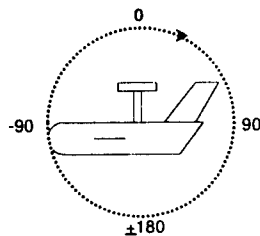
Figure A-4   Linear Array Pitch Plane Pattern, -75° Scan

16-Element Linear Array
Pitch Plane, +60° Scan
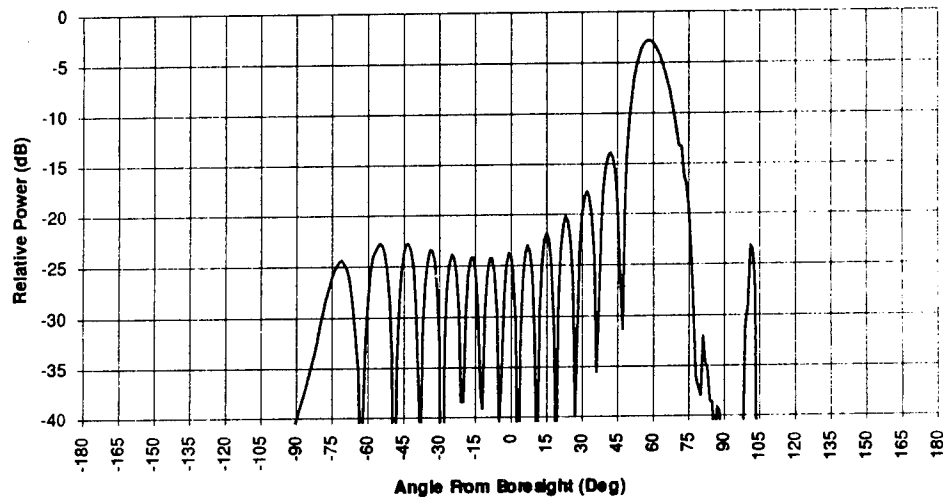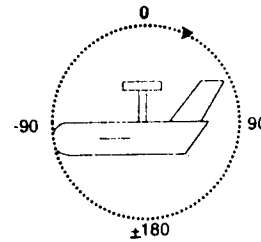
Figure A-5 Linear Array Pitch Plane Pattern, 60° Scan

16-Element Linear Array
Pitch Plane, 75° Scan
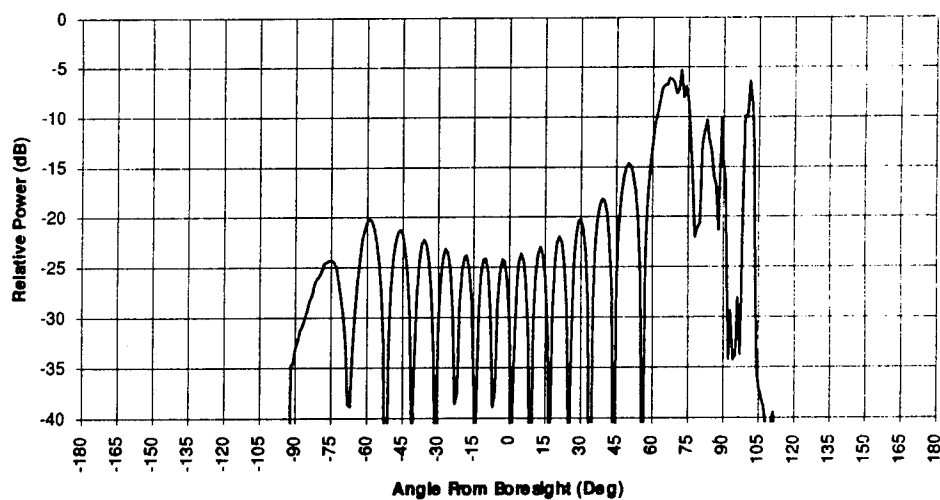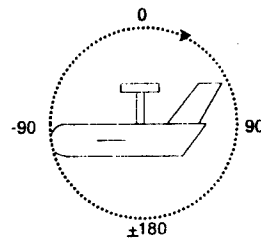
Figure A-6 Linear Array Pitch Plane Pattern, 75° Scan

Appendix B DSCS-OCSSA Communication Link Performance

**Aircraft to OCSSA-DSCS to AN/TSC-86 Ground Terminal
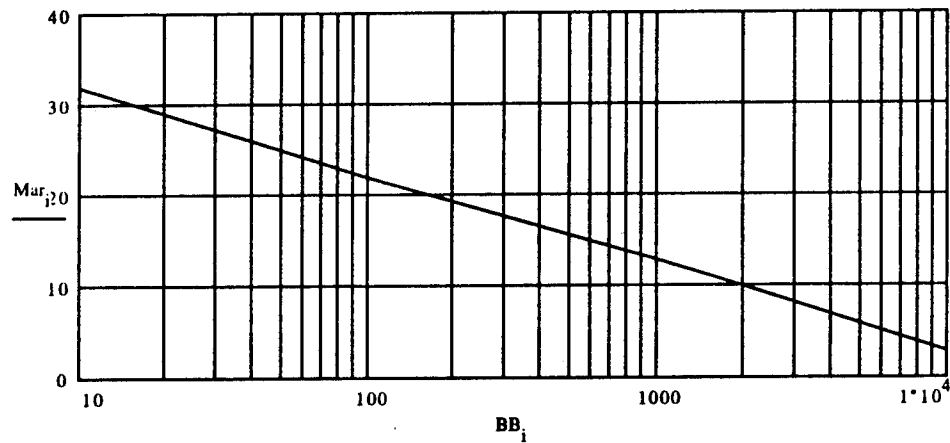Margin in dB versus Data Bandwidth in Kilohertz**
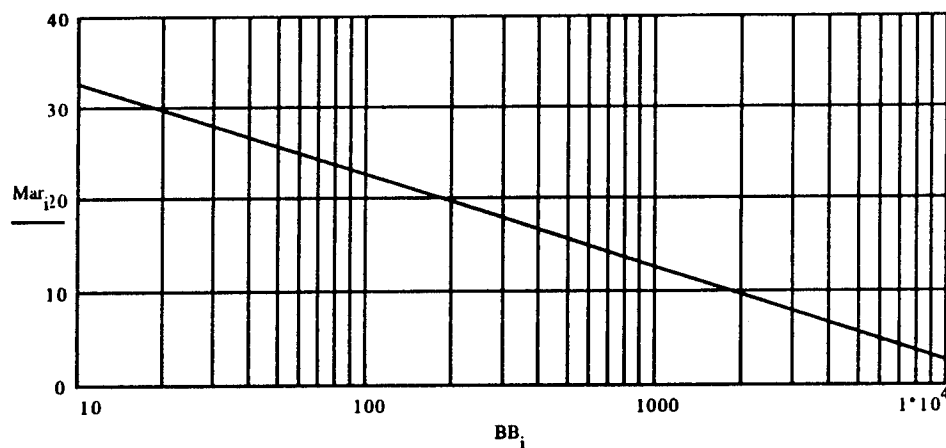
Figure B-1   OCSSA Aircraft to OCSSA-DSCS to TSC-86 Terminal Link Margin

**AN/TSC-86 Ground Terminal to OCSSA-DSCS to Aircraft
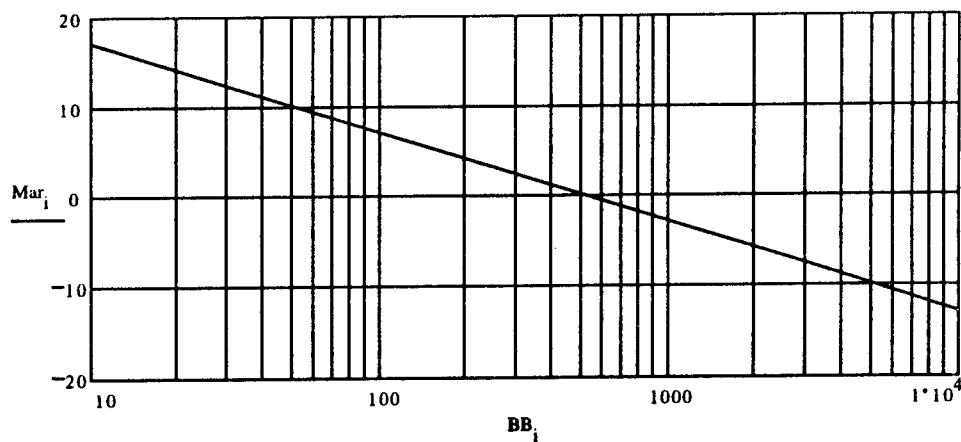Margin in dB versus Data Bandwidth in Kilohertz**
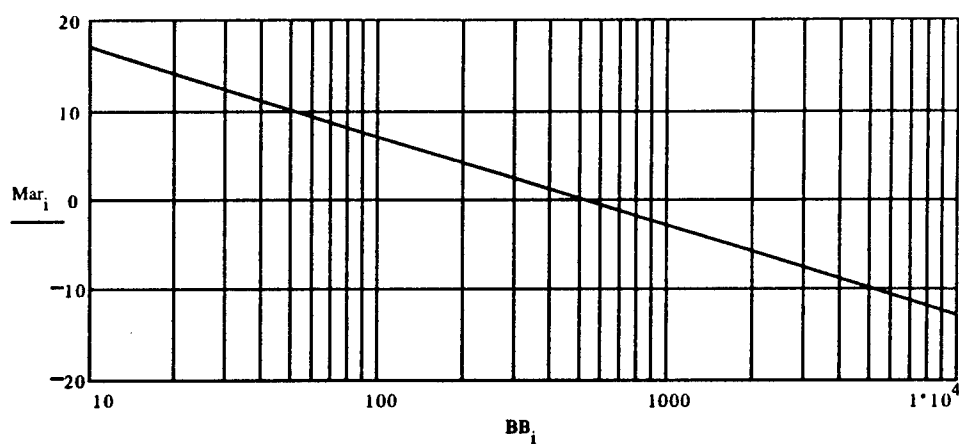
Figure B-2   TSC-86 Terminal to OCSSA-DSCS to OCSSA Aircraft Link Margin

Aircraft to DSCS III to AN/TSC-86 Ground Terminal
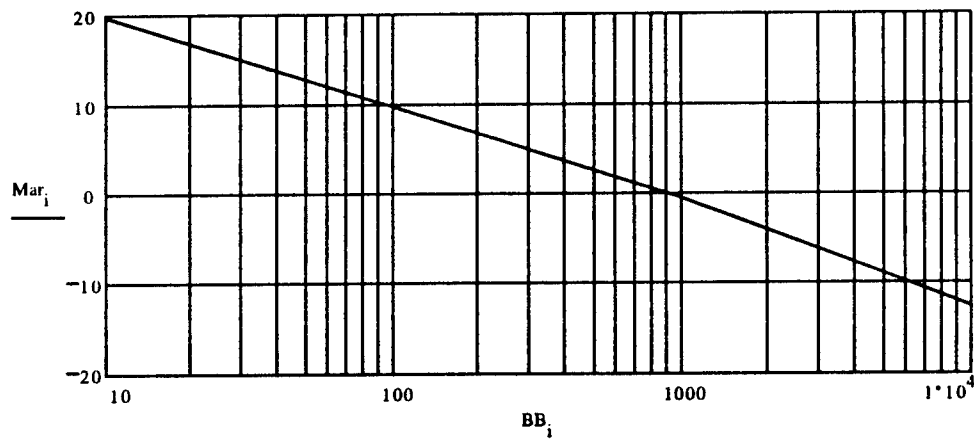## Margin in dB versus Data Bandwidth in Kilohertz
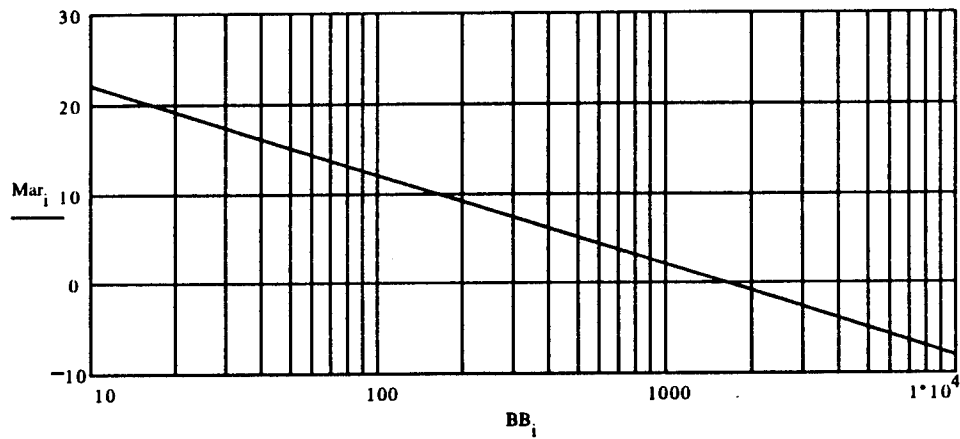
Figure B-3   OCSSA Aircraft to DSCS III to TSC-86 Ground Terminal Link Margin

AN/TSC-86 Ground Terminal to DSCS-III to Aircraft
## Margin in dB versus Data Bandwidth in Kilohertz
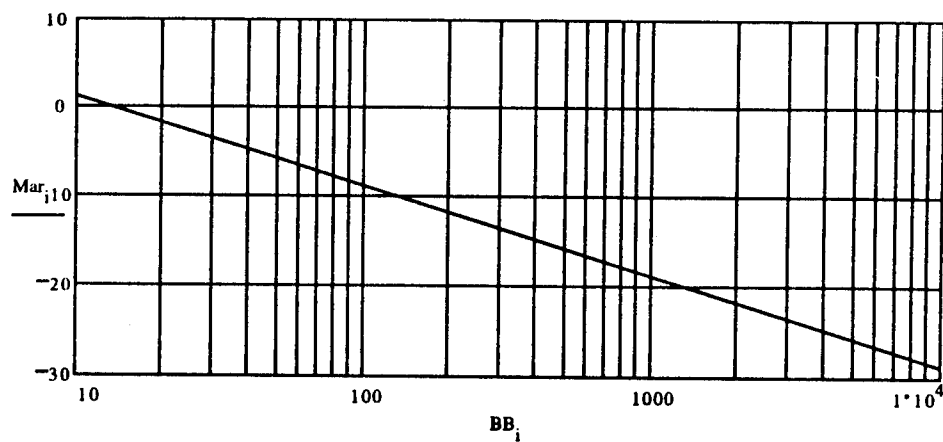
Figure B-4   TSC-86 Ground Terminal to DSCS III to OCSSA Aircraft Link Margin

Aircraft to OCSSA-DSCS to AN/WSC-6 Ground Terminal
Margin in dB versus Data Bandwidth in Kilohertz

Figure B-5   OCSSA Aircraft to OCSSA-DSCS to WSC-6 Ground Terminal Link Margin

AN/WSC-6 Ground Terminal to OCSSA-DSCS to Aircraft
Margin in dB versus Data Bandwidth in Kilohertz

Figure B-6   WSC-6 Ground Terminal to OCSSA-DSCS to OCSSA Aircraft Link Margin

Aircraft to DSCS III to AN/WSC-6 Ground Terminal
Margin in dB versus Data Bandwidth in Kilohertz

Figure B-7   OCSSA Aircraft to DSCS III to WSC-6 Ground Terminal Link Margin

AN/WSC-6 Ground Terminal to DSCS-III to Aircraft
Margin in dB versus Data Bandwidth in Kilohertz
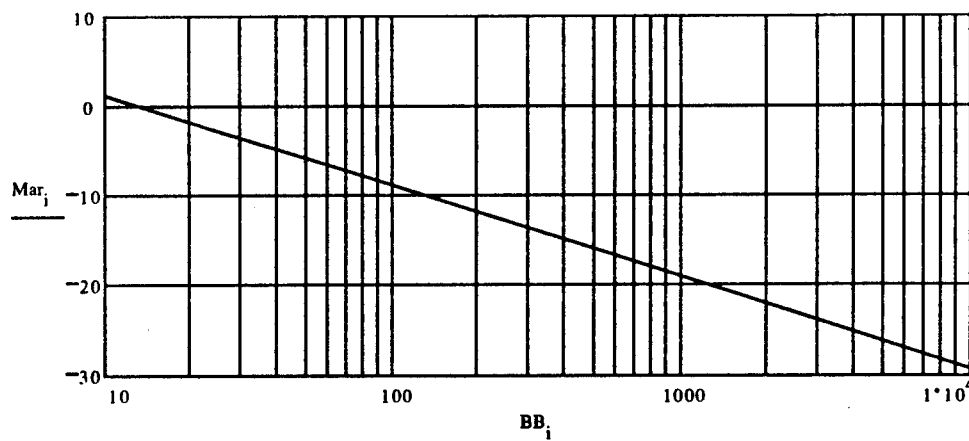
Figure B-8   WSC-6 Ground Terminal to DSCS III to OCSSA Aircraft Link Margin

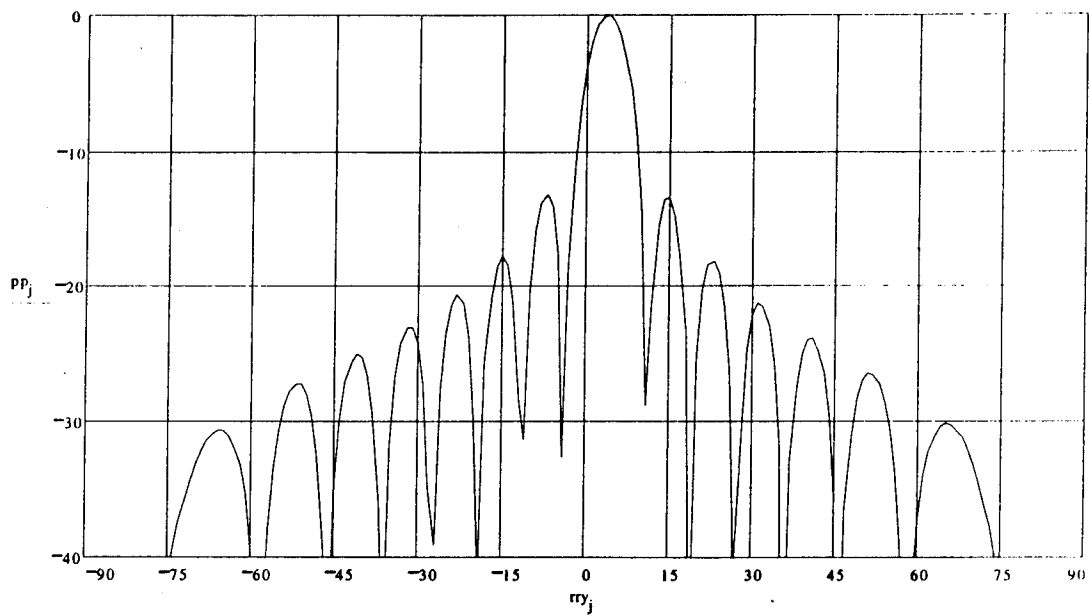Appendix C   Photonic Beamformer Airborne Array Scan Patterns
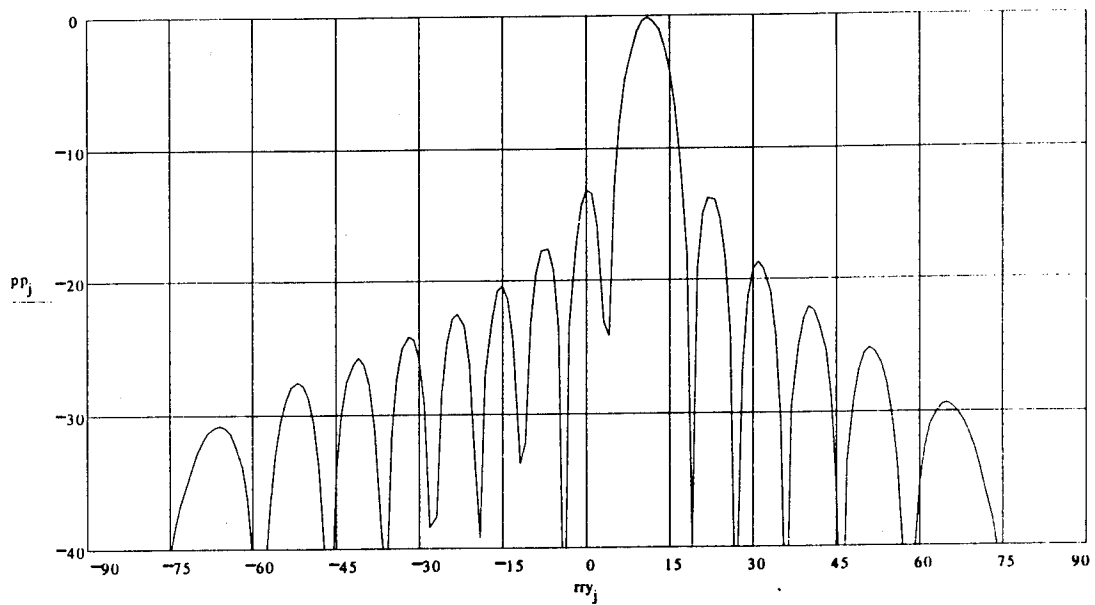
Figure C-1   Photonic Beamformer Pattern   3.7° Scan

Figure C-2   Photonic Beamformer Pattern   11.1° Scan
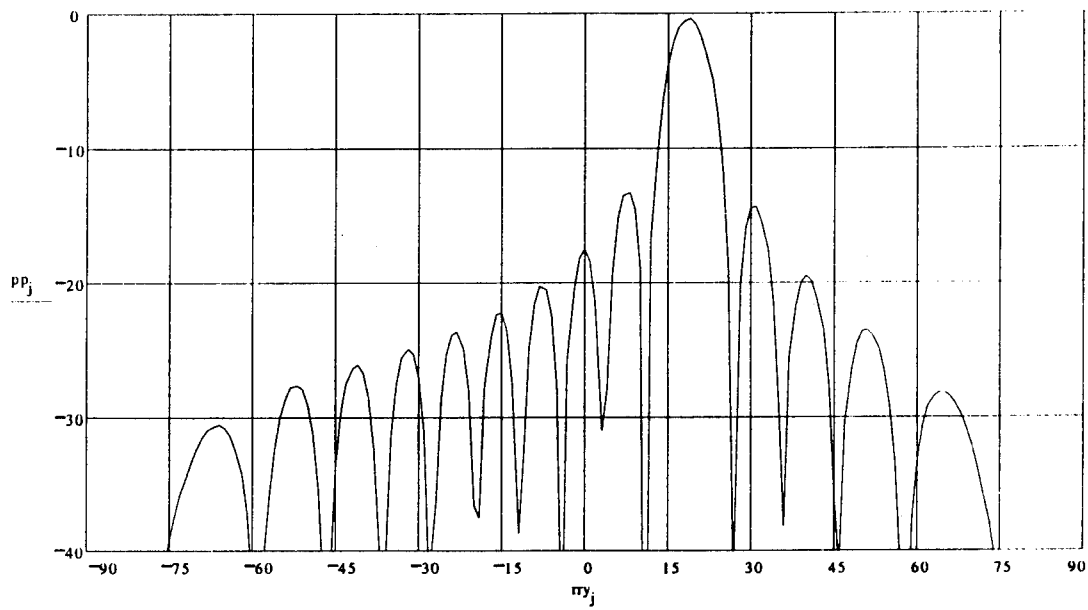
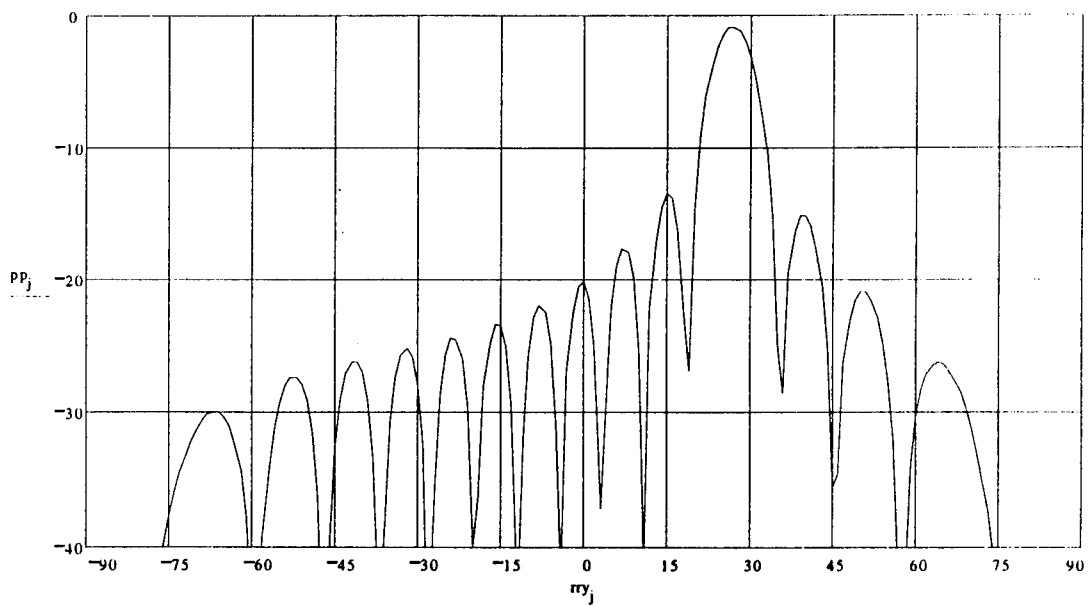Figure C-3   Photonic Beamformer Pattern   18.8° Scan

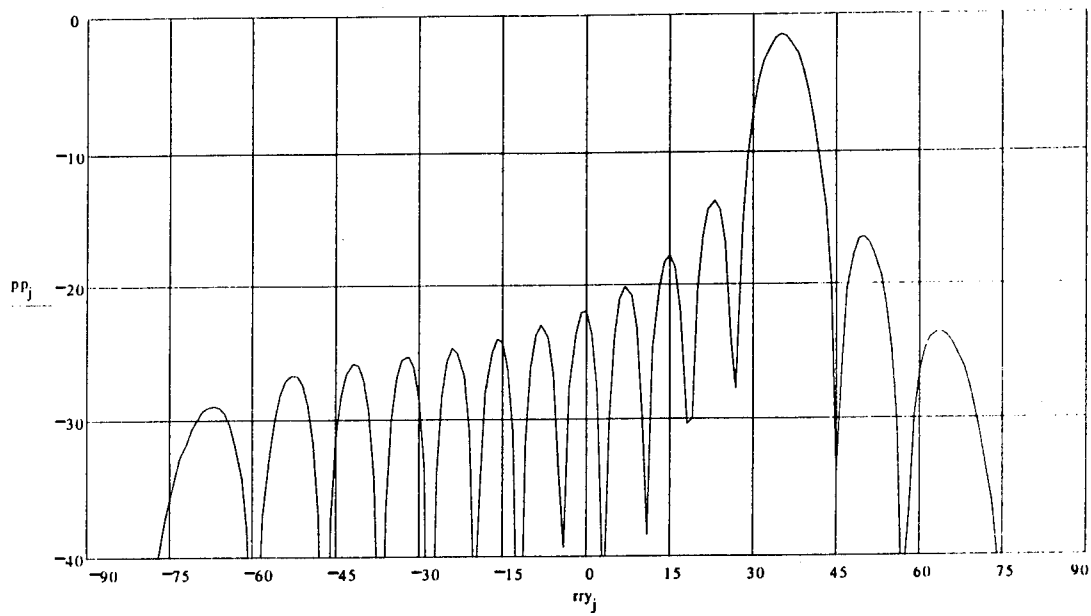Figure C-4   Photonic Beamformer Pattern   26.8° Scan

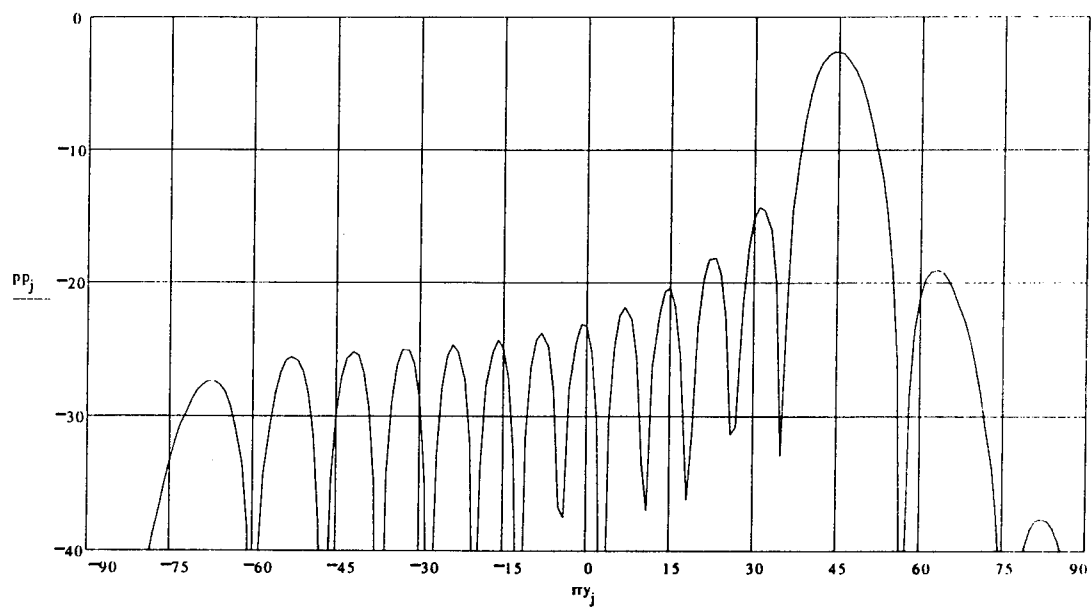**Figure C-5   Photonic Beamformer Pattern   35.4° Scan**

Figure C-6   Photonic Beamformer Pattern   45.1° Scan
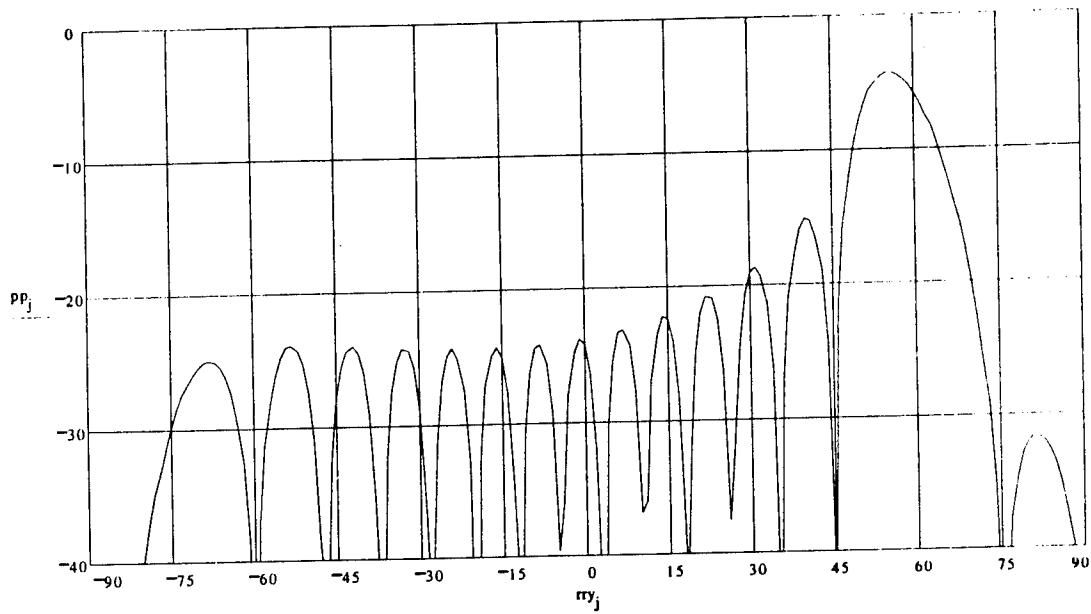
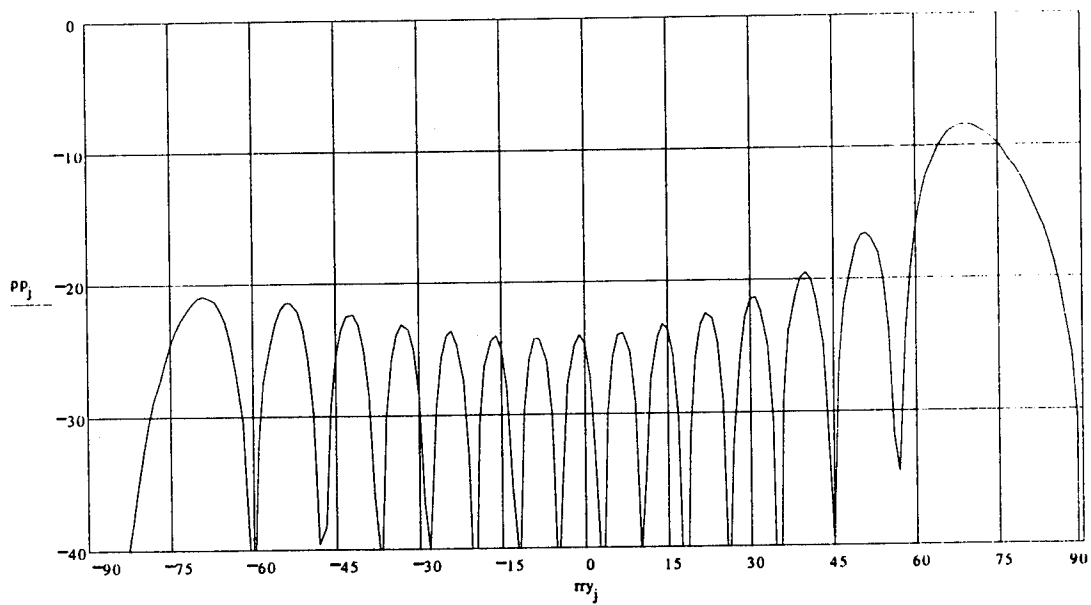**Figure C-7   Photonic Beamformer Pattern   56.8° Scan**

Figure C-8   Photonic Beamformer Pattern   75.0° Scan

Appendix D Satellite Receive Array Frequency Plan Studies

The challenge in analyzing the frequency plan for the OCSSA satellite receive phased array lies in the inability of conventional spur analysis programs and non-linear models to handle more than one LO frequency.

In order to affect a quick survey of the problem, a combination measurement and analysis task was developed.

- use initial spur analysis to find single LO bad/good spots
- bench tests using lab mixer to find spurs generated by two LO's
  with and without a signal present
- run a non-linear model in a multiple signal product finder to find
  spur coefficients
- compare measured and simulated results

Readily available test equipment was found for measurements from VHF to 2.6 GHz. Preliminary computer analysis showed a good mix for an IF between 290 and 312 MHz. For the tests, the RF frequency was 2300 and the LO frequencies were 2590 and 2612 MHz.

The test setup used for the measurements is shown in Figure D-1. The 5.9 dBm output power of the LO generators add at the mixer to about 9 dBm, a level the M18C mixer likes.
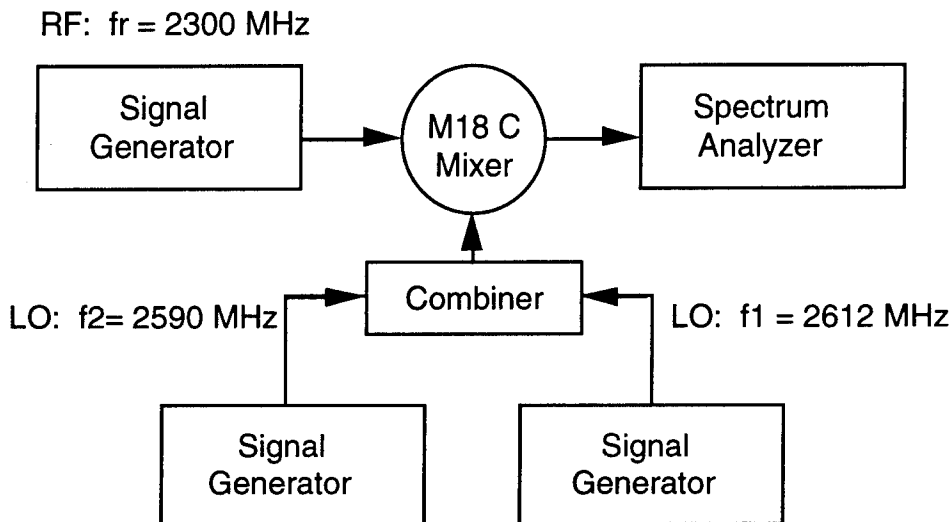
RF: fr = 2300 MHz

Figure D-1 Multiple LO Bench Test Setup

The product spurs were measured for three cases of signal power:

- P = -80 dBm (essentially no power)
- P = -20 dBm (maximum upper limit for mixer)
- P = -30 dBm (10 dB lower to look at dB/dB changes)

Figure D-2 shows the spur levels for the condition of no RF power. Operation near the minimums should be sought. (Note that the frequency scale is not linear.) This shows spurs that represent worst case degradation of performance for weak signals.
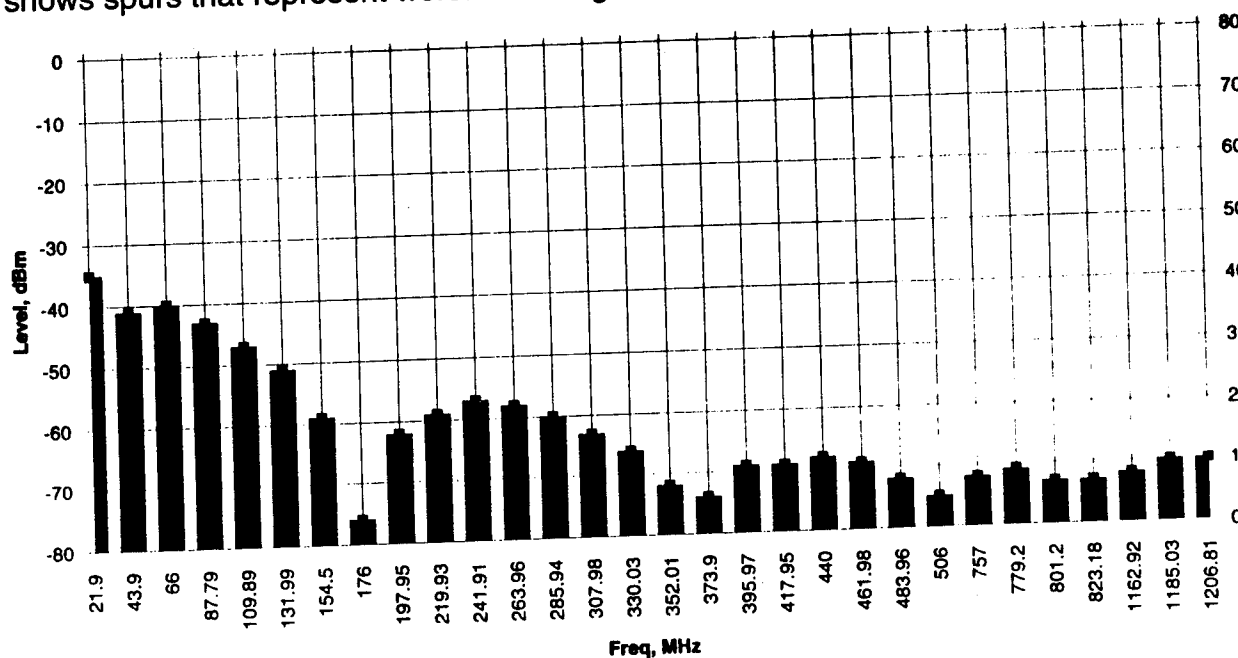

Figure D-2   Mixer Spur Levels with Two LO's and No Signal

Figure D-3 shows the effect when a signal is added and changed from no power (-80 dBm) to the maximum power (-20 dBm). This case shows the effect of strong undesired signals on the choice of frequencies. Examination of the level change of the spurs identifies the order of the spur.
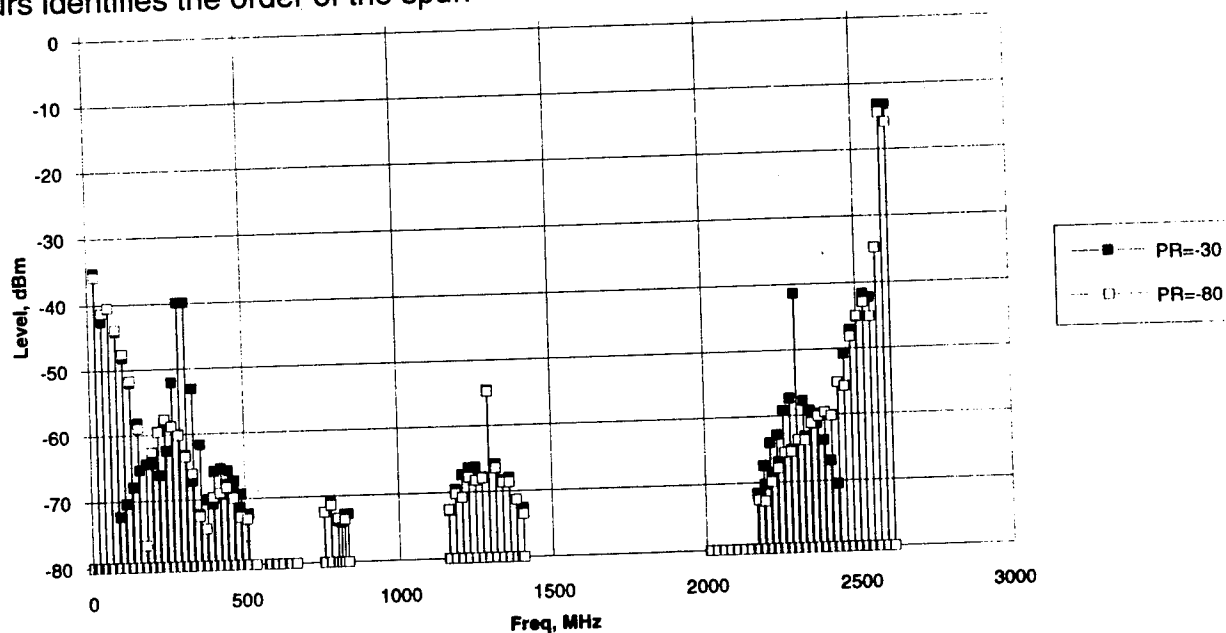

Figure D-3   Mixer Spur Levels with Two Signal Levels

Figure D-4 shows the effect when a signal is added and changed from no power (-80 dBm) to the maximum power (-20 dBm) and includes an intermediate case of a power input of -30 dBm..
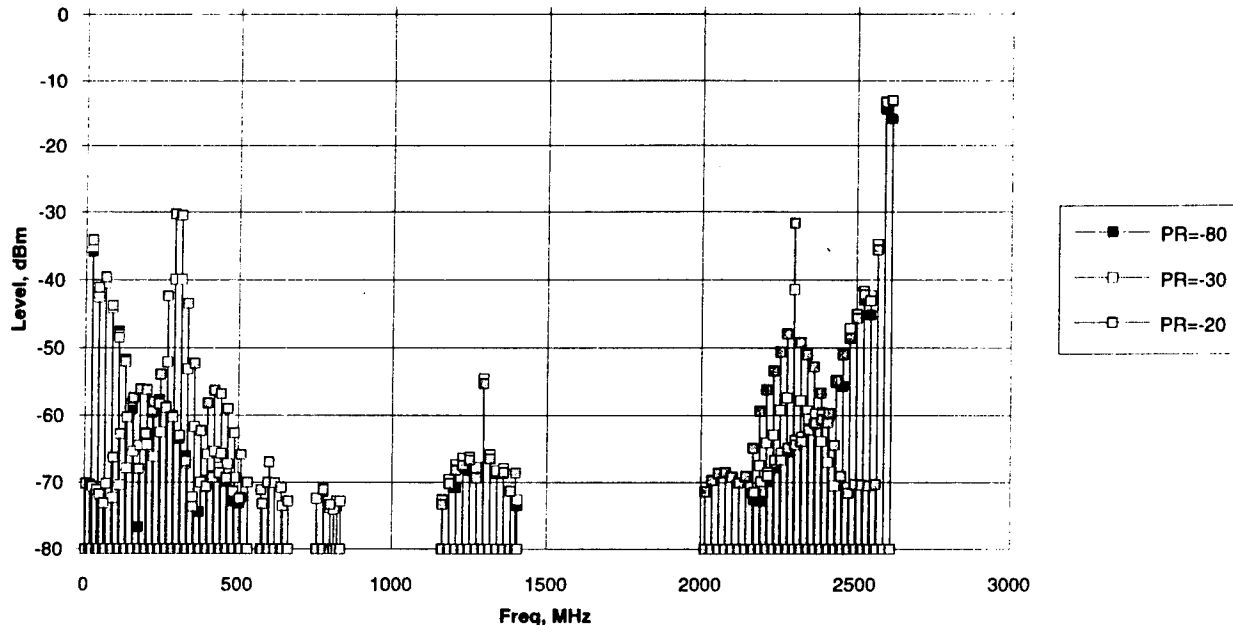

Figure D-4   Mixer Spur Levels with Three Signal Levels

Comparison of the measured spur levels with those predicted with a non-linear circuit model confirmed most of the expected spurs and identified some attributable to the generators.

At this point it appears that operation with multiple spurs does indeed create many products. However, there appears to be some usable IF bands particularly around 373 MHz. This is close to an optimum value of 1/7 of the LO frequency. The final measure of success will come when the system level spur levels are evaluated and other mixer configurations are compared.

Since the architecture is using the mixer in an unusual manner, it is most probable that a different mixer approach could help reduce spurs more. Current mixer technologies optimize for use of one LO frequency. Alternative approaches, like a resistive FET mixer, might be better because they can constrain most of their non-linearities to the second order.

MISSION

OF

ROME LABORATORY

Mission. The mission of Rome Laboratory is to advance the science and technologies of command, control, communications and intelligence and to transition them into systems to meet customer needs. To achieve this, Rome Lab:

   a. Conducts vigorous research, development and test programs in all applicable technologies;

   b. Transitions technology to current and future systems to improve operational capability, readiness, and supportability;

   c. Provides a full range of technical support to Air Force Materiel Command product centers and other Air Force organizations;

   d. Promotes transfer of technology to the private sector;

   e. Maintains leading edge technological expertise in the areas of surveillance, communications, command and control, intelligence, reliability science, electro-magnetic technology, photonics, signal processing, and computational science.

The thrust areas of technical competence include: Surveillance, Communications, Command and Control, Intelligence, Signal Processing, Computer Science and Technology, Electromagnetic Technology, Photonics and Reliability Sciences.